Volume 2

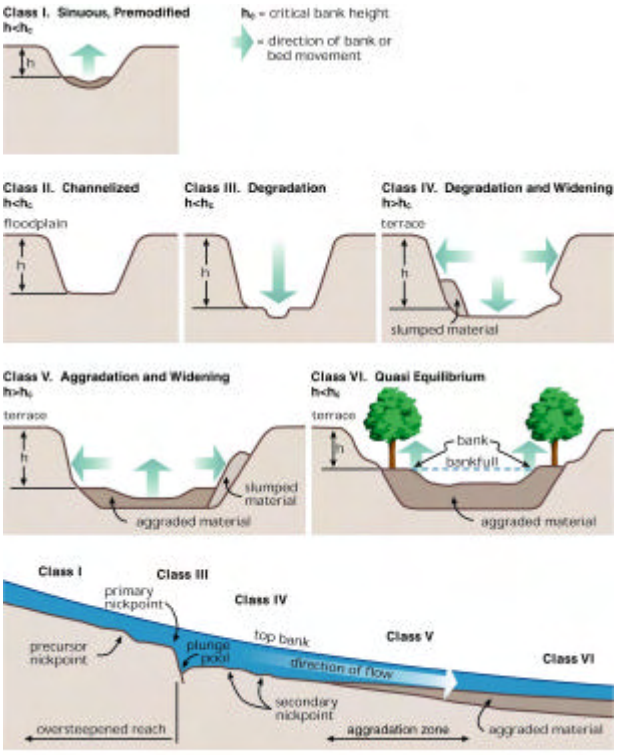

XI. Geomorphology

XI. Geomorphology

TABLE OF CONTENTS

	Page
CHARCTERIZATION OF SEDIMENTATION PATTERNS AT A MUSSEL BED ON THE OHIO RIVER NEAR OLMSTED, ILLINOIS: David S. Mueller, USGS, Louisville, KY	XI – 1
THE MANAGEMENT OF SEDIMENT ON THE J. BENNETT JOHNSTON WATERWAY: C. Fred Pinkard, Jr. and Jerry L. Stewart, USACE, Vicksburg, MS	XI – 9
GEOMORPHIC ANALYSIS TECHNIQUES APPLIED TO PACIFIC NORTHWEST RIVERS: Timothy J. Randle and Jennifer A. Bountry, USBR, Denver, CO	XI – 17
EFFECTIVENESS OF CHANNEL IMPROVEMENT WORK ON THE MISSISSIPPI RIVER: C. Fred Pinkard, Jr., James V. Ross, and Robert H. Fitzgerald, USACE, Vicksburg, MS	XI – 25
UPSTREAM IMPACTS AFTER THE 1976 FAILURE OF TETON DAM: Jennifer Bountry and Timothy Randle, USBR, Denver, CO	XI – 33
SPATIAL VARIATION OF INCISION AND DEPOSITION WITHIN A RAPIDLY INCISED UPLAND WATERSHED, CENTRAL NEVADA: Dru Germanoski and Carolyn Ryder, Lafayette College, Easton, PA; and Jerry Miller, Western Carolina University, Cullowhee, NC	XI –41
EPISODIC MOUNTAIN EROSION INFERRED FROM SEDIMENT YIELDS OVER DECADES AND MILLENIA: James W. Kirchner, University of California, Berkeley; Robert C. Finkel, Lawrence Livermore National Laboratory, Livermore, CA; Clifford S. Riebe, University of California, Berkeley; Darryl E. Granger, Purdue University, West Lafayette, IN; James L. Clayton and John G. King, USDA-FS, Boise, ID; and Walter F. Megahan, National Council for Air and Stream Improvement, Sequim, WA	XI – 49
GRAVEL ENTRAINMENT AND SCOUR IN STEEP HEADWATER CHANNELS: Alan F. Barta, USDA-FS, Boise, ID	XI – 50
A DYNAMIC PROCESS FOR ASSESSING THE IMPACTS OF GRAVEL MINING AND LAND USE CHANGES ON THE SAN LUIS REY RIVER, CA: Vernon L. Finney, USDA-NRCS, Davis, CA	XI – 58
HEADCUT ANALYSIS DUE TO SAN GORGONIO RIVER LEFT OVERBANK SAND AND GRAVEL MINING: H. M. Hu, WEST Consultants, Inc., CA; Craig Phillips, Robertson's Ready Mix, CA; and Brian J. Doeing, WEST Consultants, Inc., CA	XI – 66
ASSESSING THE GEOMORPHIC EFFECTS OF INSTREAM GRAVEL MINING ON THE MAD RIVER, HUMBOLDT COUNTY, CALIFORNIA: Kevin Knuuti, USACE, San Francisco, CA	XI – 73
HISTORIC PATTERNS OF SEDIMENTATION IN THE ATCHAFALAYA BASIN FLOODWAY SYSTEM: Lamar F. Hale, LSU Agricultural Center, Baton Rouge, LA; Nancy Powell, USACE, New Orleans, LA; Michael G. Waldon, USDI, Boynton Beach, FL; and C. Fredrick Bryan, USGS, Reston, VA	XI – 81
STREAM MORPHOLOGICAL RESPONSE TO CLIMATE AND LAND USE IN THE MINNESOTA RIVER BASIN: Joe Magner, Minnesota Pollution Control Agency, St. Paul, MN; and Lyle Steffen, USDA-NRCS, Lincoln, NE	XI – 89

THE TIRTAHARAPAN® SYSTEM: DISSOLVED, SUSPENDED, AND BED LOAD SEDIMENT LOGGER: Drs. Dirk de Hoop, Hope Hydrology, Geesteren, The Netherlands XI – 96

STATISTICAL MODELING OF LANDSLIDE HAZARD USING GIS: Peter V. Gorsevski, U. of Idaho; Randy B. Foltz, USDA-FS, Moscow, ID; Paul E. Gessler, U. of Idaho; and Terrance W. Cundy, Potlatch Corp., Lewiston, ID XI – 103

ENTRAINMENT REVISITED: HIGH-FREQUENCY MEASUREMENTS OF FORCES ON SEDIMENT PARTICLES IN TURBULENT FLOW: Jonathan M. Nelson, USGS, Lakewood, CO; Mark W. Schmeeckle, Florida St. U., Tallahassee, FL; and Ronald L. Shreve, U. of Washington, Seattle, WA XI – 110

HYDRAULIC PERFORMANCE TESTING OF STIFF GRASS HEDGES: Darrel Temple, USDA-ARS, PSWC, Stillwater, OK; and Seth Dabney, USDA-ARS, NSL, Oxford, MS XI – 118

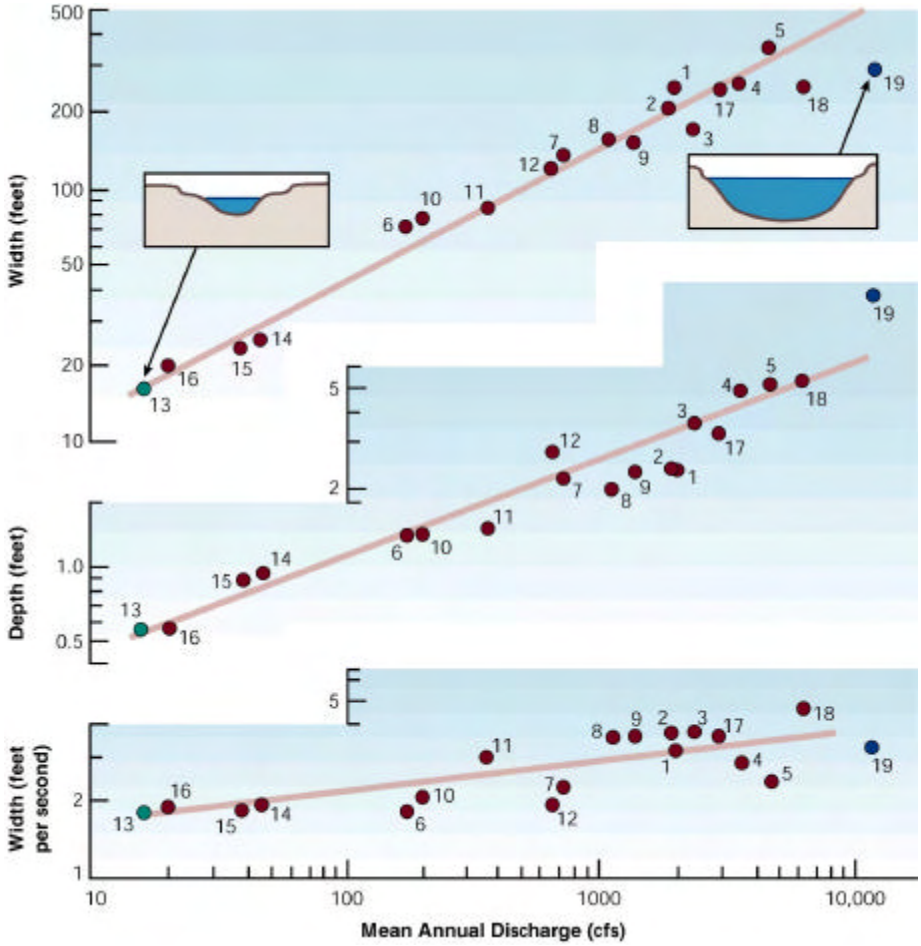

CHARACTERIZATION OF SEDIMENTATION PATTERNS AT A MUSSEL BED ON THE OHIO RIVER NEAR OLMSTED, ILLINOIS

By David S. Mueller, Hydrologist, U.S. Geological Survey, Louisville, Kentucky

Abstract: Ohio River Locks and Dams 52 and 53 are being replaced with a single facility near Olmsted, Ill. The construction and operation of this facility could adversely affect a mussel bed containing the endangered orange-footed pearly mussel (Plethobasus cooperianus) that is approximately 3 km downstream from the new facility. Sedimentation patterns and conditions at the mussel bed are being characterized through an analysis of detailed channel surveys, bed-material samples, water-velocity distributions, and bed-elevation data. The analysis of these data shows that the mussel bed has different sedimentation characteristics than the main channel in the same reach. Hourly measurements of bed elevation at discrete locations on the mussel bed showed a much greater variation than was originally believed suitable for mussel habitat. The variation in bed elevation on the mussel bed appears to be caused by sand transported as small bedforms over the mussel bed, which is primarily composed of gravel. Continued research is underway to better characterize when and where these bedforms occur. This research will help biologists develop a better understanding of the effect of sedimentation conditions on mussel habitat and mussel viability.

INTRODUCTION

Background: The U.S. Army Corps of Engineers (COE), Louisville District is replacing Ohio River Locks and Dams 52 and 53 with a single facility near Olmsted, Ill. The endangered orange-footed pearly mussel (Plethobasus cooperianus) is found in two mussel beds near the location of the new locks and dam. These mussel beds could be adversely affected by changes in sedimentation patterns that could result from the construction and operation of the new locks and dam. Studies to characterize the pre-project conditions at the mussel bed, to monitor the streambed elevation at the mussel bed, and to sample the mussel population were initiated to provide data that could be used to develop plans and strategies to protect the orange-footed pearly mussels.

The endangered orange-footed pearly mussel is an Interior Basin species that reaches an average adult size of approximately 6 cm. This large river species is historically known to occur in the Ohio, Cumberland, and Tennessee River basins. The preferred habitat for the Plethobasus cooperianus are shoal areas (depths of 3 to 10 m) of medium to large rivers with continuous flows over silt-free substrates of sand, gravel, and cobbles (U.S. Army Corps of Engineers, 1993). The Ohio, Cumberland, and Tennessee River basins contain the only three known population areas of this endangered species. The only known reproducing population is in the Tennessee River (U.S. Fish and Wildlife Service, 1993). The health of the mussel bed downstream from the Olmsted Locks and Dam was good; however, the health of the upstream bed was questionable (U.S. Fish and Wildlife Service, 1993). The viability of the species in the bed downstream from the Olmsted Locks and Dam is important because of the few known populations.

Sediment deposition and erosion patterns prior to construction of the Olmsted Locks and Dam could change during or after construction because of: (1) bed material lost during dredging for cofferdam construction, (2) creation of a temporary navigational channel, (3) changes in the water-current direction and magnitude, (4) changes in river-traffic location and volume, (5) river-side development to support construction, and (6) operation of the new locks and dam. Changes to the natural sedimentation characteristics of this river reach could affect the orange-footed pearly mussel by increasing suspended sediments, depositing fine sediments on the mussel bed, or eroding the bed. Ellis (1936) reported that some adult mussel species were smothered by as little as 0.6 cm of sediment deposition. A more recent study, however, indicated that about 50 percent of a large mussel species were able to emerge through as much as 25 cm of silt or sand (U.S. Fish and Wildlife, 1993). Additionally, if the deposited sediment is not stable the mussels may be swept off their bed. It is believed that juvenile mussels of all species would likely be smothered by more than 3 cm of sediment. U.S. Fish and Wildlife (1993) suggested that 3 cm of sediment deposition on the mussel bed for 24 hours would cause a loss of habitat. At present (2000), there is no field-verified research on the orange-footed pearly mussel to accurately specify what magnitude of change in habitat will be critical to the population.

Purpose and Scope: The sedimentation patterns and conditions at a mussel bed located in the Ohio River near Olmsted, Ill. are being characterized through an analysis of detailed channel surveys, bed-material samples, velocity distributions, and bed-elevation data. Bed-elevation data at discrete locations were collected hourly from August 1993 to June 1997. Bed-elevation data were collected more frequently at three different discharges to evaluate the presence and movement of bedforms. Detailed channel surveys and velocity distributions were collected at least twice a year from 1993 through 1998. This paper summarizes the efforts, to date, of the U.S. Geological Survey (USGS) and the COE to characterize the preconstruction sedimentation patterns at the downstream mussel bed.

DESCRIPTION OF STUDY AREA

The Ohio River flows 1579 km from the confluence of the Allegheny and Monogahela Rivers at Pittsburgh, Penn. to the Mississippi River near Cairo, Ill. (Bower and Jackson, 1981). The entire river, except for the lower 31 km (from Lock and Dam 53 to the Mississippi River), has been altered by construction and operation of locks and dams to provide a stable navigational channel. The new Olmsted Locks and Dam are located approximately 3 km downstream from Lock and Dam 53, and 27 km upstream from the confluence with the Mississippi River. The focus of this report is a mussel bed located about 3 km downstream from the new locks and dam on the right descending bank, with its center near the inflection of two opposing bends in the river (figure 1). These bends have a very large radius (small curvature). The upstream end of the mussel bed begins along the outside, downstream edge of the upstream bend and extends through the crossing and terminates on the inside of the downstream bend. The navigation channel through this reach is primarily along the left descending portion of the river.

ANALYSIS OF FIELD DATA

Bed-Material Data: The COE collected bed-material samples as part of the detailed-data collection effort and during annual mussel surveys. The bed material data from the mussel

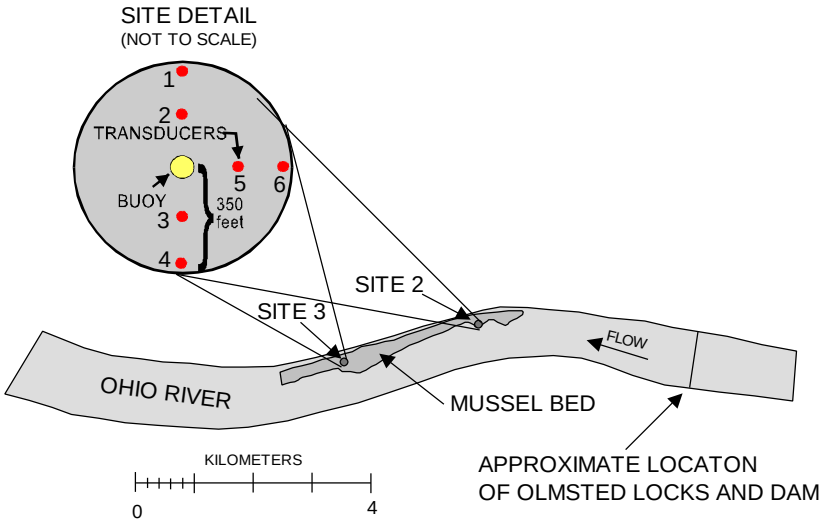

Figure 1. Location of the mussel bed.

surveys provided only 4 gradations for the 1993 and 1997 surveys and only a qualitative assessment of the size class (cobble/gravel, sand) for 1994-96. Locations of the samples were indeterminate from the data received. Geospatially referenced bed material samples were collected in 1992-94 during the annual detailed hydrographic surveys. A full sieve analysis was completed on these samples. Only the 1993 and 1994 data contained samples collected on the mussel bed. Figure 2 shows the distribution of the median bed-material size. It is clear from the graph that this reach of river is primarily a sand-bed channel with a gravel deposit extending out from the Illinois bankline. On the mussel bed, the D_{50} (grain size for which 50 percent of the material by weight is finer) is between 10 and 20 mm, and the D_{95} is between 20 and 40 mm.

Hourly Bed-Elevation Data: The USGS designed and installed a streambed monitoring system based on a multi-transducer acoustic ranging system interfaced with satellite telemetry. The transducers have an 8-degree beamwidth and operate at a frequency of 200 kilohertz. The manufacturer specifications state that the system has a resolution of 0.01 m with a range of 0.3 to 30 m. This acoustic system measures the depth to the nearest object that reflects sufficient acoustic energy to exceed a predetermined energy threshold. Fish or submerged debris could easily reflect acoustic energy exceeding the threshold, causing a false bottom measurement. To minimize the potential for false measurements, a custom measurement scheme was implemented. A measurement is

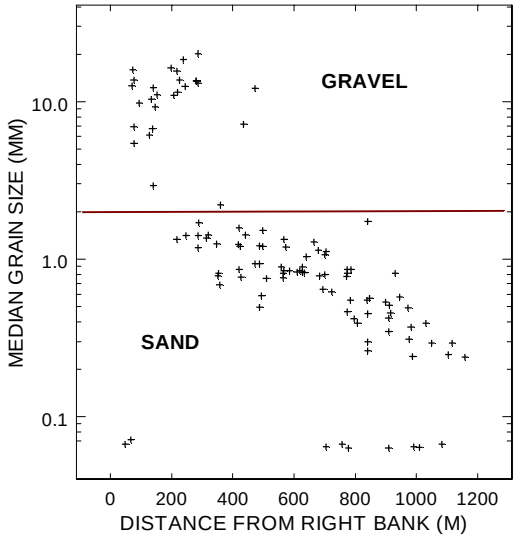

Figure 2. Median bed-material size and location for samples collected along cross sections through the mussel bed.

made every 2 minutes and the value temporarily stored. Each hour, the measurements are ranked and the minimum, median, and maximum values reported. Thus, the data from this system consists of hourly minimum, median, and maximum values for each transducer.

The original installation for real-time monitoring consisted of four sites with six transducers. The six transducers were oriented in a "T" configuration with the base of the "T" point upstream. A buoy is anchored at the intersection of the three legs of the "T" and houses all of the electronic components of the monitoring system, including the acoustic ranging system, data logger, and telemetry equipment. The transducers are deployed on a monitoring stand that consists of an H-pile driven vertically into the streambed with a 1-m horizontal I-beam extending upstream. The transducers are located at the end of the horizontal I-beam so that they are not influenced by local scour that may occur around the H-pile (Griffin, 1997). High flows from December 1993 to April 1994 severely damaged the system; subsequently only sites 2 and 3 were reinstalled.

Missing and erroneous data significantly disrupt the time series of streambed elevation measurements. Most of the transducers collected data for 70 to 80 percent of the time they were deployed. Approximately 9 percent of the missing data are accounted for by the 1994 high water, when the system was damaged. Other missing data are the result of equipment failure or interference of the measurement by debris. The distribution of the median streambed elevations show that a significant portion of these data contain erroneous measurements (figure 3) that need to be removed prior to analysis of the data.

The filter was developed to use only data collected prior to the measurement under consideration. This restriction will allow the filter to be used to screen hourly data in real-time and provide accurate real-time data that are needed by the COE to continuously monitor sedimentation conditions during dam construction. Visual inspection of the data indicates that the local trend and variation in streambed elevation change with time and (or) flow conditions. A moving window with variable size based on the standard deviation of selected measurements was used to filter the median streambed-elevation data. The size of the window was defined as eight times the standard deviation computed from the last 24 valid measurements and was centered about the last valid measurement. Data inside the window were retained as valid data and data outside the window were discarded. The most significant problem encountered in establishing the parameters for the filter were long periods of missing data. The size of the window was linearly increased from the base value of eight times the standard deviation to account for unmeasured

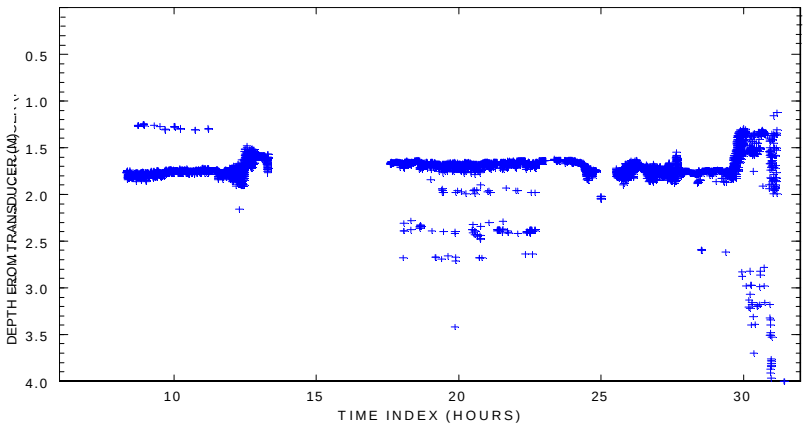

Figure 3. Sample plot of bed elevation data from a single transducer.

trends in the data. This value was increased by 0.266 for each day of missing record up to 60 days and then by 0.133 for each day of missing record beyond 60 days until a valid measurement was located. The moving standard deviation successfully eliminated data that were not consistent with the trend but maintained the high frequency variation in streambed elevation. A rapid change in the streambed elevation coupled with some missing data at site 2 (transducers 3 and 4) caused some data to be incorrectly eliminated. These data were manually retained in the data set for analysis.

The hourly bed-elevation data indicated that the mussel bed was not static. The hourly bed-elevation data indicated that the variation in elevation of the mussel bed had an inner quartile range (IQR) of less than 15 cm with 7 cm being common. Monitoring locations about 15 to 30 m off the mussel bed towards the main channel had a greater variation in elevation, with an IQR of around 50 cm. Therefore, the mussel bed is less dynamic than the main channel of the river, but the variation in bed elevation is significantly greater than what was theorized to be acceptable for mussel habitat.

Both the duration and the depth of sediment deposition are important to the viability of mussels. The median bed-elevation data were analyzed to determine the maximum duration of deposition, which was defined as the longest consecutive period that the bed remained a specified distance above a specified reference. The long-term median of all the data for each transducer was used as the reference datum. It was assumed that the magnitude of deposition remained constant during periods of missing data. Figure 4 shows a clear separation between the transducer located on the mussel bed and the two transducers at the edge of the main channel. Although the mussel bed displays different sedimentation characteristics than does the main channel, it cannot be precisely determined from these data at what threshold the mussel population will begin to be adversely affected.

Hydraulic Data: Water-surface slope, mean daily discharge, mean daily stage, and mean velocity are available for the study area during the period of data collection. Water-surface slope is computed from the difference in stage readings between the tailwater of Lock and Dam 53 and the COE gaging station at Cairo, Ill., divided by 27.2 km. The stage reported is interpolated from the stage readings at the tailwater of Lock and Dam 53 and the station at Cairo. The mean daily discharge is computed from a model operated by the COE, Louisville District. The mean velocity is determined by dividing the mean daily discharge by the cross-sectional area at a cross section that is upstream of the mussel bed near the

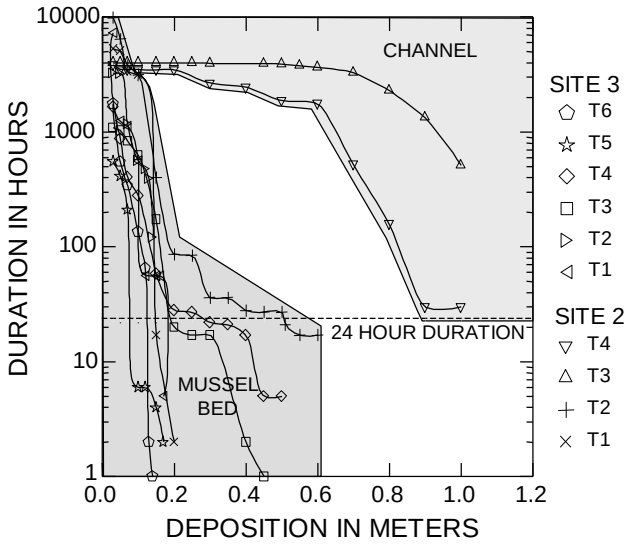

Figure 4. Plot of the magnitude and duration of sediment deposition.

axis of the new dam. The cross-sectional area of this cross section is affected by the cofferdam at the construction site. Thus, the available hydraulic variables were average values over a long reach and do not adequately reflect the hydraulics on the mussel bed. The relations between bed elevation and these average hydraulic properties were too inconsistent to be of use in characterizing the behavior of the sediment on the mussel bed.

Special Bed-Elevation Data: The filtered median streambed-elevation data showed scatter well beyond what the mussels were believed to be able to tolerate. However, no visual or statistically significant pattern was observed in the data that could be used to explain the variability in the data. Three special streambed-elevation data sets with the bed-elevation data measured every 60 seconds or less were collected to investigate the accuracy of the system and identify any causes for the data variability. These data sets were collected at three discharges (2,750; 10,400; and 13,200 m^3/s). These data clearly showed bedforms moving across the mussel bed at some monitoring locations (figures 5 and 6). The bedforms ranged from 0.10 to 0.40 m in height and had a period that ranged from less than 1 hour to about 6 hours, depending on location and flow conditions. As shown in figures 5 and 6, the hourly bed-elevation data were not adequate to characterize the bedforms with short periods (less than 4 hours).

Detailed water-velocity data collected with an acoustic Doppler current profiler, bed-material size and distribution data, and theoretical incipient motion and bedform prediction diagrams were used to evaluate the bed forms. The bed material comprising the mussel bed has been shown to be gravel with a median grain size of between 10 and 20 mm. A relation presented by Miller and others (1977) was used to compute the Shield's parameter and to evaluate what size bed material could be transported by the three discharges. This analysis indicated that it is unlikely that an appreciable quantity of material with a grain size greater than 5 cm was being transported. Bedform prediction curves from Hjulstrom (1935) and Marcelo Garcia (University

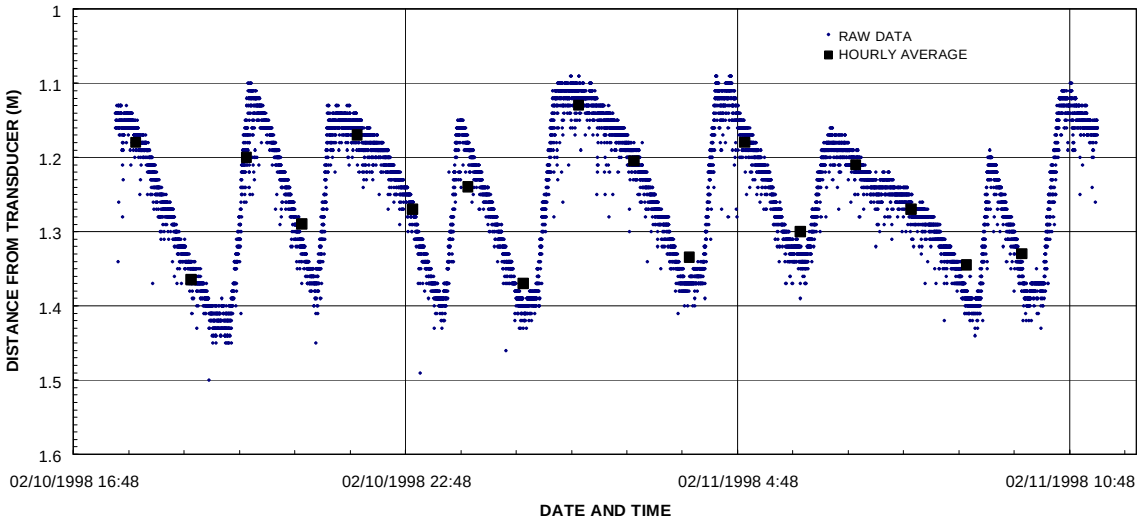

Figure 5. Example of bedforms at transducer 4 at site 3.

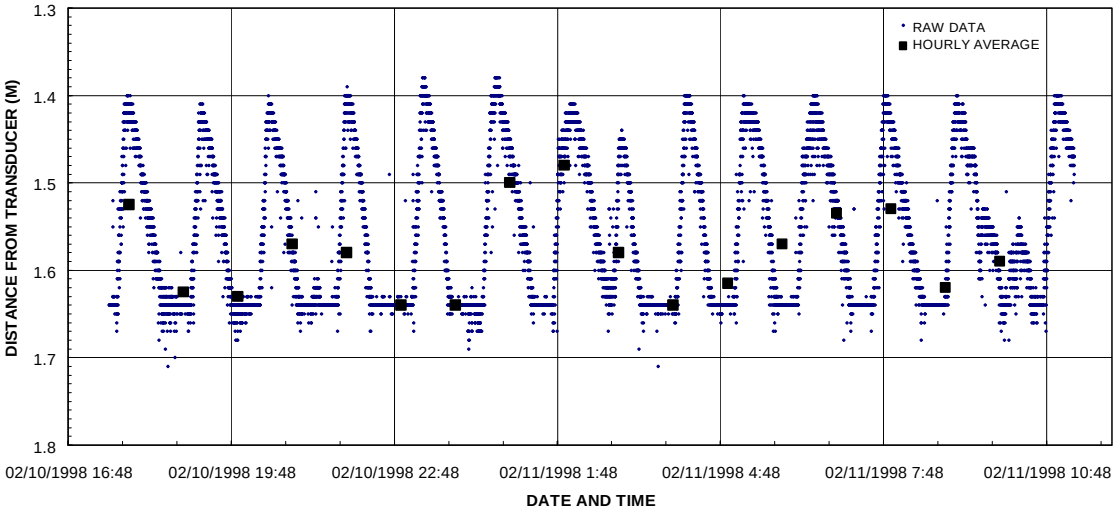

Figure 6. Example of bedforms at transducer 5 at site 3.

of Illinois, written comm., 1997) also verified that sand would likely be transported as small dunes and that gravel would not be transported. Analysis of the velocity patterns from data collected with an acoustic Doppler current profiler showed that as flow increases the maximum velocity shifts towards the mussel bed. Therefore, when velocities exceed 1 m/s, which could occur during about six months a year, sand may be swept onto and transported over the mussel bed as bedforms. This sand appears to be swept off the mussel bed as the flow recedes.

SUMMARY OF SEDIMENTATION CHARACTERISTICS

From the field data collected and analyzed, it is clear that the sedimentation characteristics on the mussel bed downstream from Olmsted locks and dam on the Ohio River are different from those in the main channel in the same reach. The bed material of the mussel bed consists primarily of gravel on a shelf extending out from the right descending bank, while the main channel is comprised primarily of sand. The bed elevation in the main channel is much more variable than that on the mussel bed. At flows up to 13,200 m^3/s, water velocities on the mussel bed do not appear competent to move the bed material comprising the bed. The change in bed elevation on the mussel bed appears to be caused by sand transported from the main channel and across the gravel mussel bed as small dunes. This transport occurs at some locations on the mussel bed when velocities reach about 1 m/s. These bed elevation changes are much greater and more dynamic than believed suitable for mussel habitat, based on previous laboratory research. Annual assessments of the mussel bed by biologists suggest that the mussel bed is viable and may be reproducing the endangered orange-footed pearly mussel. Therefore, the sedimentation characteristics of the mussel bed represent a different habitat characteristic than was anticipated for laboratory-based research, but appear to be suitable habitat for this mussel species.

FUTURE RESEARCH

Continued research is underway to better characterize when and where thebedforms occur on the mussel bed. A new acoustic ranging systemis scheduled to be installed in the fall of 2000. This new system will allow streambed elevation measurements to be collected on a user-selectable interval. Currently, readings every 2 minutes are planned. In addition, two transducers will be pointed upward and the elevation of the water surface measured to allow a water-surface slope over the mussel bed to be determined. Bed material and bed load sampling on the mussel bed at several discharges will be used to help define the size and source of the bed material being transported as small dunes. The installation of an in situ acoustic Doppler current profiler is also being investigated. Development of a two-dimensional hydrodynamic model of the study reach is planned for 2001 to allow a more detailed evaluation of the velocity vectors and their influence on sedimentation patterns.

REFERENCES

Bower, D.E., and Jackson, W.H., 1981, Drainage Areas of Streams at Selected Locations in Kentucky. U.S. Geological Survey Open-File Report 81-61, 118 p.

Ellis, M.M., 1936, Erosion Silt as a Factor in Aquatic Environments. Ecology, Vol. 17, pp. 24-42.

Griffin, M.S., 1997, Use of an Acoustic Ranging System to Monitor Sediment Deposition and Erosion for the Protection of an Endangered Mussel Below the Olmsted Locks and Dam, Illinois. U.S. Geological Survey Fact Sheet FS-127-97, 4 p.

Hjulstrom, F., 1935, Studies of the Morphological Activity of Rivers as Illustrated by the River Fyris. Bulletin of the Geological Institute, University of Uppsala, Vol. 25, pp. 221-527.

Miller, M.C., McCave, I.N., and Komar, P.D., 1977, Threshold of Sediment Motion Under Unidirectional Currents. Sedimentology, Vol. 24, No. 4, pp. 507-525.

U.S. Army Corps of Engineers, 1993, Final Environmental Impact Statement for the Replacement of Locks and Dams 52 and 53 (Olmsted Locks and Dam) Lower Ohio River, IL-KY: Louisville, Ky., U.S. Army Corps of Engineers, Louisville District, Final Supplement 1, March, 368 p.

U.S. Fish and Wildlife Service, 1993, Supplemental Biological Opinion for the Proposed Olmsted Locks and Dam, Ballard County, Kentucky: Cookeville, Tenn., 15 p.

THE MANAGEMENT OF SEDIMENT ON THE J. BENNETT JOHNSTON WATERWAY

C. Fred Pinkard, Jr., Hydraulic Engineer, USACE, Vicksburg District, Vicksburg, MS;
Jerry L. Stewart, Civil Engineer, USACE, Vicksburg District, Vicksburg, MS

Abstract: During the last three decades of the 20th century, the U.S. Army Corps of Engineers developed the lower 280 miles of the Red River in Louisiana for commercial navigation. This development included the planning, design, and construction of five locks and dams in association with an intensive channel improvement program that included channel realignments, bank stabilization works, and channel contraction. With the completion of Lock and Dam No. 4 (Russell B. Long L&D) and No. 5 (Joe D. Waggonner, Jr. L&D), the waterway was opened to commercial navigation during late December 1994.

The Red River is a heavily sediment laden alluvial river with one of the highest sediment concentrations of all major navigable rivers within the United States. Therefore, the design engineers were tasked with the responsibility of developing a system that effectively managed the incoming sediment load. This required a delicate balance of keeping velocities high enough to transport the sediment but low enough not to adversely impact navigation. The channel improvement work has reduced potential sediment problems within the navigation channel. Revetments have limited the availability of sediment that historically entered the river through bank caving. Kicker dikes on the downstream end of revetments have resulted in maintenance free crossings and dikes constructed within troublesome depositional reaches have provided the contraction required to insure adequate depths for navigation. Some maintenance dredging has been required at a few isolated locations within the navigation pools. At these trouble sites, the Vicksburg District has and continues to raise revetments and add dikes to eliminate costly dredging. Since being opened, some dredging has been required in the approaches to the locks and dams. Modifications to Lock and Dam No. 1 (Lindy C. Boggs L&D) and No. 2 (John H. Overton L&D) have greatly improved the sedimentation conditions at these structures. With the lessons learned at these two locks and dams, sediment control features were incorporated into the design of Lock and Dam No. 3, Russell B. Long Lock and Dam, and Joe D. Waggonner, Jr. Lock and Dam thus reducing potential sedimentation problems at these structures.

The development of effective sediment management features is crucial in minimizing maintenance for commercial navigation projects. This paper provides an analysis of the effectiveness of the sediment management features utilized on the Red River in providing an efficient, low maintenance navigation system.

PROJECT HISTORY

The Red River Waterway Project was authorized in 1968 with the primary purpose of providing a 9-foot deep by 200-foot wide navigation channel from the Mississippi River to Shreveport, Louisiana. A waterway project location map is provided as Figure 1. Lock and Dam No. 1 (Lindy C. Boggs L&D) located near Marksville, Louisiana was put into operation during the fall of 1984. Lock and Dam No. 2 (John H. Overton L&D), located downstream of Alexandria, Louisiana, became operational during the fall of 1987. Lock and Dam No. 3 located at Colfax,

Louisiana has been in operation since December of 1991. Lock and Dam No. 4 (Russell B. Long L&D) located near Coushatta, Louisiana and Lock and Dam No. 5 (Joe D. Waggonner, Jr. L&D) located downstream of Shreveport, Louisiana were constructed concurrently and were put into operation during December 1994. The channel realignment and bank stabilization program is essentially complete with only some raising of a few revetments and the construction of some channel control dikes at isolated trouble locations remaining. Since the waterway was opened in December 1994, a navigable channel has been maintained as far upstream as the Caddo-Bossier Port (Post Project River Mile 211.5). This port is located approximately 16 miles downstream of downtown Shreveport, Louisiana. During 2000, the Red River Waterway was renamed and dedicated as the J. Bennett Johnston Waterway in honor of the long time U.S. Senator from Louisiana who was instrumental in securing funding for project construction. Currently, the waterway project is approximately 90 percent complete. Remaining work primarily includes construction of some additional channel control works at isolated locations, the construction of visitor centers at Shreveport and Natchitoches, Louisiana, the construction of additional recreational facilities, and finalizing project mitigation.

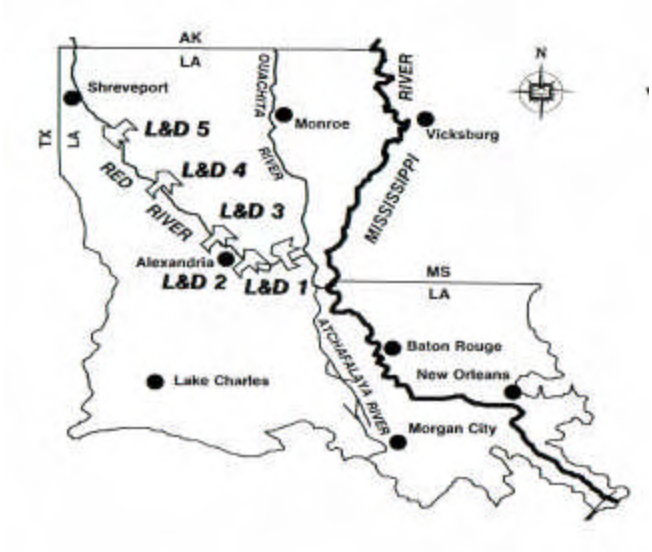

Figure 1. J. Bennett Johnston Waterway Project Map

GENERAL SEDIMENT CONDITIONS

The Red River is a heavily sediment laden stream with an average annual suspended sediment load of approximately 32 million tons at Shreveport, Louisiana and approximately 37 million tons at Alexandria, Louisiana. The suspended sediment load per square mile of drainage area on the Red River is one of the highest of all navigable rivers within the United States. In fact, at Alexandria, Louisiana the annual suspended sediment load per square mile of drainage area is almost twice that of the Mississippi River at Tarbert Landing, Mississippi. The suspended sediment load on the Red River basically consists of 25% fine sand and 75% silt. Previous studies have indicated that the bed load on the lower Red River is less than 10% of the total sediment load. The bed is primarily composed of fine to medium sand. The bed material grain size distribution at Shreveport (post project river mile 228.4) consists of approximately 5% coarse sand, 52% medium sand, 39% fine sand, and 4% very fine sand. Like most natural rivers, the bed material grain size becomes finer downstream. At Alexandria (post project river mile

88.6), the grain size distribution includes approximately 2% coarse sand, 18% medium sand, 65% fine sand, and 15% very fine sand. The Red River is a high-energy system characterized by high channel velocities. During highwater, mean channel velocities often approach 7 feet per second with maximum velocities exceeding 10 feet per second. The banks of the lower Red River generally consist of fine sand and silt. The combination of high channel velocities and easily erodible banks results in very active bank caving. Lateral migration of several hundred feet of bankline during a single highwater event is not uncommon. The primary source of sediment transported on the Red River is the erosion of unrevetted banks, especially those upstream of Shreveport. The sediment contribution from tributaries is minimal.

CHANNEL IMPROVEMENT FEATURES

The Red River Waterway Project included the construction and maintenance of a stabilized, rectified channel alignment that consists of a series of navigable bendways. Providing such a channel required stabilization of the concave bank in bends, selective channel control from the convex bank, and channel control in the crossings. Due to the sediment conditions on the Red River, sedimentation was a critical factor in the design of these waterway channel improvement features. The project design utilized to the maximum extent possible, the natural erosive action and the large sediment transport capacity of the high-energy river in developing the navigation channel. At the same time, the large sediment load provided a challenge to the design engineers in providing and maintaining a low maintenance channel.

Channel Realignments. Many bends within the waterway reach of the Red River were too tight to be navigated by the Red River Waterway channel design tow. Therefore, these bends were realigned via a channel cutoff across the neck of the old bendways. For these channel realignments, the pilot channel concept was used. This construction procedure includes excavating a pilot channel of smaller section than the desired channel section and allowing the natural erosive action of the river to develop the pilot channel to its ultimate size. This method of channel realignment reduced the project cost by significantly reducing required excavation.

Within the waterway reach of the Red River, 36 channel realignments were constructed that shortened the river by almost 50 miles. The pilot channels excavated for these realignments ranged from 80 feet to 200 feet wide. The excavated width was based on the probability of the pilot channel developing. The major factors that impact development are the slope advantage of realigning a long bendway with a shorter channel and the erodibility of the soils through which the pilot channels are excavated. The pilot channels with the greatest probability of development were those with the greatest slope advantage and those that traverse the more easily erodible soils. Of the 36 channel realignments, 33 adequately developed within relatively short time periods. Once the pilot channels were opened, development typically occurred quickly, usually within no more than a couple of highwater events. The 3 pilot channels that had trouble developing were excavated through backwater deposits of stiff clay. During highwater, the slowly developing pilot channels constricted the channel and significantly increased local channel velocities. These increased channel velocities resulted in the pilot channels being difficult to navigate. Therefore, all 3 pilot channels were widened by mechanical dredge.

Project criteria included the preservation of the old bendways that were at least a mile long for recreational and environmental purposes. Of the 36 realignments, 24 were of sufficient length to be preserved. The construction of these 24 realignments resulted in the creation of approximately 5,900 acres of oxbow bendways. The bendways were preserved by constructing a non-overtopping closure dam across their upstream ends. This closure dam prevents the sediment laden river flow from entering the bendway from upstream and also helps facilitate the development of the pilot channel by forcing all of the river flow through it. The downstream end of the oxbow bendways are left open to the river to allow fish migration and recreational access and to allow an interchange of water with the river. However, undesirable sediment deposition that threatens to limit or at some locations eliminate river access occurs in the downstream end of the oxbow bendways. The severity of this deposition varies and is dependent upon several factors including the alignment of the old bendway with the realigned channel and the location of the old bendway within the pool. During 1996, the Vicksburg District completed an evaluation of the oxbow bendways. This evaluation recommended the dredging of a small low water channel through the deposited sediment in the downstream end of selected oxbows to maintain continuous access to the old bendway from the river. At most of these bendways, a small access channel is naturally maintained without any dredging. The Vicksburg District monitors 13 of the oxbow bendways. During the past 3 years, some dredging has been required. In both 1998 and 1999, 6 oxbow bendways were dredged while during 2000, 4 were dredged. At each of these bendways, a 20-foot wide channel with a bottom elevation of 5 feet below the permanent minimum pool level is dredged. Dredging is not required throughout the oxbow bendway but is limited to the very downstream end. In fact, the length of these access channels varies, but typically ranges from 500 feet to 2000 feet.

Bank Stabilization. The types of revetment used on the Red River Waterway were trenchfill, stonefill, and timber pile revetments. At those sites at which the desired bankline alignment was located landward of the existing bankline, trenchfill revetment was used. This type revetment includes the excavation of a trench along the desired channel alignment and filling the trench with stone. As the bankline continues to erode, the trench is undermined and the stone in the trench launches down the face of the bank, thus stabilizing the bank and maintaining the desired channel alignment. Trenchfill revetments have proved very effective on high-energy rivers like the Red River that primarily traverse easily erodible soils. At those sites at which the desired bankline alignment was located riverward of the existing bankline, stonefill revetment, timber pile revetment, or a combination of the two were used. These type revetments protect the bank by inducing sediment deposition behind the revetment and thus build the bankline out toward the revetment. In the shallow sections along the desired alignment, stonefill revetment is used. In the deeper river sections, timber pile revetment, with some stone placed around the toe of the piling is used. Once sediment deposition has occurred behind these revetments, the revetments are raised or "capped-out" by placing additional stone on top of the deposited sediment along the revetment alignment. This construction procedure results in a less costly revetment than initially constructing the revetment to its ultimate height.

Dikes. Channel crossings are natural sediment deposition locations. Project design studies determined that to maintain navigation depths, channel widths must be limited to 450 feet in crossings in the upper reaches of the pools where depth is critical and 600 feet throughout the remainder of each pool. To provide this limiting channel crossing width, kicker dikes are

provided on the downstream end of revetments. These dikes are an extension of the revetments and reduce sediment deposition in the crossings by contracting the channel and thus keeping velocities high enough to prevent excessive sediment deposition. Once raised to their ultimate height, kicker dikes on the Red River have proved very effective in maintaining an adequate navigation channel in the crossings.

In the very upper ends of the pools where channel depths are most critical, navigation depths are maintained by the construction of additional contraction structures (ACS). These structures are stone dikes that extend from the convex bank to contract the channel. The contracted channel creates a deeper channel due to bed scour. The ACS constructed on the Red River have been and continue to be very effective in maintaining a developed navigation channel within the upper most reach of each pool.

Figure 2. Crain Revetment Kicker Dike

Figure 3. Hog Lake ACS

Except for a few isolated locations, the channel throughout the Red River Waterway has adequately developed. In those isolated reaches, troublesome sediment deposition has occurred, resulting in some channel dredging. At these sites, the District continues to raise revetments and construct channel control dikes to limit sediment deposition. As these structures are completed, additional channel development has occurred. The Vicksburg District continues to monitor channel conditions and is committed to providing a low maintenance navigation channel throughout the waterway project reach. Table 1 includes the dredging quantities by pool from 1989 through 1999 except for 1992. Quantities from 1992 have been omitted because the dredging record for that year is incomplete. This data shows that the 9-mile reach from Lindy C. Boggs Lock and Dam to the mouth of the Black River (identified as Below L&D1) has required considerable dredging, averaging over 1,000,000 cubic yards per year. Stages within this reach are not controlled by any downstream structure but are dependent upon backwater from the Mississippi River. Therefore, this reach is subject to large variations in stages including extremely low stages. The channel within this reach has been greatly contracted in an effort to reduce sediment deposition. However, even with this channel contraction, dredging is required regularly. Within all the pools with the exception of Pool 5, some dredging has been required. No dredging has been required in Pool 5 because the navigation channel is only maintained as far upstream as the Caddo-Bossier Port. In Pools 1 through 4, varying amounts of dredging have been required with the most dredging occurring in the upper end of Pool 3. Within each pool,

the dredging is limited to a few isolated locations. Since the Red River is dynamic, problem sites occasionally develop as the hydraulics and geometry of the channel changes. As problems develop, the District designs and constructs applicable channel control features to reduce the deposition. For example, dredging was required in Pool 1 during the early 1990's but was limited to one location, the Vick–Barbin crossing. As a result, a kicker dike was constructed off the downstream end of the Vick Revetment and dredging was eliminated at this crossing. In Pool 3, substantial dredging has been required primarily in the upper end of the pool. As a result, the revetments were capped-out at Kadesh, Socot, and Campti and dikes were constructed at Powhatan and downstream of the Highway 6 Bridge at Grand Ecore. In Pool 4, sediment deposition hindered navigation at two locations (Eastpoint and Westdale) within the upper reach of the pool. As a result, channel control dikes were constructed at Eastpoint. At each of the locations discussed above, the additional channel control work has helped reduce the need for costly maintenance dredging.

Table 1. Historic Dredging In Red River Pools

	Dredging Quantities (cubic yards)					
Year	Below L&D 1	Pool 1	Pool 2	Pool 3	Pool 4	Pool 5
1999	591,782	37,306	47,240	271,122	21,363	0
1998	1,416,730	136,065	124,418	728,944	140,381	0
1997	414,594	20,573	0	231,762	0	0
1996	0	0	77,547	319,489	0	0
1995	426,283	0	0	1,126,915	258,980	0
1994	843,404	0	0	N/A	N/A	N/A
1993	1,323,493	0	0	N/A	N/A	N/A
1992	Data Record Not Complete					
1991	2,127,066	354,000	0	N/A	N/A	N/A
1990	1,791,417	460,053	0	N/A	N/A	N/A
1989	1,237,031	131,215	0	N/A	N/A	N/A

LOCKS AND DAMS

The physical layout of locks and dams can and often does result in eddies and slack water areas. These areas are natural sediment deposition zones. Therefore, great care must be taken on heavily sediment-laden rivers to design locks and dams that minimize sediment deposition while at the same time are safe for all waterway users. During the first highwater after Lock and Dam No. 1 (Lindy C. Boggs L&D) was opened during the fall of 1984, significant sediment deposition occurred at 4 primary locations. These problem areas were (1) in the upstream lock approach channel, (2) along the riverside lockwall, (3) in the downstream lock approach channel, and (4) against the downstream lock miter gates. During the design of this structure, model studies indicated that sediment deposition would occur in each of these areas but not to the extent that actually occurred. This sediment deposition resulted in damage to the lower miter gates. Repair of this damage closed the lock and dam and therefore, closed the river to navigation for approximately 3 months. Analyses indicated that areas of channel expansion and flow separation created sediment deposition inducing slack water and eddies at this lock and dam. Two-

dimensional numerical model studies were used to evaluate the problems and aid in the determination of appropriate solutions. The results of these studies indicated that structural measures were required to either reduce the amount of sediment deposition or at least relocate the deposition to more manageable areas of the channel. These measures included constructing dikes in the upstream approach channel, raising the wall that separates the downstream lock approach channel and the dam outlet channel, and laying back the right descending bank downstream of the dam. The dikes were constructed from the right descending bank in the upstream approach channel to contract the channel with the hopes of limiting sediment deposition there. The I-wall was raised to prevent sediment-laden flow from overtopping the wall during higher water, thus moving the troublesome sediment deposition away from the lower miter gates. The bank downstream of the dam was realigned to create more desirable flow patterns in the dam outlet channel. As Table 2 shows, even with these modifications, dredging is still required at Lindy C. Boggs Lock and Dam. However, the dredging is less than that required before these measures were incorporated and is now limited to more manageable areas. Since these features were incorporated in the mid-1980', the lock has not been closed due to sediment deposition problems. The District continues to evaluate structural measures to reduce sediment deposition at this structure.

Table 2. Historic Dredging At Red River Locks and Dams

	Dredging Quantities (cubic yards)				
Year	Boggs L&D	Overton L&D	L&D No. 3	Long L&D	Waggonner L&D
1999	664,384	203,637	32,932	58,930	21,956
1998	812,367	195,587	81,114	49,937	18,040
1997	390,068	238,389	113,111	73,134	30,033
1996	180,275	45,794	33,128	23,396	0
1995	640,342	245,803	129,246	41,923	32,540
1994	685,761	223,275	65,733	N/A	N/A
1993	1,060,385	590,500	279,764	N/A	N/A
1992	Data Record Not Complete				
1991	809,001	114,180	N/A	N/A	N/A
1990	1,482,097	464,785	N/A	N/A	N/A
1989	966,297	266,041	N/A	N/A	N/A
Average	769,098	258,799	105,004	49,464	20,514

As a result of the sediment deposition problems experienced at Lindy C. Boggs Lock and Dam, the District anticipated some sediment deposition at John H. Overton Lock and Dam. However, several design features at John H. Overton Lock and Dam that differ from Lindy C. Boggs Lock and Dam indicated a reduction in sediment deposition problems could be expected. These features included a cross section at the structure that more closely represented that of the natural river section, no separation between the lock structure and the dam structure, and fixed guidewalls instead of floating guidewalls. However, even with these changes, the potential for deposition within the approach channels remained. Both physical and numerical model studies

were conducted to determine if additional structural measures were needed. As a result, a stone sediment control dike extending downstream from the riverside lockwall and a narrowing of the approach channels were incorporated. Subsequent to opening this lock and dam, sediment deposition occurred in the vicinity of the upstream miter gates and the downstream lock approach channel. To reduce the deposition at the miter gates a high velocity scour jet system was installed during July 1988. This system has been very successful in limiting sediment deposition at the miter gates. As Table 2 shows, some dredging is required at John H. Overton Lock and Dam but quantities are about one third of those at Lindy C. Boggs Lock and Dam.

Based on the experience gained at the two lower locks and dams and on physical and numerical model studies, the design of Lock and Dam No 3, Russell B. Long Lock and Dam, and Joe D. Waggonner, Jr. Lock and Dam included structural modifications aimed at significantly reducing sediment deposition. At all three of these structures, the downstream guidewall was moved from the landside of the lock to the riverside, uncontrolled pipes were provided through the downstream lock sill, and like John H. Overton Lock and Dam, a channel cross section that closely approximates the natural river section was provided. At both Russell B. Long Lock and Dam and Joe D. Waggonner, Jr. Lock and Dam, more elaborate scour jet systems were installed at both the upstream and downstream miter gates. As Table 2 shows, required dredging at Lock and Dam No. 3 is significantly less than that at the lower two locks and dams with average volumes being less than 15 percent of those dredged at Lindy C. Boggs Lock and Dam. Table 2 also shows that required dredging at Russell B. Long Lock and Dam and at Joe D. Waggonner, Jr. Lock and Dam is minimal when compared to the lower two locks and dams. The historic dredging indicates that the District learned its lessons well with Lindy C. Boggs Lock and Dam and John H. Overton Lock and Dam and designed, constructed, and are now operating the upper three locks and dams with very limited maintenance dredging required.

CONCLUSIONS

The fact that the Red River is a high-energy system with a high sediment transport capacity was both an asset and a hindrance in the design, construction, operation, and maintenance of the waterway project. These characteristics were an asset in that they reduced the project cost by providing for the development of project features. These features included pilot channels, trenchfill revetments, and capping-out of stonefill and timber pile revetments. The sediment conditions were a hindrance because they resulted in troublesome deposition at the locks and dams that required costly removal by dredging. Also, the availability of sediment transported by the river required the costly construction of transverse dikes in depositional reaches and kicker dikes on the downstream end of revetments in crossings.

Since the waterway was opened, dredging has been required in the approach channels to the locks and dams and to a lesser extent within the navigation channel within the pools. Modifications to the locks and dams have reduced the required dredging but still some dredging is required. Within the pools, the Vicksburg District continues to cap-out revetments and construct channel control dikes to reduce dredging within the navigation channel. However, given the flow and sediment conditions on the Red River, required dredging to provide and maintain a viable commercial navigation system has been and continues to be of manageable quantities.

GEOMORPHIC ANALYSIS TECHNIQUES APPLIED TO PACIFIC NORTHWEST RIVERS

Timothy J. Randle and Jennifer A. Bountry, Hydraulic Engineers
U.S. Bureau of Reclamation, Technical Service Center, Sedimentation and River Hydraulics Group
P.O. Box 25007 (D-8540), Denver, Colorado 80225

INTRODUCTION

The study of geomorphic processes in a river system can provide crucial information for resource managers. Every river system is unique and a geomorphic study often becomes a research effort. When resource management issues are at stake, researchers must provide accurate information to managers in a timely and cost-effective manner. Researchers must decide how best to collect and analyze data from river systems within the time and budget constraints of a given study. Some investigators may attempt to assert too much with too little data while other investigators attempt to collect and analyze too much data or don't focus the research on topics of interest to resource managers. The best method for determining when to appropriately obtain and analyze data is still the scientific method: formulate a set of hypotheses and determine the type of data and analyses that are needed to test these hypotheses. The collection and analysis of data without any hypothesis to test is often a wasteful exercise. The research hypotheses need to be driven by resource management questions if the research is to provide useful information to resource managers.

The geomorphic data collection and analysis techniques that were applied by the U.S. Bureau of Reclamation (Reclamation) to six different rivers in the Pacific Northwest are presented in this paper. All of the six rivers have steep channel gradients with gravel beds. Each river is being studied for unique reasons and, in each case; a cooperative study effort has been established with several different agencies and individuals who are interested in the results. This paper discusses which study approaches were the most useful to accomplishing the study goals and which approaches were not as useful. In addition to the literature reviews, the types of data collection activities for these river studies included:

- field reconnaissance by ground and air
- topographic surveys of the river channel, floodplains, and terraces
- bed-material size gradation measurements
- stream gaging of discharge and sediment load
- collection and analysis of historical maps, ground photographs, and aerial photography
- collection and analysis of tree ring samples
- collection and analysis of soil samples and radiocarbon ^{14}C dating

Analysis methods applied to these studies include orthorectification of aerial photographs, contour mapping of the river channel and floodplain, geomorphic mapping, hydraulic modeling, and sediment transport analysis and modeling. While each of the geomorphic studies discussed in this paper are unique, the lessons learned from these studies can assist in preparing study plans for other Pacific Northwest Rivers.

PILGRIM CREEK NEAR MORAN, WYOMING

Pilgrim Creek flows from a 50-mi^2 drainage of the Teton Wilderness Area near Moran, Wyoming. Although Pilgrim Creek has no long term stream gage, the annual mean flow was estimated to be 52 ft^3/s with a mean annual runoff of 14 inches. The highest peak flow recorded was 2,250 ft^3/s on June 5, 1997, which was very close to the 100-year flood peak. The lowest mean-monthly flows, 8.8 ft^3/s, occur during January and February (U.S. Department of the Interior, 1998). Pilgrim Creek has large sediment loads of sand, gravel, and cobbles. The creek flows across an alluvial fan within Grand Teton National Park before entering Jackson Lake on the Snake River. Jackson Lake is a naturally deep lake (maximum depth of 400 feet) that was raised 40 feet by the construction of Jackson Lake Dam. Originally, a timber-crib dam was privately constructed during 1906-1908, but that dam failed soon after its construction in 1910. The left abutment of the dam had been built on the Pilgrim Creek alluvial fan near the active channel of Pilgrim Creek. Before a new dam could be constructed, the downstream most portion of the creek had to be moved so that it entered the lake farther upstream from the dam site. Reclamation rebuilt a larger dam at this location, which was completed in 1916 (Piety and others, 1998).

Ever since the dam's reconstruction, Reclamation has been managing Pilgrim Creek to stay away from Jackson Lake Dam and to enter the reservoir rather than the Snake River channel downstream. Management activities of the creek have included the excavation of the river gravels to construct channels and dikes across the alluvial fan. However, in 1996, the granting of a permit

for channel maintenance activities became a controversial issue. The U.S. Army Corps of Engineers was not willing to grant a permit to construct dikes with river alluvium. However, an emergency permit was granted under the condition that Reclamation fully study the continuing need to build dikes and channelize the creek (Piety and others, 1998). The key questions for this study included:

- Is the river still aggrading across the alluvial fan?
- What is the risk of the creek causing erosion of Jackson Lake Dam?
- What is the risk of the creek entering the Snake River downstream from Jackson Lake Dam?

The study concluded that the creek was transporting its sediment load through the upper reach of the alluvial fan. However, coarse sediments had been aggrading the middle reach of the alluvial fan and causing channel avulsions. Geomorphic analysis including radiocarbon ^{14}C dating determined that the Pilgrim Creek channel had not changed its course across the upper alluvial fan during the past 2000 years. Analysis of historic aerial photographs revealed that the creek channel was wide, straight, and braided through the upper fan reach and that channel avulsions had occurred in the middle reach of the alluvial fan during the last several decades. After the coarse sediments had deposited in the middle fan reach, the creek channel was narrow and meandering in the lower fan reach. Cross-section surveys of the creek channel revealed that the longitudinal slope decreased in the middle fan reach. Sediment load measurements and transport calculations indicated that the sediment transport capacity was relatively high through the upper fan reach, but that it decreased through the middle and lower fan reaches. Analysis of sediment samples from the creek bed proved that the coarse gravel and cobble-sized sediments were not being transported all the way through the lower fan reach.

During the 1980's, Reclamation had excavated a straight pilot channel through the middle fan reach of the alluvial fan. During the course of the study, Pilgrim Creek flows were unusually high from the 1997 spring snowmelt. Hydrologic analysis of the discharge data indicated that the maximum flow that year was near the magnitude of the 100-year flood peak. The unusually high flows from the 1997 spring snowmelt caused the new pilot channel to erode and become wider and steeper through the middle fan reach. The high flows also caused the channel through the lower fan reach to erode its banks and become wider and straighter. The straightening of the channel also made it steeper and gravels were transported through the entire middle fan reach and through most of the lower fan reach for the first time. The observations and measurements that were made during the high flows of 1997 were valuable for understanding the physical processes of Pilgrim Creek and for making future predictions. The risk of Pilgrim Creek having a channel avulsion and causing damage to Jackson Lake Dam or entering the Snake River downstream from the dam was judged to be very low. The Pilgrim Creek Maintenance Program had ultimately been successful in forcing Pilgrim Creek into a stable channel that now enters Jackson Lake much farther upstream than the channel location of the early 1900's.

For the aggrading channel of Pilgrim Creek, the field measurements of bed-material surface size, radiocarbon dating of terrace soils, and channel topography were all very useful. Survey data of the Snake River channel, downstream from Pilgrim Creek, were never used. The analysis of aerial photographs, river hydraulics, and sediment transport capacity were necessary to support the study conclusions.

TETON RIVER NEAR DRIGGS, IDAHO

Teton Dam near Rexburg, Idaho suddenly failed on first filling of the reservoir in 1976. Although several studies have been done on the catastrophic impacts to people and property downstream from the dam, the impacts of the dam failure on the 17-mile reach of the former reservoir area were never formally evaluated. To determine what impacts did occur in this upstream canyon reach (from the filling of Teton Reservoir and subsequent failure of Teton Dam), a geomorphology and river hydraulics study was completed by Reclamation during 1997-2000, more than 20 years since the dam failure (Randle and others, 2000; Bountry and Randle, 2001). When Teton Dam failed, the reservoir was 270 feet deep (at the dam) and drained in less than 6 hours. The filling and the subsequent rapid draining of the reservoir triggered more than 200 landslides in the river canyon that was inundated by the former reservoir. Debris material from these landslides covered river terraces and buried the river channel in several locations. In addition, many existing riffles were enlarged by landslide debris and, in some locations, new rapids were formed. A complex of 27 rapids now exists in the river canyon creating slow-velocity pools upstream of each rapid. In 1997, a 100-year flood resulted in only minor reworking of the landslide debris that had deposited in the river channel. The study concluded that it would take centuries of natural weathering to erode the large boulders that comprise the existing rapids. The annual mean flow of the Teton River is 843 ft^3/s. With a total drainage area of 890 mi^2, the mean annual runoff is 13 inches. Except for the dam failure, the highest peak flow recorded was 11,000 ft^3/s on February 12, 1962 and the lowest mean-daily flow recorded was 199 ft^3/s.

Predam aerial photographs and contour maps of the river canyon were compared with recent aerial photographs and a new survey of the existing river channel. This comparison was made to document the impacts of reservoir filling and dam failure and to put these impacts in the context of natural processes. The logistics of a bathymetric survey in this remote river canyon were very difficult, but the data were essential to the study. Historical photographs and analysis of soil samples showed that landslides have been occurring in the canyon for thousands of years, but that this natural process was greatly accelerated by the failure of Teton Dam. Several deep pools and riffles were present at the time of the dam failure, but have been enlarged due to the deposit of additional landslide debris. In two separate locations, the landslide debris has created new rapids with more than 16 feet of drop in the water surface. These rapid complexes have significantly raised the water surface of the river relative to predam conditions.

Bed-material data from the river channel was used to evaluate the impacts of landslides on sediment transport. It was determined that sand and gravel-sized sediments are being trapped in the four upstream most pools of the former reservoir. Hydraulic modeling was performed to predict water depth, velocity, and the travel time of water for a given discharge. Water-temperature data were collected concurrently throughout the river canyon to determine if summer flows were being warmed as they passed through downstream river pools. The temperature data indicated that river flows were being warmed by 1 to 2 °F. The hydraulic modeling results correlated this warming with an increase in the travel time of water through the deeper and slower river pools. Bathymetric surveys of the channel bottom, comparison of current and historic aerial photographs and maps, and the modeling of river hydraulics were very useful for documenting the impacts of dam construction and failure.

ELWHA AND GLINES CANYON DAMS, ELWHA RIVER NEAR PORT ANGELES, WASHINGTON

The Elwha River flows northward from the Olympic Mountains of northwest Washington State to the Straight of Juan de Fuca near the town of Port Angeles, Washington. The upper watershed of the Elwha River is located within Olympic National Park and within a Wilderness Area (U.S. Department of the Interior, 1996). With a mean annual flow of 1,508 ft^3/s, and a drainage area of more than 270 mi^2, the Elwha River is the fourth largest river on the Olympic Peninsula. The mean annual runoff is 76 inches. The highest peak flow recorded was 41,600 ft^3/s on November 18, 1897 and the lowest mean-daily flow recorded was 10 ft^3/s on October 3, 1938.

Private companies constructed two large dams on the Elwha River during the early 1900's. Elwha Dam, constructed during the period 1910-13, is a 105-foot high concrete gravity dam that forms Lake Aldwell 8 miles upstream from the river's mouth. Glines Canyon Dam, built in 1927, is a 210-foot high concrete arch dam that forms Lake Mills 13 miles upstream from the river's mouth. When the dams were first built, they were significant producers of electricity on the Olympic Peninsula. Today, the dams are operated in a run-of-the river mode and generate about 40 percent of the electricity needs for the Diashowa America paper mill in Port Angeles, Washington. These two large dams have no facilities for the upstream passage of anadromous fish and their removal would provide an opportunity to restore an entire watershed to near natural conditions (U.S. Department of the Interior, 1996).

The U.S. Department of the Interior has recently purchased Elwha and Glines Canyon Dams in preparation for their removal. One of the major challenges in removing these two dams is the management of nearly 18 million yds^3 of sediment trapped within the two reservoirs. Of this total sediment volume, 13 million yds^3 is trapped behind Glines Canyon Dam in Lake Mills and 5 million yds^3 is trapped behind Elwha Dam in Lake Aldwell. About one half of the sediments in Lake Mills is coarse grained (sand, gravel, and cobble-sized) and the remaining half is fine grained (clay and silt-sized). Some of the fine-grained sediments are transported through the reservoirs while the remainder is deposited along the reservoir bottoms. All of the coarse-grained sediments are trapped within the reservoirs as delta deposits located at the upstream end of each reservoir. The width of these reservoir deltas is large, about ten times greater than the width of the alluvial river channel.

The Lake Mills drawdown experiment (Childers and others, 2000) was crucial to learning about the erodibility of reservoir sediments. Lake Mills was drawn down 18 feet over a one-week period and then the lake elevation was held constant for one additional week. This drawdown experiment exposed the upper layer (12 to 18-foot thickness) of coarse delta sediment to direct erosion by the Elwha River. Several types of data were collected throughout the drawdown experiment including:

- river discharge
- suspended sediment concentration and water quality
- bed load
- particle size gradations and chemical composition of the upper delta layer
- repeat cross section measurements of the delta surface (above and below water)
- time-lapsed photography of the delta erosion
- aerial photography

During the reservoir drawdown, vertical incision through the coarse delta sediments was very rapid, but the width of erosion was much less than the reservoir delta width. The eroded sediments redeposited in the receded lake and formed a new delta immediately downstream of the initial delta front. Once the reservoir was drawn down 18 feet, the lake elevation was held constant for another week. During the period of constant lake elevation, lateral erosion processes dominated the continued erosion of the exposed delta, especially at the downstream end. The width of erosion was near zero at the delta's upstream end, but increased at a parabolic rate in the downstream direction until the erosion width equaled the reservoir width at the delta face (Randle and others, 1996).

The Lake Mills drawdown experiment provided critical data for a new sediment erosion model and helped lead to the conclusion that the reservoir sediment erosion could be managed by controlling the rate of reservoir drawdown and that not all of the sediments would be eroded from the reservoir. The new reservoir sediment erosion model was an empirically based mass balanced model (Randle and others, 1996). This model predicted the rates and final quantities of fine and coarse-grained sediments eroded from each reservoir. The standard HEC-6 model (U.S. Army Corps of Engineers, 1993) was applied, using measured cross sections of the downstream river channels, to predict the potential for sediment deposition. The selected plan for managing the 18 million yds^3 of reservoir sediment is to concurrently remove both dams, in controlled increments, over a two-year period. Rates of sediment erosion, transport, and deposition are to be intensively monitored during dam removal. These rates will be monitored to determine if they match the predicted values within acceptable limits before proceeding with the next increment of dam removal (U.S. Department of the Interior, 1996).

SAVAGE RAPIDS DAM, ROGUE RIVER NEAR GRANTS PASS, OREGON

Savage Raids Dam is located in south-central Oregon, on the Rogue River, just 5 miles upstream from the town of Grants Pass. The annual mean flow of the Rouge River is 3,372 ft^3/s. With a total drainage area of 2,459 mi^2, the mean annual runoff is 19 inches. The highest peak flow recorded was 152,000 ft^3/s on December 23, 1962 and the lowest mean-daily flow recorded was 744 ft^3/s. Savage Rapids dam was built in 1921 to divert river flows for irrigation. The dam is 40 feet tall and creates a backwater pool that extends ½ mile upstream during the non-irrigation season and 2 ½ miles upstream during the irrigation season. The reservoir width is relatively narrow, only two to three times greater than the width of the river (Bountry and others, written communication, 2000). Although the dam has fish ladders, these ladders are old, do not meet current regulations, and only allow limited fish passage. Dam removal has been proposed to restore fish passage to natural conditions. The dam would be replaced with two pumping plants that would deliver water to the irrigation canals. A sediment study was requested by the Grants Pass Irrigation District to determine the sediment-related impacts of dam removal.

The volume and quality of the reservoir sediments were the critical properties to be determined. Previous estimates of the reservoir sediment volume had ranged from 0.5 million to 1 million yds^3. These estimates were based on limited information and seemed large for a reservoir of this size. Because the reservoir is significantly drawn down during the winter flood season (non-irrigation season), river conditions exist in the upper two miles of the reservoir during the period of maximum sediment inflow. Therefore, sediment was not able to significantly deposit along the upper two miles of the reservoir, but it did deposit in the 2-mile reach immediately upstream from the dam where the permanent pool was established. The techniques that were used to determine a more accurate estimate of the sediment volume included a visual inspection of the shoreline during a low reservoir pool, dive team examinations of the reservoir bottom, bathymetric surveying of the reservoir bottom, and core drilling of the reservoir sediments. Based on these more accurate techniques and a knowledge of reservoir operations, the reservoir sediment volume was determined to be only 200,000 yds^3. This volume is roughly equivalent to a 2-year sediment supply from the Rogue River. The reservoir sediments were found to consist of 71 percent sand, 27 percent gravel, and 2 percent silt and clay. Chemical testing of the reservoir sediments did not find any contaminants in concentrations significantly greater than natural background levels. These sediments would not pose any hazard to water quality, fish and wildlife, or human uses if released downstream of the dam (Bountry and others, written communication, 2000). Without drill-hole data and without an analysis of reservoir operations, the previous estimates of the reservoir sediment volume were significantly too high. Drill hole data from the deep areas of the reservoir were necessary to accurately determine the reservoir sediment volume and chemical composition.

A bathymetric survey of the downstream river channel was performed to develop river cross sections. The HEC-6t sediment transport model (Thomas, 1996) was used to simulate the erosion of sediments from the reservoir and their transport downstream. Model results indicate that the majority of sediments would be eroded from the reservoir within the first year following dam removal. The downstream transport of this sediment is dependent on the magnitude and duration of river flows following dam removal.

DUNGENESS RIVER NEAR SEQUIM, WASHINGTON

The Dungeness River is a gravel and cobble-bed stream located on the Olympic Peninsula of northwestern Washington State. The river flows northward about 30 miles from the base of Mount Deception in the Olympic Mountains to the Strait of Juan De Fuca near the town of Sequim. The watershed has a drainage area of more than 156 mi^2, a portion of which is located within the boundaries of Olympic National Park. The river is steep, falling about 3,300 feet in 28 miles for an average slope of 0.022. The river slope is steepest in the upper watershed canyons, but decreases downstream. The downstream most 10 miles of river flows across a piedmont surface, composed of glacially-derived sediment and outwash. The channel in these lower 10 miles has incised into this material since the Pleistocene (about 10,000 years ago) and meandered some, but within a relatively narrow corridor. The annual mean flow of the Dungeness River is 380 ft^3/s with a mean annual runoff of 33 inches. The highest peak flow recorded was 7,120 ft^3/s on November 24, 1990 and the lowest mean-daily flow recorded was 65 ft^3/s.

There has been a sharp decline in the numbers of salmon returning from the ocean to spawn in the Dungeness River. Two species of salmon are now listed as endangered. The upstream watershed has been affected by logging and the associated road building. The lower ten miles of river have been affected by the construction of levees, dikes, bridges, bank armoring, and by irrigation withdrawals and the removal of large woody debris. The physical processes of the Dungeness River are being studied to determine the degree to which natural processes have been impacted by human development. A comprehensive study approach has been initiated because the processes are complex and interdependent. The following types of data have been collected and analyzed during the course of the study (Piety and others, written communication, 2000):

- A network of more than 60 river cross sections was established with monuments along the lower 10 miles of the river in 1997. Data from this cross-section network define the channel geometry and slope and will serve as a baseline for future monitoring. The data were also used in a hydraulic model to identify reaches of low sediment transport capacity and to document the hydraulic impacts of levees, dikes, and bridges.

- The sediment grain-size distribution of the river-bed material was measured at various locations along the lower 10 miles of the river. Both the surface and sub-surface layers of the bed material were measured in the field. These data were collected to determine if the coarse gravel and cobble-sized sediments were being transported all the way to the estuary.

- Suspended sediment load and bed load rates were measured to determine sediment yield rates from the upstream watershed and to verify predictive sediment transport equations. Sediment modeling can then be applied to estimate rates of channel degradation, aggradation, or avulsions.

- Current and historic aerial photographs and maps were examined to determine the historical boundaries of the channel, rate of channel migration, and if the channel was subject to avulsions. Soil samples were collected from river terraces for radiocarbon ^{14}C dating to determine how many years it had been since the channel had abandoned the terraces.

- Time lapsed photography was also taken at three locations along the river channel to determine if large woody debris caused the formation of gravel bars and to determine the rates at which the bars are formed.

HOH RIVER NEAR FORKS, WASHINGTON

The Hoh River is a gravel and cobble-bed stream also located on the Olympic Peninsula of northwestern Washington State. The river flows westward about 60 miles from the base of Mount Olympus to the Pacific Ocean near the town of Forks, Washington The watershed has a drainage area of more than 253 mi^2 a large portion of which is located within the boundaries of Olympic National Park. The river is steep, falling about 5,000 feet in 58 miles for an average slope of 0.016. The river slope is steepest in the upper watershed canyons and decreases in the downstream direction. In the downstream most 30 miles, the average slope decreases to 0.0025. The river is meandering and flows through very high glacial terraces all the way to its mouth. Bedrock outcrops have been observed in the channel at several locations along the river. The annual mean flow of the Hoh River is 2,524 ft^3/s with a mean annual runoff of 135 inches. The highest peak flow recorded was 54,500 ft^3/s on November 24, 1990 and the lowest mean-daily flow recorded was 252 ft^3/s.

There has also been a sharp decline in the numbers of salmon returning from the ocean to spawn in the Hoh River. Logging and the associated road building have affected the upstream watershed. Landslides and debris flows are common throughout the drainage. Roads are adjacent to the channel and floodplains along the downstream 30 miles of the river. In some locations, the riverbanks have been extensively armored with rip rap to stop active bank erosion. The physical processes of the Hoh River are being studied to determine the degree to which natural processes have been impacted by human development.

This study is just beginning. Data collection activities in the year 2000 have included a river channel survey along the lower 31

miles of river and preliminary comparison of current and historic aerial photographs. The river channel survey was performed from a raft using global positioning system instruments and a depth sounder. The channel survey data will be useful for hydraulic modeling and future monitoring. Installation of cameras with automatic timers is being planned to produce time-lapsed videos at areas of active bank erosion to determine how certain reaches are presently responding to engineered log jams or how they may respond in the future. The analysis of current and historic aerial photography is expected be very useful in evaluating changes in river channel location.

SUMMARY AND CONCLUSIONS

Field reconnaissance was performed by various means, including driving and walking along the river channels, on all six river studies. Helicopters were chartered to view and photograph the river channels and mountain watersheds of Pilgrim Creek, the Dungeness River, and the Hoh River. Rafts were used to observe and measure the bottom topography along the Teton River, Rouge River, and Hoh River. The use of rafts would not have been practical on either Pilgrim Creek or the Dungeness River because the flow rates were too low on these wide, shallow channels. When practical, the use of helicopters and rafts was found to be a very effective way of observing channel and watershed processes including the presence of landslides, debris flows, sediment erosion and deposition, and the interactions between river hydraulics, sediment transport, and large woody debris.

Topographic survey of the river channel, floodplains, and terraces was performed on all six river studies either by wadding the channel or from a raft. The survey data were measured along cross section lines perpendicular to the channel flow. Additional channel data were easily measured between cross sections when the data were collected from a raft (e.g., Teton River, Rouge River, and Hoh River). In all six studies, the survey data were used to document the river-channel geometry and slope and as a basis for future monitoring. The survey data were used for the numerical modeling of river hydraulics and sediment transport. One-dimensional hydraulic models were used to predict the average channel velocity and depth for a range of discharges on each river study. Hydraulic model results were also used to predict reaches of low sediment transport capacity where channel aggradation can occur.

Sediment particle size measurements were performed on five of the six rivers. Depending on the river being studied, measurements were made on the river bed surface layer, the underlying bed layer, and throughout the thickness of the reservoir sediments. Present or future aggradation of the riverbed is a significant issue for all of the rivers being studied. Sediment particle size measurements of the river-bed surface, for various locations along the river channel, were compared to determine if coarse sediments were being transported through the study reach or if they were being deposited along the channel. This comparison was helpful for studies of Pilgrim Creek, Teton River, Dungeness River, and will likely be helpful for the Hoh River study. Degradation of the riverbed was not a significant issue for any of the river studies. Thus, measurements of the underlying bed-material layer were not particularly useful. For the case of the two dam removal studies, the sediment particle size measurements of the reservoir sediments were crucial for the sediment transport modeling of the downstream river channels. However, the sediment particle size data were not useful for predicting aggradation of the downstream river channels because sediment particle mixing is not expected to occur between the eroding reservoir sediments and the existing coarse sediments of the downstream river channel.

Stream gaging of discharge and sediment loads was performed on Pilgrim Creek, Elwha River, and the Dungeness River. Water discharge was measured on all six rivers that were being studied. The sediment load measurements were expensive and required the use of large bed-load samplers (6 by 12 inches) operated from a small crane. However, these data were valuable for determining a sediment budget and for numerical modeling of the sediment transport. This type of data would have been valuable for all of the six river studies.

Collection and analysis of historical maps, ground photographs, and aerial photography were performed for all six river studies. This collection and analysis were very valuable when the historic data existed, especially when it was available prior to significant water resources development.

Collection and analysis of tree ring samples were valuable for determining the minimum age of channel abandonment for the study of Pilgrim Creek. This has not yet been applied to the other river studies where the tree growth is much more rapid or where the age of trees is less than the period already described by aerial photography.

Collection and analysis of soil samples for radio carbon-14 dating were found to be very valuable for determining how many years it had been since an alluvial terrace had been abandoned by the river channel. This data was used to determine the lateral boundaries of the historic channel. This data would not be as useful in canyon reaches where the river channel is confined by bedrock.

Time lapsed photography was applied to the Elwha and Dungeness River studies to help others better understand natural processes and to observe these processes at times when the investigators could not be there, especially during floods. Normally,

river channel changes are only documented on an annual, or even less frequent, basis and it is difficult to determine the magnitude or number of floods that caused a particular change. By documenting changes over a daily time scale, a better understanding of natural processes in relation to changes in discharge was gained. The time-lapsed photography was found to be very popular with resource manager and the public and a very useful way to continuously observe natural processes. This technique will likely be applied to the Hoh River study.

Sediment transport modeling was applied to the two dam removal studies to predict the amount and timing of sediment deposition in the downstream river channels. Calculations of sediment transport capacity have been or will be made for the other river studies to predict reaches where sediment deposition is likely. Sediment transport modeling could also be applied to the other river studies, but the expense and effort have not yet been justified given that the important study conclusions can be made from simpler analysis of the available data. However, numerical models can be powerful and important predictive tools that can explain process linkages. Their successful application normally depends on the ability of the modeler to build or adapt an existing model that can properly account for the important channel processes, and their linkages, for a given river. The generic application of a model to a complex river can often produce misleading or incorrect results.

Recommended Steps for Successful River Study:

1. Field reconnaissance to characterize the river channel properties (such as slope, width, and sediment size of the bed and banks) and determine the local resource management goals, problems, and questions.

2. Review literature, data, photographs, and maps to understand historical changes of the river.

3. Formulate research hypotheses that can explain river processes and ultimately answer the questions of resource managers.

4. Design data collection and analysis programs that can be used to test the research hypotheses.

5. As new information is learned from step 4, formulate and test new research hypotheses until the study goals can be accomplished. This step should involve frequent discussions with resource managers to determine if the study findings will cause them to change or adapt their management goals and objectives.

6. When justified, develop predictive models to explain important river channel processes.

7. Write and present a study report than can be understood by resource managers and other interested parties.

REFERENCES

Bountry, J.A.; Randle, T.J.; Link, R.A.; Yahnke, J.; Bullard, K.L.; Black, R., September 2000, written communication, draft report in progress: Savage Rapids Dam Sediment Evaluation Study, Rogue River, Oregon, U.S. Department of the Interior, Bureau of Reclamation, Denver, Colorado.

Bountry, J.A.; Randle, T.J. (March 2001), "Upstream Impacts After the 1976 Failure of Teton Dam," in *Proceedings of the Seventh Federal Interagency Sedimentation Conference*, in Reno, Nevada.

Childers, D.; Kresch, D.L.; Gustafson, A.S.; Randle, T.J.; Melena, J.T.; Cluer, B., September 2000, Hydrologic Data Collected During the 1994 Lake Mills Drawdown Experiment, Elwha River, Washington, Water-Resources Investigations Report 99-4215, U.S. Geological Survey, Tacoma, Washington, 115 pages.

Piety, L.A. and Randle, T.J., October 1998, Physical Processes of Pilgrim Creek in Context With the Operations and Maintenance History for the Pilgrim Maintenance Program, Jackson Lake Dam, Minidoka Project, Wyoming and Idaho," U.S. Department of the Interior, Bureau of Reclamation, Denver, Colorado, 116 pages.

Piety, L.A.; Randle, T.J.; Bountry, J.A.; Link, R.A., January 2000, written communication: Geomorphology of the Lower Dungeness River, Draft Progress Report for Fiscal Years 1998 and 1999, Dungeness River, Washington, U.S. Department of the Interior, Bureau of Reclamation, Denver, Colorado, 63 pages.

Randle, T.J.; Young, C.A.; Melena, J.T.; Ouellette, E.M., October 1996, Sediment Analysis and Modeling of the River Erosion Alternative, Elwha Technical Series PN-95-9, U.S. Department of the Interior, Bureau of Reclamation, Boise, Idaho, 138 pages.

Randle, T.J.; Bountry, J.A.; Klinger, R.; and Lockhart, A., May 2000, Geomorphology and River Hydraulics of the Teton River Upstream of Teton Dam, Teton River, Idaho, U.S. Department of the Interior, Bureau of Reclamation, Denver, Colorado, 50 pages.

Thomas, W.A., March 1996, HEC-6t Sedimentation in stream networks, User's Manual, Version: h6tr514," Mobile Boundary Hydraulics, Vicksburg, Mississippi.

U.S. Army Corps of Engineers - Hydrologic Engineering Center, August 1993, HEC-6 Scour and deposition in rivers and reservoirs, User's Manual, Version 4.1.

U.S. Department of the Interior, November 1996, Elwha River Ecosystem Restoration Implementation, Final Environmental Impact Statement," Olympic National Park, Washington, 281 pages.

U.S. Department of the Interior, November 1998, Pilgrim Creek Maintenance Program, Jackson Lake Dam, Minidoka Project, Wyoming/Idaho, Technical Findings Report, Appendices, Bureau of Reclamation, Boise, Idaho, pages 3-1 to 3-10.

EFFECTIVENESS OF CHANNEL IMPROVEMENT WORK ON THE MISSISSIPPI RIVER

C. Fred Pinkard, Jr., Hydraulic Engineer, USACE, Vicksburg District, Vicksburg, MS; James V. Ross, Civil Engineer, USACE, Vicksburg District, Vicksburg, MS; Robert H. Fitzgerald, Civil Engineer, USACE, Vicksburg District, Vicksburg, MS

Abstract: The Mississippi River has long been a major contributor to the physical and economic development of our nation. However, at the time that the United States was first settled, the Mississippi River was a natural alluvial stream characterized by a wide, shallow channel, numerous shifting sandbars, and large fluctuations in stage. The river was active and freely meandered across its floodplain. In this natural state, the river could not provide a dependable channel to meet the nation's commercial navigation needs nor could it provide for the efficient passing of flood flows.

To meet both navigation and flood control needs, a dependable, low maintenance channel had to be developed. Initially, dredging was conducted to provide adequate depths for navigation and levees were constructed to ease flooding problems. However, these measures alone proved ineffective. Then in 1927, a great flood devastated the entire Mississippi River Valley. As a result of this flood, Congress passed the Flood Control Act of 1928. This legislation authorized the U. S. Army Corps of Engineers to develop a system of flood control and navigation improvements for the Lower Mississippi River. To provide an efficient navigation channel, the banks of the river had to be held in place. The Corps of Engineers initiated a comprehensive bank stabilization program to meet this need. The use of revetment consisting of articulated concrete mattress (ACM) on the lower bank in conjunction with stone paving on the upper bank has proved to be most effective in controlling the erosion of the river's banks. However, revetment alone was not sufficient to provide a low maintenance channel. During low water periods, substantial dredging was required to maintain adequate channel depths. As a result of this continued dredging, a system of rock dikes was developed to provide adequate depths through trouble reaches. Now approximately 90 percent complete, the channel improvements have greatly reduced the expensive dredging requirements. Dredging within the Vicksburg District is now only required in isolated problem reaches.

Even with the proven success of the channel improvement program, additional work is required. With continued construction of the remaining planned channel improvement structures and continued maintenance of existing structures, an efficient navigation channel will be provided on the Mississippi River for decades to come.

BASIN CHARACTERISTICS

The Mississippi River drainage basin is the third largest in the world, exceeded in size only by the Amazon River in South America and the Congo River in Africa. The Mississippi River drains 41 percent of the lower 48 states, including all or parts of 31 states, extending from New York in the east to Montana in the west. The Ohio, Missouri, Tennessee, Arkansas, and Red River basins are part of the Mississippi River basin. The Mississippi River flows some 2,350 miles from its source at Lake Itasca in Minnesota to the Gulf of Mexico. The Lower Mississippi River Valley extends from just below Cape Girardeau, Missouri for approximately 600 miles to

the Gulf of Mexico. The lower valley ranges in width from 30 miles to 125 miles with an average width of 45 miles and includes parts of Missouri, Illinois, Kentucky, Tennessee, Arkansas, Mississippi, and Louisiana.

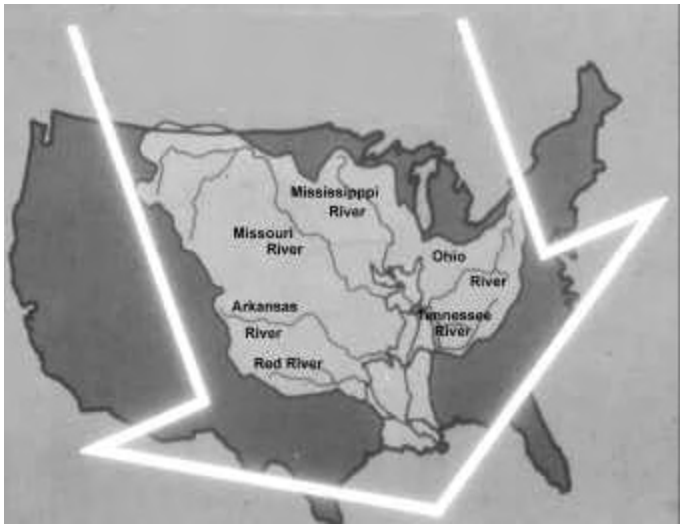

Figure 1. Mississippi River Drainage Basin

On the Mississippi River, flows, stages, and channel velocities vary over a wide range. During the 1928 through 1998 period, the average flow at Vicksburg, Mississippi was 601,000 cubic feet per second (cfs). The minimum recorded flow during this 71-year period was 93,800 cfs during August 1936 while the maximum recorded flow was approximately 2,060,000 during the 1937 flood. During that period, flows ranged on average from a low of around 202,000 cfs to a high of about 1,344,000 cfs. River stages also vary greatly. During the 1928 through 1998 period, the average annual low stage at Vicksburg was 48.6 feet, National Geodetic Vertical Datum (NGVD), the average stage was 65.4 feet, NGVD, and the average annual high stage was 86.8 feet, NGVD. Based on these averages, stages typically varied almost 40 feet from annual highwater to low water. The lowest stage ever recorded at Vicksburg was 39.2 feet, NGVD during February 1940 while the highest stage recorded was 102.2 feet, NGVD during the 1927 flood. Channel velocities typically range from about 2 to 3 feet per second during low water to over 10 feet per second during highwater.

The Mississippi River is a natural alluvial river that carries a large sediment load. Available data indicates that the annual suspended sediment load at Tarbert Landing, Mississippi (River Mile 306.3) has varied from about 100,000,000 tons to over 575,000,000 tons with an average annual suspended sediment load of approximately 240,000,000 tons. This sediment load equates to 213 tons per square mile of contributing drainage area per year. Sieve analyses indicate that on average, this suspended sediment load consists of 22 percent sand and 78 percent fine material (silt and clay). Studies have indicated that over time, the measured suspended sediment load on the Mississippi River has significantly decreased primarily due to the construction of the channel improvement features, closure of multipurpose reservoirs, and improved land use management procedures. However, since the measured suspended sediment load is predominantly silt and clay, which are not found in large quantities in the bed, the total measured suspended sediment

load could have decreased without any decrease in the bed material load. In fact, as pointed out by Biedenharn (1995), the river through most of the Vicksburg District has a much steeper slope and larger stream power (QS) today than it did prior to the 1930's. Therefore, since studies (Nordin and Queen, 1992) show that the bed material size (D_{50}) of the river has not changed significantly since the early 1930's, it is possible that the bed material load is higher today than it was prior to that time. This conclusion would mean that more sediment of the size that deposits in the navigation channel and historically required removal by dredging is carried by the river today.

NAVIGATION DEVELOPMENT HISTORY

The Mississippi River has long been recognized as a valuable transportation benefit. Native Americans traveled the river by canoe for centuries before the European explorers arrived. The Europeans used the river for settlement expansion and small-scale commercial navigation to transport goods such as furs and supplies. The introduction of the steamboat during the early 19th century ignited an explosion of development along the river. However, the river was unpredictable and many steamboats fell victim to hazardous snags, shifting sandbars and high channel velocities. As early as 1820, the Federal Government recognized the importance of improving the Mississippi River for navigation. In that year, Congress appropriated funds for the preparation of a survey, maps, and charts of the Ohio and Mississippi Rivers. In 1824, the Corps of Engineers initiated channel improvement work by removing snags in the Mississippi River below the mouth of the Missouri River. For several years thereafter, channel improvement work was sporadic and limited to localized areas. All channel improvement work halted during the Civil War. As the country began to heal after the war, the need for more substantial Federal involvement in improvements of the river for navigation and flood control was generally recognized. In 1879, Congress established the Mississippi River Commission (MRC) to coordinate engineering operations within the Mississippi River Valley. The MRC was assigned the primary duties "…to take into consideration and mature a plan or plans and estimates as will correct and permanently locate, and deepen the channel and protect the banks of the Mississippi River; improve and give safety and ease to the navigation thereof; prevent destructive floods; promote and facilitate commerce, trade, and the postal service…". In 1894, dredging began on the river. The success of these dredging operations prompted Congress in 1896 to authorize a 9-foot deep by 250- foot wide navigation channel from Cairo, Illinois to the Gulf of Mexico, to be maintained by dredging alone. However, dredging alone was not entirely effective in providing the required navigation channel and did not provide for the overall development needs of the valley. Then in 1927, the most disastrous flood in the history of the Lower Mississippi River Valley occurred. This flood inundated an area of about 26,000 square miles. During this flood, levees were breached, cities and towns were flooded, industry was paralyzed and crops were destroyed. Over 200 lives were lost and over 600,000 people were displaced. As a result of this flood, Congress passed the Flood Control Act of 1928, the nation's first comprehensive flood control and navigation act. This act increased the authorized navigation channel width to 300 feet and initiated a policy of river improvement and systematic construction of the channel improvement feature. The act also authorized the Mississippi River and Tributaries (MR&T) Project. Every year since the Flood Control Act of 1928 was passed, Congress has appropriated funds for the MR&T Project. One of the major components of the MR&T Project is channel improvement and stabilization for providing and maintaining an efficient navigation alignment,

increasing the flood carrying capacity of the river, and for protection of the levee system. To provide for this component, an intense program of revetment and dike construction was initiated and is on-going today. The estimated total cost of the MR&T channel improvement program is $1,140,000,000. Through 1999, $718,412,000 (63%) has been expended. The channel improvement program is scheduled for completion in 2021 assuming adequate funding continues to be provided.

Waterborne commerce on the Mississippi River has increased from 30 million tons in 1940 to over 500 million tons today. This tonnage includes such commodities as agricultural products including various grains, coal and coke, petroleum products, sand, gravel, and stone, salt, sulphur and other chemicals, among others. Without this valuable transportation system, the railways and highways would be much more crowded. One standard barge that is 35 feet wide and 195 feet long can carry 1,500 tons of cargo. One of these barges has the capacity of 15 railroad cars or 60 18-wheeler trucks. Therefore, it would require 5,000,000 railroad cars or 20,000,000 18-wheeler trucks to transport the tonnage that moves on the Mississippi River today. The Mississippi River also provides an important link in the mobilization of our nation's defense forces. Therefore, the on-going development of the channel improvement program has resulted in the Mississippi River continuing to thrive as a crucial link for the country's economic development.

BANK STABILIAZTION

As is common on natural alluvial rivers, the Mississippi River has historically experienced bankline migration. As evidenced by the numerous oxbow lakes and meander scars that exist today, the Mississippi River freely meandered across its floodplain. In this natural state, the river was wide and shallow with numerous shifting sandbars. To provide a dependable navigation channel, the banks of the river had to be held in place along the desired alignment. Therefore, an intense program of bank stabilization was initiated. In the past, several types of revetment have been used including willow, lumber, and asphalt mattresses. While these types of revetment proved somewhat successful, the most economical and effective means of protecting the banks continues to be a revetment composed of articulated concrete mattress (ACM) on the lower bank and stone paving on the upper bank. The current method of ACM placement is unique and is the result of years of research and development.

The use of ACM is restricted to large rivers due to the size of the floating plant required to place the mat. Therefore, in the Vicksburg District, ACM has only been used on the Mississippi River and on the lower Red River below the mouth of the Black River. The mat placement process includes several phases. The first phase involves the clearing of the bank. Many of the banks on the lower Mississippi River are covered with vegetation that must be removed. Caving banks are usually very steep. Therefore, to insure the stability of the revetment, the bank is graded to a flatter slope. The banks are graded by a large floating diesel-electric powered dragline. The clearing and grading of the banks are conducted on a schedule so that work is completed just prior to the arrival of the mat-sinking unit. This minimizes the potential for erosion of the freshly graded bank, reducing the overall cost of the operation and producing a better product. Natural vegetation re-establishes itself quickly along the stabilized top bank following completion of the revetment construction.

The ACM consist of individual units of mat that are pre-cast and stored at strategically located casting fields along the river. Each unit contains 20 separate concrete blocks that are held together by corrosion-resistant wire embedded in the concrete. Each block is 4 feet long, 14 inches wide, and 3 inches thick, resulting in each unit being 25 feet long by 4 feet wide. The surface of the mat is roughened during the casting process by dragging a large wire brush type tool over the uncured concrete after it is placed into forms. Use of the roughened mat improves the aquatic habitat provided by the river by increasing the surface area for growth of macro-invertebrates which retain and recycle organic materials that would otherwise be lost from the system as well as providing a food source for fish and birds with recreational, ecological, and economical value. Once the revetment season begins, the ACM units are loaded onto barges and transported to the construction site. Once on site, the units are loaded on a specially designed mat-sinking barge. The units are wired together into a mattress that is 140 feet wide and anchored to the bank with cables. As the mat is assembled, the sinking barge moves out into the river along the mooring barge. As the sinking barge moves, the ACM is launched off the barge and covers the river bottom. Placement of the mat continues to beyond the deepest part of the channel. The mat sinking plant is then moved upstream to lay the next section of mattress. This process continues with each succeeding mattress overlapping the previous mattress in a manner similar to shingles on a roof until the desired length of bank has been revetted. Once the ACM is in place, placing stone riprap on the graded upper bank completes the revetment process.

Figure 2. Stacked ACM in Casting Field

Figure 3. ACM Placement

ACM is placed during the low water season. On the lower Mississippi River, the revetment season typically extends from early August until all scheduled revetment placement is complete, usually in November. The location and amount of revetment placed each year is based on a prioritization of needed stabilization work and available funding. Through 1999, over 284 miles of revetment have been placed on the Mississippi River within the Vicksburg District with only 10.5 miles of revetment remaining. Therefore, the revetment construction program is approximately 96.4 percent complete.

CHANNEL CONTROL

Dikes: The channel improvement feature that has had the greatest impact on dredging is the contraction of the channel with dikes. Dikes are constructed on the Mississippi River to contract

the width of the low water channel to provide and maintain adequate depth for navigation. Historically, dikes have been constructed of timber pile or stone or a combination of the two materials. Since stone is more permanent, this construction material is now used exclusively for dike construction. Dikes on the Mississippi River are constructed to a sufficient height to maintain an efficient low water channel but low enough so as not to hinder the passage of flood flows. Dikes within the Vicksburg District are typically constructed so as to provide a 3000-foot minimum width between the riverward end of the dike and the opposite bank of the river. The Vicksburg District has been constructing channel control dikes on the Mississippi River since the early 1960's. As of 1999, over 270 dikes totaling approximately 114 miles have been constructed. The dike construction program is approximately 76 percent complete with just over 36 miles of dikes remaining. One of the environmental features currently used by the Corps of Engineers is the notched dike concept. By leaving a notch in selected dikes, the navigation channel can be maintained while at the same time providing diverse habitats for a variety of species including fish and the endangered least tern. The intended result is to insure that flow is maintained in secondary channels that would otherwise be greatly reduced or even eliminated during low water periods. The size and location of the notch in dikes is determined by the overall configuration of the river channel at each specific location. The Vicksburg District typically provides 100-foot wide notches with the bottom elevation of the notch varying by site. The District's current plan is to notch all future dikes that are constructed across secondary channels. All existing dikes that extend across secondary channels that require raising in the future to maintain the navigation channel will also be notched at the time they are raised. The Vicksburg District first constructed notched dikes on the Mississippi River during the mid-1980's. Since that time, some 47 notched dikes have been constructed within the District.

Figure 4. Channel Control Dikes

As previously mentioned, the Federal Government has been involved in dredging the Mississippi River since the 1890's. As the MR&T bank stabilization and channel control programs progressed, less dredging has been required to provide and maintain an efficient navigation channel. Records indicate that required dredging within the Vicksburg District often exceeded 10,000,000 cubic yards per year during the 1960's and the first half of the 1970's. However, during those years, only a minimal amount of dike construction had been completed. Figure 5 presents a graphical comparison of the annual dredging conducted on the Mississippi River within the Vicksburg District versus the cumulative amount of completed dike construction. As

the figure shows, in 1970 over 19,200,000 cubic yards were dredged. By that time, a total of less than 35 miles of dikes had been constructed. As the dike construction continued, the amount of dredging required to maintain a safe and dependable low water navigation channel drastically decreased throughout the 1970's. In 1980, just over 5,000,000 cubic yards of dredging was required and almost 65 miles of dikes were complete. In 1988, only 3,200,000 cubic yards were dredged even though the basin was experiencing a severe low water with river stages falling lower than had occurred in several decades. At Vicksburg, the low stage recorded in 1988 was the lowest in almost a quarter century. During 1996, 1997, 1998, and 1999, less than 1,000,000 cubic yards per year were dredged. So far in 2000, only about 1,100,000 cubic yards have been dredged. However, a severe drought that began in the late spring and early summer of 1999 continued to impact the stages on the lower Mississippi River valley into the late winter of 1999 and the spring of 2000. Stages during late 1999 and early 2000 approached the extreme low stages experienced in 1988. As a result, increased dredging has been required over that required in the most recent previous years. However, even with this extreme low water, dredging has been far less than required in 1988 with total combined 1999 and 2000 dredge volumes only slightly exceeding half of the dredging required in 1988. Much of this reduction can be attributed to the additional dike construction completed since 1988. In 1988, 75 miles of dikes had been constructed. By 1999, over 114 miles of dikes were complete.

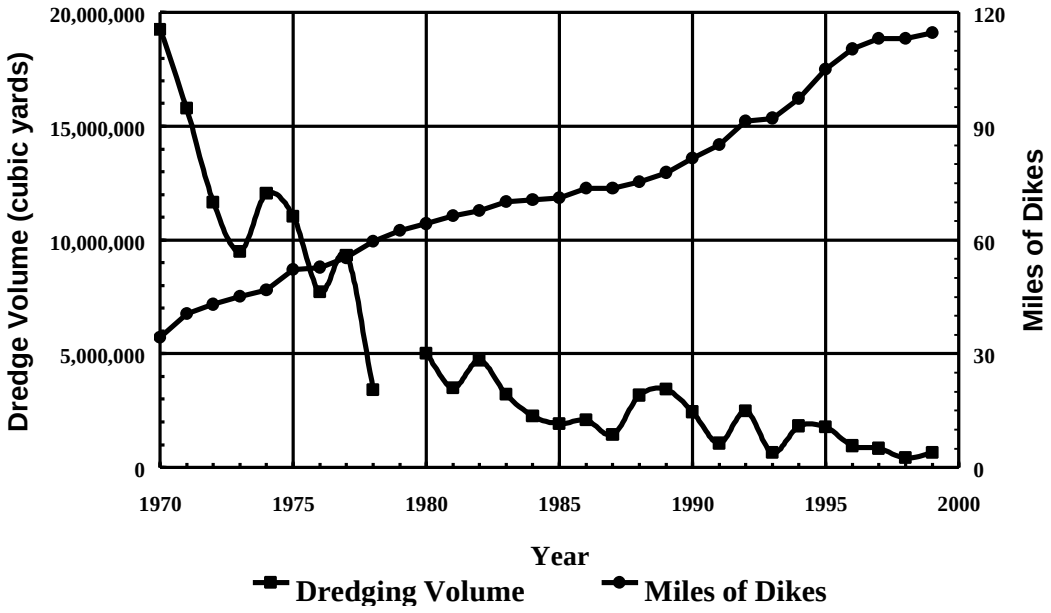

Figure 5. Mississippi River Dredging Versus Dikes in Vicksburg District

Bendway Weirs: A relatively new method of providing adequate navigation width in bends is bendway weirs. This concept as developed by the U.S. Army Corps of Engineers St. Louis District is used to reduce the depth on the outside of bends and thus naturally widen the channel on the point bar. Bendway weirs are totally submerged stone structures that extend from the outside of the bend and are angled upstream. The bendway weirs are constructed so that commercial tows can navigate over the structures without experiencing excessive turbulence. The position and alignment of the bendway weirs alter the river's secondary currents so that channel deepening along the outside of the bend is controlled.

Continued navigation problems at Victoria Bend (River Mile 595) prompted the Vicksburg District to construct bendway weirs at this location in 1995. A total of 6 weirs were constructed to an elevation of 20 feet below the Low Water Reference Plane (LWRP). The LWRP is defined as the stage associated with the flow that is equaled or exceeded 97 percent of the time. Subsequent surveys indicate that the navigation channel through the bendway has experienced some widening. Even with this additional channel width, navigating the bend remains difficult at certain flows. However, since construction of the bendway weirs, the towing industry, in general, believes that the navigation conditions are improved.

CONCLUSIONS

The Mississippi River indeed has been and remains a major contributor to the physical and economic development of the nation. It carries the runoff from rainfall and snow melt for about 41 percent of the contiguous United States plus a small portion of Canada along with about 240,000,000 tons of sediment annually to the Gulf of Mexico. The river also supplies water for over 18 million people and unnumbered industries and power plants. Currently, over 50,000,000 tons of commerce are transported on its navigation channel annually. Since their inception in the 1800's, the channel improvement works completed by the Corps of Engineers have contributed significantly to the efficient operation of this mighty river and its service to the nation. More recently, the systematic placement of channel training structures have significantly reduced the need for costly dredging to maintain a safe and dependable navigation channel.

REFERENCES

Biedenharn, David S., 1995, Lower Mississippi River Channel Response: Past, Present, and Future, Dissertation for Degree of Doctor of Philosophy, Colorado State University, 127.

Nordin, C. F. and Queen, B. S., 1992, Particle Size Distributions of Bed Sediments Along the Thalweg of the Mississippi River, Cairo, Illinois to Head of Passes, Potamology Program (P-1), Report 7, U.S. Army Corps of Engineers, Lower Mississippi Valley Division, Vicksburg, Mississippi.

Robinson, Michael C., Ethridge, Loyde T., U.S. Army Corps of Engineers, Lower Mississippi Valley Division, Mississippi River Commission August 1984, History of Bank Protection Through The Use Of Revetments.

U.S. Army Corps of Engineers, Mississippi River Commission, September 1992, Lower Mississippi River Environmental Program, Report 19, Effects of Surface Texture of Articulated Concrete Mattress Blocks on Their Habitat Value.

U.S. Army Corps of Engineers, Mississippi River Commission and Lower Mississippi Valley Division, March 1976, Flood Control In The Lower Mississippi River Valley.

U.S. Army Corps of Engineers, St. Louis District, August 1993, DP-1110-1-1, Bendway Weirs Brochure.

UPSTREAM IMPACTS AFTER THE 1976 FAILURE OF TETON DAM

By Jennifer Bountry and Timothy Randle, Hydraulic and Sedimentation Engineers, Bureau of Reclamation, Department of Interior, Denver, Colorado

Abstract: The construction and subsequent failure of Teton Dam in 1976 changed the physical and biological characteristics of the Teton River canyon for 17 river miles (RM) upstream from the dam site. This paper discusses the results from a study that analyzed the existing geomorphology and river hydraulics upstream of the dam site, and the changes that have occurred as a result of the reservoir inundation and subsequent failure of Teton Dam (Randle, et al, 2000). Results from this study will assist in managing Reclamation withdrawn lands in and around the Teton River canyon upstream from the Teton Dam site. In addition, models developed from this study can be utilized as predictive tools for addressing various alternatives for modifying rapid and pool formations caused as a result of the dam failure.

PROJECT BACKGROUND

The construction of the Teton Basin Project, Lower Teton Division, was authorized by Public Law 88-583 on September 7, 1964. This project would have provided supplemental irrigation water for approximately 110,000 acres in the Fremont-Madison Irrigation District, for flood control operation, and for recreation and fish and wildlife mitigation measures (Schuster and Embree, 1980). The 17-mile-long reservoir was to have a total capacity of 288,000 acre-feet and a surface area of 2,100 acres.

Filling of the reservoir began October 3, 1975, and continued until June 5, 1976, when Teton Dam failed (Jansen, 1980). The reservoir was at elevation 5301.7, about 272 feet deep at the dam, and 22.6 feet below the planned maximum pool elevation when piping caused the embankment to fail. Approximately 250,000 acre-feet of water and 4 million cubic yards of embankment material were sent down the river in about 6 hours (Lloyd and Watt, 1981). The destruction downstream from the dam was extensive, reaching to the upper end of American Falls Reservoir, 95 miles downstream. This paper focuses on the impacts upstream of the dam caused by landslides induced from the filling of the reservoir and rapid draw down following the failure of the dam.

DATA COLLECTION

Data were collected in 1997, 1998, and 1999 along portions of the Teton River between the Teton Dam site and the Felt Dam Powerhouse, 19 river miles upstream (figure 1). The data collected consist of new aerial and ground photographs, measurements of riverbed topography, water surface elevations, water and air temperatures, preliminary particle size analysis of landslide material, and bed-material particle size distributions. Additional data collected on the riparian vegetation are presented in a separate report (Beddow, 1999). The channel topography data were used to create a hydraulic model and a set of bathymetric maps for the Teton River pools from the confluence with Bitch Creek to the confluence with Canyon Creek (12 river miles) and in the borrow ponds just upstream from the Teton Dam site.

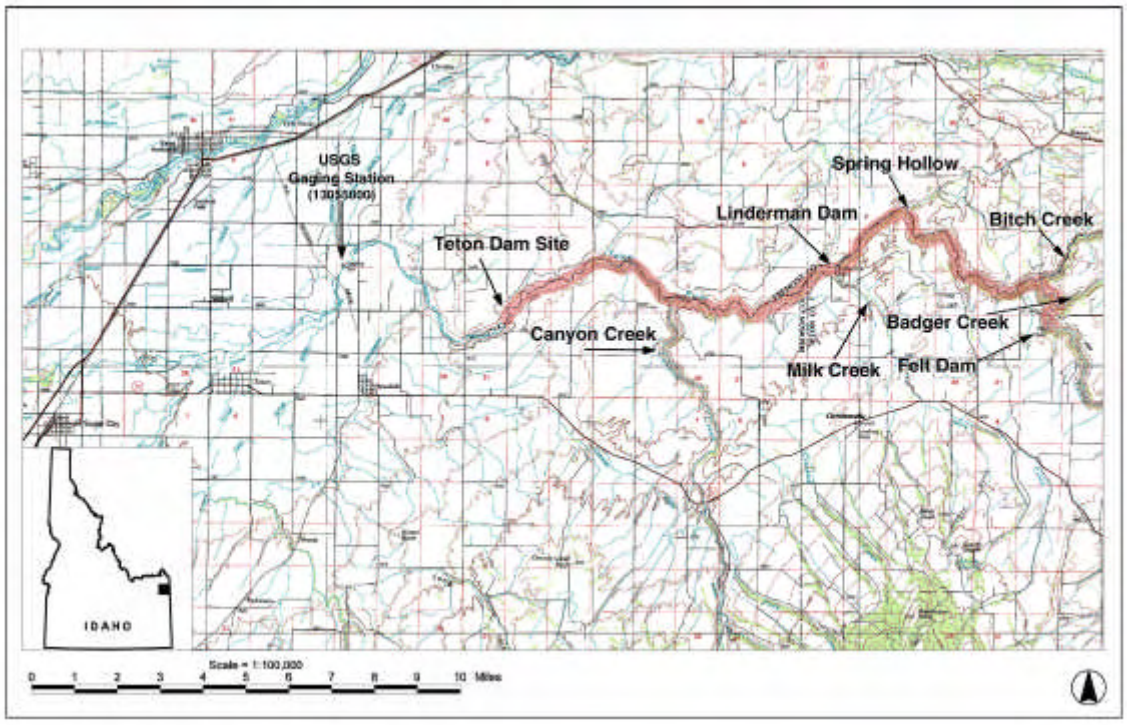

Figure 1. Location map for Teton River study showing study reach extending 19 miles from Felt Dam Powerhouse downstream to the Teton Dam site.

LANDSLIDE EFFECTS ON RAPID AND POOL FORMATION

Landslide activity in the former reservoir area started with the filling of the reservoir. The June 5, 1976, dam failure activated more than 200 landslides along the reservoir rim, due to the filling and the rapid drawdown of the reservoir. Approximately 1,460 acres of canyon slopes were submerged by the reservoir, and 34 percent (500 acres) failed (Magleby, 1981). Approximately 3.6 million cubic feet of landslide debris moved downslope to the canyon floor, with some reaching and blocking the river. While a large amount of landslide debris reached the valley floor, much of the debris remained on the lower portion of the canyon slopes.

Most of the landslides were shallow surface slumps, earth flows, debris flows, and rockfall. The thickness of the landslide debris ranged from less than 5 feet to about 25 feet normal to the slope. Particle size evaluation of landslide material was completed during the 1998 field investigations along the Teton River, but should be considered preliminary, due to the small data sample. The size of the landslide material ranges from silt to boulders greater than 10 feet across. Most of the material in the landslides consists of rock fragments from 3 inches to 3 feet across.

In the former reservoir area, the Teton River canyon is narrowest at the upstream end and tends to become progressively wider in the downstream direction. When landslides naturally occurred in the wider reaches of the Teton River canyon (prior to Teton Dam),

the river channel was able to move laterally around the debris fan or incise through the area of finest material, and, consequently, deep pools were not able to persist. In contrast, when landslides occurred in the narrow reaches of the canyon, the river channel was completely blocked, the riverflows were forced to spill over the coarse debris, and persistent, deep pools were formed upstream.

In the 5-mile reach downstream from the confluence with Canyon Creek to the dam site, the landslide debris associated with the filling and rapid drawdown of Teton Reservoir landed on high terraces and typically did not reach the river channel. Therefore, landslides downstream from Canyon Creek did not significantly affect the river channel and its hydraulics. In the 12 miles upstream from the confluence with Canyon Creek, the Teton River canyon was narrow enough that the landslide debris fans typically reached the river channel. These debris fans formed new rapids in some locations and enlarged pre-existing riffles in other locations. Landslides that occurred centuries ago through natural geologic processes formed the pre-existing riffles.

Currently, the river channel contains several long, slow velocity pools that are backed up by short, steep riffles or rapids formed from landslide debris. Since the failure of Teton Dam in 1976, 27 rapids and pools have persisted in the reach upstream from Canyon Creek (figures 2 and 3). Landslide debris was also deposited in pools upstream from some of these rapids.

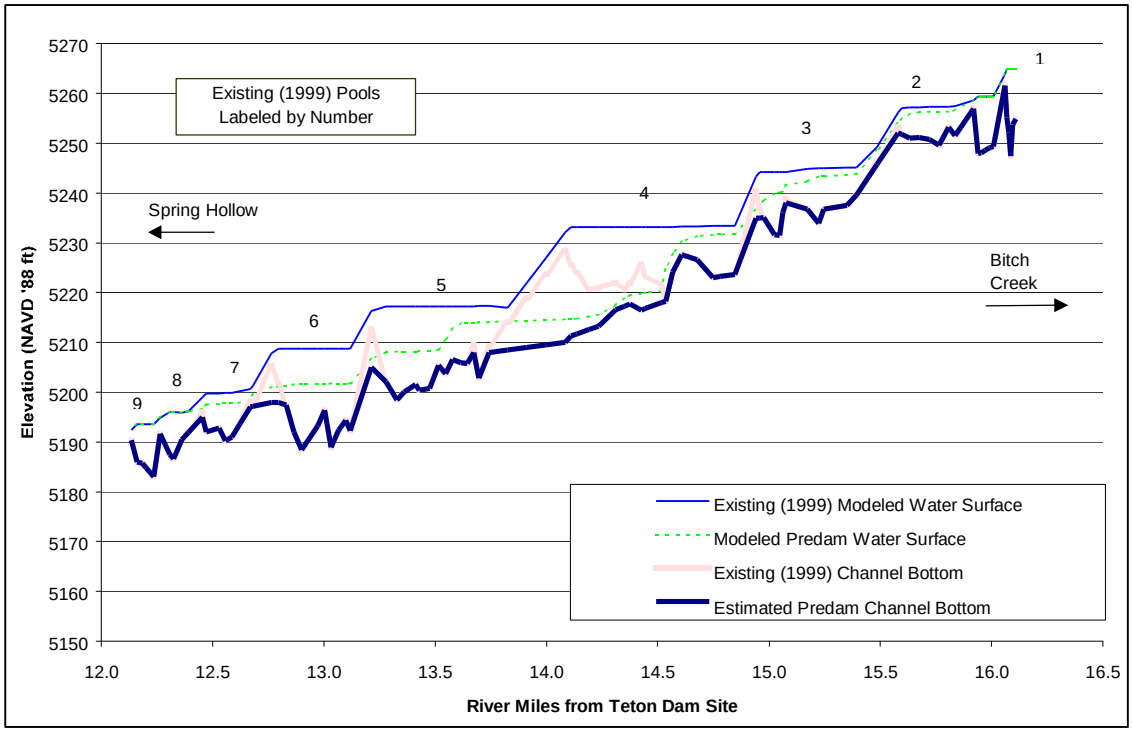

Figure 2. Existing (1999) and Predam (1972) Water Surface and Thalweg Profiles Corresponding to a Discharge of 1,000 cfs for the Teton River from River Mile 12 to River Mile 17 (upstream extent of former reservoir inundation).

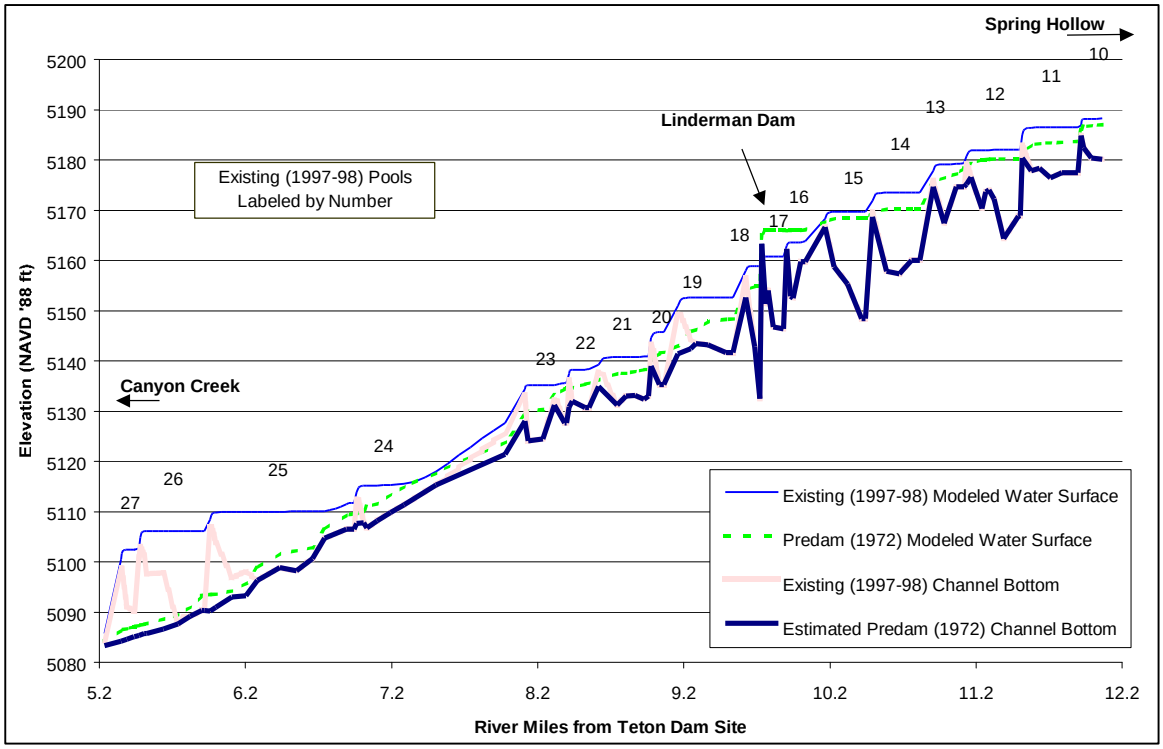

Figure 3. Existing (1999) and Predam (1972) Water Surface and Thalweg Profiles Corresponding to a Discharge of 1,000 cfs for the Teton River from River Mile 5 (downstream most rapid formed from landslide induced rapid following failure of dam) to River Mile 12.

Prior to the construction of Teton Dam, two rapids and several small riffles existed between the confluence with Bitch Creek and Spring Hollow. One of these rapids is now inundated by a new rapid formed from the dam failure (rapid 1). There were no major rapids present along the Teton River between the Teton Dam site and Spring Hollow (based on inspection of aerial photographs). However, 13 riffles and deep pools existed in the 4-mile reach downstream from Spring Hollow (RM 8 to RM 12). It is estimated that water depths in these pools ranged from 5 to 20 feet. The landslides that occurred in 1976 enlarged many of the existing riffles into rapids and, subsequently, increased pool water surface elevations by 2 to 5 feet (an increase much less than the pool depths). These deep pools measured in 1997 downstream from Spring Hollow must have been present in 1972, because they could not have been created in 1976.

No large landslides occurred in the half-mile reach downstream from RM 8.0, and the river channel was left relatively unaffected by the initial filling of the reservoir and subsequent failure of Teton Dam. The reason that no large landslides occurred in this reach is likely due to the general northeast-southwest orientation of the canyon in this location. Most of the river canyon is generally oriented in an east-west direction so that the south side of the canyon (left side looking downstream) is more shaded, retains more moisture, and develops thicker soil and forest growth than the north (right) side. The north side of the canyon gets more sun and has less moisture; thus, the canyon-wall surface is typically composed of exposed bedrock. Subsequently, nearly all of the large landslides in 1976 occurred on the south side of the canyon. In the half-mile reach

downstream from RM 8.0, both sides of the canyon have significant sun exposure, and there was relatively little soil development and forest growth on either side of the canyon. Consequently, the landslides that did occur in this reach were shallow, and the river channel and hydraulics were left relatively unaffected.

LARGEST IMPACTS ON TETON RIVER UPSTREAM OF THE DAM SITE

In the Bitch Creek to Spring Hollow reach, the 1976 landslides had the greatest impact on a 2-mile stretch of river where 3 major rapids now exist, creating a 30.5-foot drop over 3 pools (4, 5, and 6). Pool 4 is the longest of the pools, stretching over 4,000 feet. In the Spring Hollow to Canyon Creek reach, the 1976 landslides had the greatest impact on the Teton River channel in the 2-mile reach upstream from Canyon Creek. In 1972, there was no evidence of deep pools present. However, there are four new major rapids and pools (24, 25, 26, and 27) in this reach today, with pool depths ranging from 9 to 19 feet. The four landslide rapids in this reach have a total drop of 26 feet over a distance of 2.1 miles.

These rapids and pools must be viewed in sequence. For example, the downstream-most rapid (informally known as Parkinson's Rapid) has one of the largest drops in water surface of 16 feet. The relatively short pool that was formed behind this rapid inundates much of the next rapid upstream (informally known as Little Parkinson's Rapid). If the downstream-most rapid were removed, the next rapid upstream would have an even larger drop than the drop through the existing Parkinson's Rapid.

WATER TRAVEL TIME AND TEMPERATURES

The travel time of water flowing through the Teton River canyon from the confluence with Bitch Creek to the confluence with Canyon Creek has increased as a result of the landslide debris fans forming rapids and long, slow-velocity pools in the river channel. At a typical July flow of 1,000 cubic feet per second, the travel time of water has increased from predam conditions by about 6 hours (from 8 to 14 hours). Part of this increase is due to the formation of pools 4, 5, and 6, which have a much higher water surface and deeper depths than predam conditions. The remainder of the increase is due to the four new large rapids between RM 5.3 and RM 7.4. Travel time of water has not changed in the reach between Canyon Creek and the borrow ponds (RM 1.5 to 5.0). Water travel times may have significantly increased through the two large borrow ponds near the dam (RM 0.4 to 1.5), but the magnitude is not precisely known. The two borrow ponds combined are just over 1 mile in length, contain a total water volume of 1.6 million cubic yards (1,000 acre-feet), and potentially increase water travel times by up to 12.5 hours. However, flow patterns through the borrow ponds are complex, due to the presence of a side channel which can bypass flow around the lower borrow pond and the potential for horizontal eddy currents, density currents, and vertical recirculating zones within each borrow pond. The slow moving, or nearly stagnant, water near the borrow pond surface would undoubtedly be warm during the summer months. However, the warm surface water may not necessarily mix with the inflowing river water (which may form a density current) and may not result in a substantial increase in water travel time.

Increased temperature is postulated to result from the increased travel time, and shallow, lower velocity, larger surface area pools resulting from the many small landslides induced by inundation and dam failure that are partially blocking flow. The construction and subsequent failure of Teton Dam has likely increased summer river water temperatures by 1 to 2 degrees Fahrenheit (ºF). Temperatures have increased because flows today move slower through the river pools enlarged by 1976 landslides and through the borrow ponds excavated for the construction of Teton Dam. The loss of riparian trees, especially in the reach downstream of Canyon Creek, also would have contributed to increased river temperatures. Suitable temperatures for trout probably still exist in the deeper portions of the borrow ponds and river pools upstream from Canyon Creek. Most of the temperature gain occurs along the reach of river between pool 24 (7-½ miles upstream of Teton Dam) downstream to Canyon Creek and in the borrow ponds.

During the water temperature monitoring period, all of the data loggers recorded at least one or more temperatures above 60 ºF. Although the 1- to 2-ºF increase in water temperature appears small, the increase could be significant if the natural water temperatures needed by Teton River fish species were already near their threshold. It seems likely that fish can find cooler water temperatures at deeper depths known to exist, but not monitored in this study, as needed during the warmer period of the diurnal cycle. This would suggest that the "lifestyle" of native fish may be affected by forcing them to seek deeper depths during mid- to late afternoon.

BED-MATERIAL COMPOSITION AND SEDIMENT TRANSPORT CAPACITY

In the former reservoir area, the enlargement and development of the 27 pools from the dam failure has affected the river's capacity to transport sediment. The increase in water travel time found in some of the pools has increased the sediment trap efficiency in those pools. This means that finer-grained sediment particles (i.e., sand, silt, and clay) may settle out along the pool bottom and become part of the channel bed material. The change in bed-material particle size, caused by the 1976 landslides, cannot be precisely determined because there is no predam data available. However, bed-material observations and samples collected in the pools upstream from Canyon Creek were compared with the general characteristics of the channel upstream from pool 1 and downstream from Canyon Creek, which is a gravel-bed river.

Upstream from the former reservoir inundation area, the river channel is extremely steep and narrow. The sediment transport capacity in this reach is presumably high, as a result of the river gradient, narrow widths, and high velocities. Between Bitch Creek and pool 1 (the first pool backed up by a landslide-formed rapid), the river has shallow, uniform depths, and the channel bed primarily consists of 3-inch to 6-foot-diameter boulders.

On the basis of sediments observed along the channel bed, measured pool depths and channel widths, and computed water travel times, pools 1-3 appear to be near the maximum storage capacity for sand, and pool 4 has been the major sediment trap along the river. Eventually, pool 4 will fill in to a maximum storage capacity, and fine-grained

sediments will be further transported downstream. Because of its long travel time (over 1 hour), pool 5 will be the next major sediment trap in the river system. The process to nearly fill pool 4 has taken over 20 years and can be expected to take near this amount to fill in pool 5.

The sediment particles along the channel bottom of the pools in the Spring Hollow to Canyon Creek reach are definitely finer than the bed material downstream from Canyon Creek. Silts and clay-sized sediments have deposited along the channel bed in the longer and slower pools. The largest pools (25 and 26) were formed as a result of landslides in 1976 and occurred in a reach (RM 5.5 to RM 6.9) where deep pools were not present in 1972. Therefore, it is likely that the bed material of these pools is much finer today (dominated by sand, silt, and clay) than it was in 1972 (likely dominated by gravel, cobble, and boulder).

PREDICTED EVOLUTION OF RAPIDS

Landslide activity has been an ongoing natural geomorphic process in the Teton River canyon ever since the placement of the Huckleberry Ridge tuff and uplift of the Rexburg Bench. These landslides have been naturally creating rapids and pools in the narrowest reaches of the Teton River canyon for thousands of years. For example, a debris flow that occurred during the last decade enhanced a major rapid and pool in the narrow reach between Badger Creek and Bitch Creek. This reach of the river is upstream from the area inundated by Teton Reservoir. However, fluvial processes have also been at work for thousands of years. This is why all the major rapids formed by prehistoric landslides have been reduced to small rapids and riffles.

Landslides in the Teton River Canyon are an integral part of the canyon evolution. The construction and failure of the Teton Dam have rapidly accelerated those processes in the portion of the river canyon below the high elevation of the former reservoir. The 1976 landslides also significantly reduced the volume of source material available (below the former reservoir level) for future landslides. Therefore, the probability and quantity of future landslides (initiated below the elevation inundated by the former reservoir) have been significantly reduced over the next several centuries to thousands of years.

The 1976 landslides removed material from the lower canyon slopes which could tend to make the upper canyon slopes less stable. However, there is no evidence (through September 1999) that large landslides have occurred in the upper canyon slopes in the last two decades since the failure of Teton Dam. Although the upper canyon slopes have been relatively stable during the last two decades, the probability of future localized landslides on the upper canyon slopes (initiated at elevations above the former reservoir level) may have increased because of material removed from the lower canyon slopes.

The debris fans and rapids formed by the 1976 landslides will eventually be eroded by riverflows, but this process could take centuries. Since 1976, the finer-grained material in the debris fans has been reworked by riverflows, but the coarsest material was left behind, and the rapids and pools are still present. The snowmelt runoff of 1997 produced

the largest flood peak since 1976 and was approximately equal to the 100-year flood. Even this large magnitude flood was only capable of minor reworking of the debris forming each rapid. Therefore, the existing rapids are most likely too large to be eroded by a single flood, and the river will take centuries of abrasion and weathering to erode the rapids. This, of course, reflects the rates of natural processes which have been occurring for many thousands of years.

REFERENCES

Beddow, E., March 1999, Teton River management plan, vegetative resources, draft currently in review, U.S. Bureau of Reclamation (Reclamation) Ecological Planning and Assessment Group, Technical Service Center, Denver, Colorado.

Bowser, S., January 1999, Teton River water temperature investigation report, U.S. Bureau of Reclamation (Reclamation) Land Suitability and Water Quality Group, Technical Service Center, Denver, Colorado.

Carter, B.H., 1976, Field inspection of shallow slides on the Teton Reservoir, Teton Project, Idaho, Reclamation memorandum from Regional Director, Boise, Idaho, to Director of Design and Construction Engineering and Research Center, Denver, Colorado.

Jansen, R.B., 1980, Dams and public safety, a water resources technical publication, U.S. Department of the Interior, Water and Power Resources Service.

Lloyd, L., and J. Watt, March 1981, Post failure landslides, Teton Reservoir, Minidoka Project, Idaho, U.S. Department of the Interior, Water and Power Resources.

Magleby, D.N., 1981, Post Failure Landslides, Teton Reservoir, Minidoka Project, Idaho, U.S. Department of the Interior, Water and Power Resources Service, Boise, Idaho.

Randle, T.J., Bountry, J.A., Klinger, R., Lockhart, A., March 2000, Geomorphology and River Hydraulics of the Teton River Upstream of Teton Dam, Teton River, Idaho,U.S. Department of the Interior, Bureau of Reclamation, Technical Service Center, Denver, Colorado.

Schuster, R.L., and G.F. Embree, April 1980, Landslides caused by rapid draining of Teton Reservoir, Idaho, in Proceedings of the Eighteenth Annual Engineering Geology and Soils Engineering Symposium, hosted by Boise State University.

CONTACT INFORMATION

Jennifer Bountry
PO Box 25007, D8540
Denver, CO 80225-0007
Email: jbountry@do.usbr.gov
Phone: (303) 445-3614

Timothy Randle
PO Box 25007, D8540
Denver, CO 80225-0007
Email: trandle@do.usbr.gov
Phone: (303) 445-2557

SPATIAL VARIATION OF INCISION AND DEPOSITION WITHIN A RAPIDLY INCISED UPLAND WATERSHED, CENTRAL NEVADA

Dru Germanoski, Professor and Head, Geology and Environmental Geosciences, Lafayette College, Easton, PA; Carolyn H. Ryder, Geology and Environmental Geosciences, Lafayette College, Easton, PA; Jerry R. Miller, Whitmire Professor of Environmental Science, Department of Geosciences and Natural Resource Management, Western Carolina University, Cullowhee, N.C.

INTRODUCTION

The Great Basin of central Nevada is characterized by north-northeast trending ranges that are separated by intermountain basins. The mountain ranges contain numerous small, watersheds, many of which possess wet meadow (or wetland) ecosystems along their riparian corridors. These ecosystems are characterized by shallow water tables that support water-loving plant assemblages (Castelli and Chambers, 2000) and that provide important habitat for a number of endemic, migratory, and endangered species. Many of the wetland areas have been affected by episodes of axial channel instability during the late Holocene. We have been studying a number of these watersheds in the Toiyabe, Toquima, and Monitor Ranges to develop an understanding of drainage basin response to small scale climate change and land use (Chambers et al, 1998; Miller et al, in press).

The most recent episodes of instability have been dominated by channel incision. In addition to the physical destabilization of the stream channel itself, channel incision often results in the degradation of riparian ecosystems. Channel downcutting can, for example, de-water wet meadows by lowering the groundwater base level. In many cases, the net result is a shift from wet to mesic or dry meadow plant assemblages. Extensive field reconnaissance in central Nevada has demonstrated that wet meadows are typically located immediately upstream of mid- to late Holocene age side-valley alluvial fans that prograde into the mainstem valleys. The fans are characterized by coarse bed material that armors the channel floor against erosion. However, once this armor is breached, incision progresses upvalley into the adjacent meadow through knickpoint migration.

The basins that we examined have a common history of hillslope erosion and valley-sedimentation associated with the onset of the post neoglacial drought approximately 2500 years BP, followed by one or more episodes of channel incision (Chambers et al, 1998; Miller et al, in press). The most recent period of downcutting began as much as 290 years ago and many systems are still actively incising or are in the incipient stages of incision (Miller et al, in press). During episodes of channel incision, erosion is not uniformly spaced throughout any single drainage system and downcutting in one place produces sedimentation in other locations. Whereas the stratigraphic record is sufficient to allow the erosional and depositional history to be deciphered with respect to major events, the exact spatial distribution of incision and deposition is not clear. Moreover, episodes of channel incision are fairly prolonged in most systems, occurring over periods of years, decades, and perhaps centuries. Consequently, it is very difficult to reconstruct

the sequence of events and the spatial distribution of incision and deposition in any single basin. Furthermore, because the period of incision is prolonged, it is not clear whether groundwater flow contributes significantly to channel erosion.

In May, 1998, Marshall Canyon in the Toiyabe Range just south of Austin, Nevada was incised catastrophically over a period of days in response to spring rainfall and the melting of a large winter snowpack. The pattern of erosion and deposition was not spatially consistent down the length of the channel. Rather, erosion, sediment transport, and deposition occurred in discrete zones along the riparian corridor. The basin also experienced an episode of erosion following a wildfire in 1981 that was followed by above average precipitation in 1982 and 1983. Although we did not study the effects of that episode of erosion in detail, we did reconnoiter the basin in 1992 while studying the impacts of the wildfire on an adjacent watershed (Germanoski and Miller, 1995). Reconnaissance of the Marshall Creek shortly after it was incised in June, 1998 suggested that groundwater discharge and groundwater sapping were integral to the erosion process.

STUDY AREA

Marshall Canyon is a 4.9 square kilometer drainage basin positioned on the western slope of the Toiyabe Range approximately 2 kilometers south of Austin, Nevada (Figure 1). The Toiyabe Range is located in central Nevada and extends north-northeast for approximately 193 kilometers (Figure 1). Marshall Creek drains west into the Reese River valley. Four perennial springs have been mapped at the head of Marshall Canyon and serve as the Austin municipal water supply.

The drainage basin is underlain by quartz monzonite and granodiorite of the middle Jurassic age Austin pluton (Stewart and McKee, 1977). Soils are poorly developed and hillslopes are mantled by grus that has accumulated from weathering of the underlying crystalline rocks. The coarse-grained grus may also represent lag deposit formed as finer grains were removed by erosion in the past, particularly during the post Neoglacial drought (Miller et al, in press). Vegetation in Marshall Canyon consists of nettles, wild roses, willows, sagebrush, and grasses. Sagebrush and grasses grow on the valley floor and on valley sides and willows and roses are restricted to the riparian corridor. Aspen groves grow near springs at the head of the drainage.

The climate in Austin, Nevada, is semi-arid to arid. The average summer and winter temperatures are 21° C and -1° C, respectively. Average annual precipitation is 38.8 centimeters. Precipitation occurs primarily between November and May. June through October are dry with occasional thunderstorms (Stewart and McKee, 1977). Austin does not receive much precipitation in the form of rain. Most of the precipitation falls as snow that may persist until late spring and produce significant runoff. Streams in 1973,

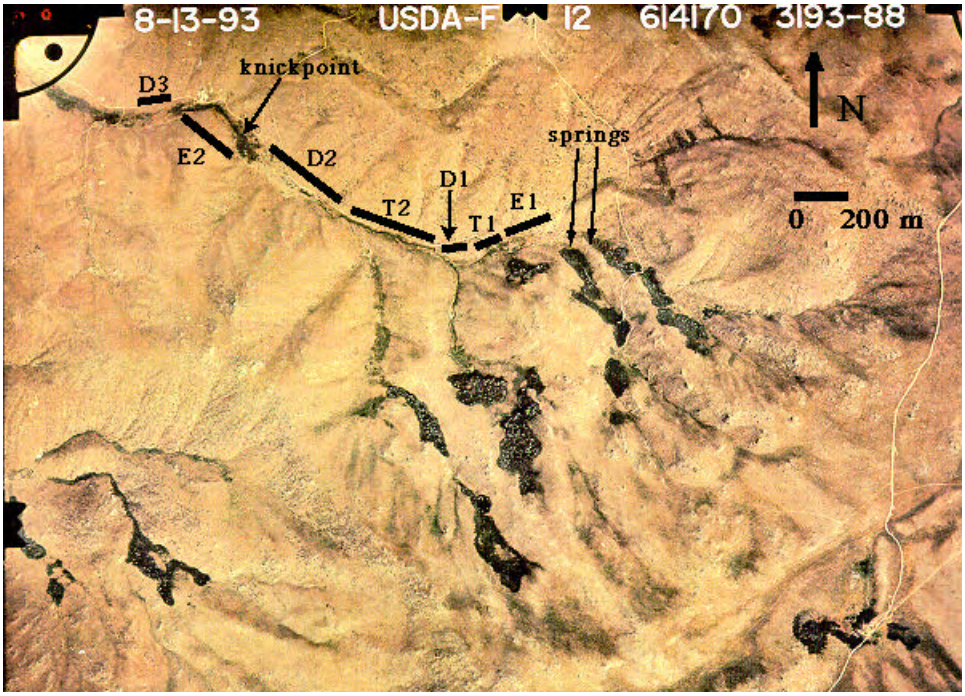

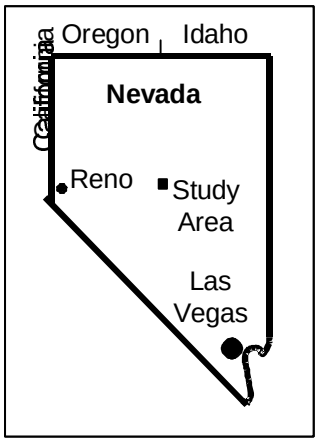

Figure 1. Location map showing distribution of erosional (E), transport (T), and depositional (D) reaches along Marshal Creek.

1975, 1978, 1983, and 1984 experienced relatively high discharge; 1983 had the highest discharge for the period of record (Miller et al, in press).Marshall Canyon is roughly rectangular in shape. The basin pinches out at the point of lowest relief, which is at the mouth of the canyon to the west. The drainage basin is approximately 3.5 kilometers long with a maximum relief of approximately 840 meters, and can therefore be described as being relatively steep and rugged.

METHODOLOGY

The drainage basin was reconnoitered in 1992 and areas of erosion and deposition that occurred in response to the 1981 wildfire were noted. After the 1998 erosional event, zones of erosion, sediment transport, and deposition were mapped on an aerial photograph. The distinction between sediment deposited in 1982-83 and 1998 was based on the degree of weathering and cementation as viewed in hand dug pits and exposures produced by channel incision. The 1983 deposits were partially cemented and more cohesive than those created in 1998. The thickness of both deposits was also determined using the burial depths of vegetation. A longitudinal profile was surveyed along the channel using a Leica total station. Measurements were taken at 20-meter intervals for

1440 meters downvalley. Additional points were surveyed to identify features of interest such as terraces, knickpoints, or the locations of cross-valley profiles. A series of 18 cross-valley profiles were measured along the valley floor using a tape measure, stadia rod, and Abney level. Cross profiles were positioned at 100-meter intervals. Additional cross-valley profiles were measured in areas of significant incision or deposition.

PATTERNS OF EROSION AND DEPOSITION

The 1982-83 event created at least two major zones of erosion that are separated by a zone of deposition. However, it is unclear whether more complex patterns of erosion and deposition were produced during the 1980s because we were not specifically studying Marshall Canyon when we examined the basin in 1992, and some of the alluvial deposits may have been reworked by the 1998 event. Observations made in June 1998, immediately following valley incision, indicate that there were two distinct erosional zones, three distinct transport zones, and three depositional zones. The two segments of channel that were entrenched in 1982-83 served as transport zones during the 1998 event. The major depositional zone received sediment during both episodes of instability. Following the initial pulse of deposition, the depositional zones were re-incised to varying degrees. Thus, there was a shift in process dominance through time.

The zones of erosion, transport, and deposition associated with the 1998 event are mapped on the aerial photograph shown in Figure 1. Each zone is numbered consecutively from upstream to downstream. Erosion zone 1 begins below the confluence of springs located at the head of the drainage and extends for approximately 160 meters downstream. It suffered the greatest amount of erosion in 1998, reaching maximum depths of approximately 6 meters. The main gully was flat-floored and approximately 7-10 meters wide with vertical channel walls. It terminated upstream in three amphitheater-shaped, vertical headcuts that were separated by narrow "islands" of valley fill. There were no surface channels feeding two of the three headcuts, but the middle headcut may have received some runoff from a nearby road. The incision that occurred along this reach damaged the water supply lines to the town of Austin. As a result, a pipe was installed at the base of the headcut almost immediately after incision occurred to re-supply Austin with water from the springs. In addition, the channel floor was armored with rip-rap to limit further erosion and damage to the new piping. The trench was subsequently filled, and the valley floor reseeded, in late July, 1999.

Below the deeply incised reach, sediment was routed through a V-shaped transport zone (transport zone 1) that was produced by incision in 1982-83. The transport zone was approximately 3 meters deep, 9 meters wide at the valley floor and tapered to less than a meter wide at the thalweg. It extended downstream for approximately 100 meters. Valley gradient in the transport zone was 0.12 (Figure 2). In 1998, localized deposition and subsequent incision produced isolated inset terraces within the reach. Vegetation preserved on the banks of the channel indicated that this segment was not significantly modified either by erosion or deposition during the 1998 event. Sediment evacuated from erosion zone 1, and routed through transport zone 2, was deposited downstream in

depositional zone 1 (Figure 1). The deposited sediment formed a discrete lobe-shaped feature that began as an inset channel fill that then spilled out over the valley floor. The inset fill was comprised of sediment as much as 0.5 meters thick (and was later incised to form an inset terrace). The overbank lobe of debris was 60 meters long, exhibited a maximum width of 11 meters, and ranged in thickness from a maximum of 0.4 meters to a minimum of 0 meters at the margins. The average thickness was approximately 0.15 meters. The valley gradient decreased from 0.12 in transport zone 1 to 0.080 to 0.055 in the depositional zone 1 (Figure 2).

The vast majority of the sediment produced by incision in erosion zone 1 was passed through depositional zone 1 to a second V-shaped transport zone (transport zone 2) that was also carved by erosion in 1982-83 (Figure 1). Transport zone 2 was nearly 300 meters long, as much as 4.5 meters deep, and tapered in width from as much as 10 meters at the valley floor to approximately 2 meters at the thalweg. The channel gradient increased from depositional zone 1 through transport zone 2 (Figure 2). Similar to transport zone 1, the integrity of rose bushes and other vegetation lining the trench walls indicate that this channel segment was not significantly altered by erosion or deposition during the 1998 event.

Transport zone 2 discharged sediment into a very large depositional zone where most of the sediment produced by upstream erosion was deposited. The morphology of the depositional lobe is very similar to that of depositional zone 1. The deposit begins as an inset channel fill within the lower reaches of transport zone 2 and then spread out as a discrete lobe across the valley floor. The inset fill (now preserved as several inset terraces) is located in the lower 75 meters of transport zone 2. The inset terraces are less than 0.5 meters thick, but are continuous along the reach. The depositional lobe on the valley floor is almost 400 meters long and has a maximum width of 75 meters. Sedimentary deposits completely filled the pre-existing channel to a depth of as much as 1.5 meters and then spread out across the valley floor to a maximum thickness of 0.4 meters. The deposit split into two lobes at its downstream end. The valley floor gradient decreases from 0.105 at the downstream end of transport zone 2 to as low as 0.045 (Figure 2). The valley floor reaches its maximum width of 80 meters along this depositional reach. Both the lobe of debris and the channel were re-incised to depths ranging from 0.5 to 1.5 meters following the initial phase of deposition. The 1998 deposits are locally cut into a sequence of stair step terraces with scarp heights on the order of centimeters to tens of centimeters. Observations made in June 1998 indicate that this incision occurred almost immediately after sedimentation ceased. Indeed, we suspect that this incision may have occurred during the waning stages of the maximum discharge event in May, 1998. The geomorphology of depositional zone 2 was complicated in June 1998 when a bulldozer was used to divert water from a gully that formed on the north side of the valley into the main channel on the south side of the valley. Examination of the stratigraphy exposed in the gullies, along with observations made in 1992, indicate that depositional zone 2 is also composed of sediment produced by incision of transport zones 1 and 2 during 1982-83. The grain size distributions for sediment samples collected in erosion zone 1 (the main source of 1998 sediment), depositional zone 2 (1982-83 and

1998 samples), and depositional zone 3 (1998 sample) are remarkably similar. The median grain diameter for each sample is approximately 1 mm and the size distribution curves are parallel to nearly superimposed.

The valley floor in depositional zone 2 is wide, gently sloping, and covered by wild rose thickets and willows along the channel. In many respects it is morphologically similar to wet, mesic, and dry meadows complexes that we have studied in other mountain drainages in central Nevada (Miller et al, in press). The natural channel is not deeply incised where it traverses the meadow (average incision ranges from less than 0.5 to 1.5 meters). However, depositional zone 2 transitions very abruptly downstream into an incised segment via vertical headcuts produced by two channels. These channels are now migrating headwardly into the meadow of the depositional zone. We refer to the reach below the headcuts as erosion zone 3 (Figure 1). Incision along this segment appears to have begun well before the 1998 event and is currently ongoing, albeit slowly. The surface channels feeding the headcuts possess very little flow and morphologically consist of very narrow, vertical slots. The larger of the two headcuts is 1.9 meters high and has a maximum width of 25 centimeters at the valley floor. Downstream the entrenched channel widens to 4 meters at the top of the channel bank.

Erosion zone 3 grades smoothly into deposition zone 3. Deposition zone 3 consists of a sediment lobe approximately 71 meters long with a maximum width of 21 meters. The deposit ranges from a maximum of 0.2 meters to 0 at the margins. This sediment may have been derived from as far away as erosion zone 1 as suggested by the near coincidence of grain size distribution curves.

DISCUSSION

Eyewitness accounts of the 1998 event describe it as a "mud flow" or a "slurry". These descriptions along with other observations suggest that the initial erosion and headcut migration in erosion zone 1 resulted from groundwater saturation of the valley fill. The site is located below the confluence of two mapped springs, one of which served as the water supply for the town of Austin. The water supply manager who has been involved in horizontal drilling near the springs stated that, " the groundwater hangs up on a clay seam and bedrock and pours out of the sand." There was absolutely no evidence that any of the three headcuts were fed by significant surface water runoff. In fact, the valley floor upstream of two of the headcuts is devoid of channelized flow and a small channel less than 10 centimeters deep and less than a meter wide heads above the third headcut. We speculate that prolonged snowmelt in the spring of 1998 was able to recharge the shallow groundwater aquifer and saturate the alluvial fill to the point of failure. These observations strongly suggest that groundwater seepage and sapping played a critical role

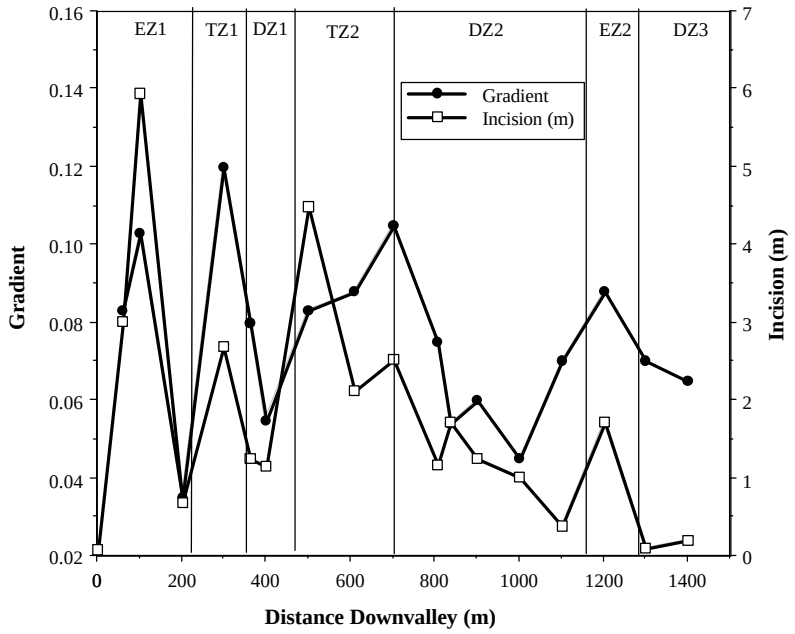

Figure 2. The relationship between erosion, deposition, and channel gradient. Segments labeled EZ are erosion zones, segments labeled TZ are transport zones, and segments labeled DZ are depositional zones. Transport zones 1 and 2 were entrenched in 1982-83 and depositional zone 2 was a depositional zone in 1982-83 and 1998.

in initiating erosion of the valley fill in erosion zone 1 in 1998. Groundwater erosion also appears to have played a prominent role in the incision of the meadow at the lower end of depositional zone 2 where significant seepage is visible at the base of the headcut. The morphology of the headcut and surface channel (which is 1.9 meters high and 0.25 meters wide), combined with the observation that flow increases dramatically at the base of the headcut, suggest that this channel was cut largely by groundwater. Currently, the headcut is migrating upstream through groundwater sapping.

Although sapping and valley fill saturation may have been very important in generating erosion, the fact that sediment deposited in depositional zones 1, 2, and 3 are characterized by planar laminations indicate that, once the sediment was mobilized, it was transported and deposited by fluvial processes rather than by debris flow or hyperconcentrated flow. Furthermore, the re-incision of the inset terrace and sediment lobes in the transport and depositional zones indicates that the event evolved from a sediment laden transport and depositional event to a more sediment starved flow. Because we did not witness the erosional event we hesitate to say the event was indeed a debris flow or hyperconcentrated flow. Nonetheless, we are confident of the assertion that groundwater played a prominent role in the early phase of the event and that it continues to be important in the evolution of the headcut located in erosion zone 2.

Maximum erosion in the 1998 event occurred in areas where the valley gradient was steepest (Figure 2). This is true for both erosion zones 1 and 2. Likewise, transport

zones 1 and 2, which were eroded in 1982-83, were incised in relatively steep portions of the valley floor (Figure 2). This is not surprising. Incision would be expected to occur where channel gradients, and shear stress are high. Nonetheless, the result is significant because there is a rational explanation for the nonuniform pattern of geomorphic processes. Deposition occurred where channel gradients decreased and valley floor widths increased (Figure 2). The inset terraces in the downstream ends of transport zones 1 and 2, where valley gradients are still fairly high, suggest that sediment backfilled into these transport zones after sediment was deposited in depositional zones 1 and 2 (Figure 2). However, erosion was not exclusively controlled by valley morphology. Although valley gradients were steep in transport zones 1 and 2, significant incision did not occur, apparently because these reaches had already been entrenched and the deep V-shaped channels were efficient at routing sediment downstream. Thus, the distribution of incision and deposition was controlled by channel gradient, valley width, channel history, and the availability and nature of groundwater reservoirs.

These observations are helpful in the evaluation of the patterns of erosion and deposition in other mountain drainages throughout central Nevada. Perhaps of greater importance, the influence of groundwater on incision has provided insights that are otherwise, easily overlooked. The implications are that: (1) once incision is initiated in a wet meadow, and the groundwater reservoir is tapped, groundwater seepage and sapping may play an increased role in the erosion process, and (2) in addition to basic controls such as valley gradient, the erosional history of the drainage network may well dictate where erosion, transport, or deposition occurs.

REFERENCES

Castelli, R. M., J. C. Chambers, and R. J. Tausch. 2000. Soil-plant relations along a soil-water gradient in Great Basin riparian meadows. Wetlands 20(2): 251-266.

Chambers, J.C., Farleigh, K, Tausch, R.J., Miller, J.R., Germanoski, D., Martin, D., and Nowak, C. 1998. Understanding long- and short-term changes in vegetation and geomorphic processes: The key to riparian restoration? Rangeland Management and Water Resources Proceedings. Edited by D.E. Potts. American Water Resources Association 101-110.

Germanoski, D. and Miller, J.R. 1995. Geomorphic impact of wildfire in an arid watershed, Crow Canyon, Nevada. Physical Geography 16(3):266-279.

Miller, J.R., Germanoski, D., Waltman, K., Tausch, R.J., and Chambers, J.C. Influence of Late Holocene hillslope processes and landforms on modern channel dynamics in upland Watersheds of Central Nevada. In press Geomorphology.

Stewart, J.H. and McKee, E.H. 1977. Geology and mineral deposits of Lander County, Nevada. Nevada Bureau of Mines and Geology Bulletin 88.

EPISODIC MOUNTAIN EROSION INFERRED FROM SEDIMENT YIELDS OVER DECADES AND MILLENNIA

James W. Kirchner, Department of Earth and Planetary Science, University of California, Berkeley, CA, 94720-4767, (510) 643-8559, kirchner@seismo.berkeley.edu;
Robert C. Finkel, Center for Accelerator Mass Spectrometry, Lawrence Livermore National Laboratory, Livermore, CA;
Clifford S. Riebe, Department of Earth and Planetary Science, University of California, Berkeley, CA;
Darryl E. Granger, Department of Earth and Atmospheric Sciences, Purdue University, West Lafayette, IN;
James L. Clayton and John G. King, Rocky Mountain Experiment Station, USDA Forest Service, Boise, ID;
Walter F. Megahan, National Council for Air and Stream Improvement, Sequim, WA

Abstract Documenting erosion rates, patterns, and processes is crucial for understanding how mountainous regions evolve, for assessing the erosional impacts of land use, and for predicting how sediment loading will affect stream ecosystems. At 32 watersheds on the Idaho batholith, we measured catchment-scale sediment yields over 10,000-year timescales using in-situ cosmogenic ^{10}Be in alluvial quartz grains, and compared these with conventional measurements of sediment yields over much shorter timescales (10-84 yr, mean=24). Here we show that at every site, long-term rates of sediment yield (55-327 T km^{-2} yr^{-1}, mean=145) are many times higher than rates measured over years or decades (2.5-30.0 T km^{-2} yr^{-1}, mean=10.5). The discrepancy between short-term and long-term sediment yields averages 17-fold, and is consistent across catchments ranging over five orders of magnitude in size, from small experimental watersheds (0.2 km^2) to large river basins (35,000 km^2). Neither methodological differences nor climatic changes can explain the mismatch; instead, these measurements indicate that long-term average sediment yields are dominated by episodic erosion events that are too rare to be reliably observed in typical sediment yield studies. Our data show that conventional sediment yield measurements, even when made over decades, can greatly underestimate long-term average rates of sediment delivery, and thus greatly overestimate the lifespan of engineered reservoirs. Our observations also indicate that sediment delivery is extremely episodic, sporadically subjecting mountain stream ecosystems to extensive disturbance.

GRAVEL ENTRAINMENT AND SCOUR IN STEEP HEADWATER CHANNELS

Alan F. Barta, Research Geomorphologist, Rocky Mountain Research Station, U.S.D.A. Forest Service[1], 316 East Myrtle Street, Boise, ID 83702-7678 (Phone: 208-373-4393, Fax: 208-373-4391, Email: abarta@fs.fed.us).

Abstract: Steep headwater channels differ markedly from lower gradient channels in their morphology and the processes that control sediment transport. These differences are important considerations for land and water management decisions as the response of these channels to changes in water or sediment supplies can also be very different than for lower gradient channels. Gravel deposits in steep streams provide important habitat for spawning fish and benthic invertebrates. This paper summarizes observations of gravel entrainment and scour in steep streams in California and suggests techniques for predicting the stream discharge required for gravel entrainment in similar systems. These techniques are of two general types, those based upon flow hydraulics and those based upon a consistent correlation between entrainment and flows of a specific magnitude or frequency.

INTRODUCTION

Predicting the discharges that transport bed material in steep streams is useful for a host of practical applications and presents a significant challenge to those who seek to understand sediment mechanics and stream morphology. The practical utility of accurately estimating entrainment and transport would include specifying flows for river maintenance, assessing the impacts of land use changes or reduced sediment supply from upstream dams, and reserving water rights to maintain aquatic habitat. The challenge lies in the greater complexity of the flow and sediment transport mechanics of steep streams (Furbish, 1993). Accurately estimating the flows that entrain gravels in steep boulder-bed channels is useful even though these gravels usually only compose a small proportion of the streambed because they provide important habitat for benthic organisms and spawning fish (Kondolf *et al.*, 1991). Typically, these gravels are found in isolated pockets protected by local flow obstructions. Flow around and over obstructions is complex and depends strongly on the geometry of individual boulders and the local channel morphology. Thus, prediction of entrainment from conventional hydraulics and bedload transport theory is impractical (Barta *et al.*, 1994).

Sediment transport has been correlated with a range of flow variables, often with the goal of finding an effective regional predictor. For example, the discharge producing the largest cumulative transport in alluvial streams has been correlated to floods that occur about every 1.5 years and to the discharge that fills the river channel (Wolman and Leopold, 1957; Wolman and Miller, 1960; Woodyer, 1968; Pickup, 1976). Also, it has been suggested that the flow initiating transport in gravel-bed rivers is a constant proportion of the discharge that fills the channel (Parker, 1979; Andrews, 1984).

In alluvial channels, a consistent correlation between flow frequency and some measure of sediment transport depends implicitly on the assumption that the river channel adjusts its size and shape to the imposed range of discharge and sediment supply (Mackin, 1948; Leopold and Maddock, 1953). Only if this adjustment is consistent across a range of channel types and environments might one expect that a particular flow frequency would be related to some measure of transport. This assumption of self-adjusted channels does not usually hold for steep mountain streams because they are not always free to adjust their size and shape (e.g. due to the presence of bedrock or large boulders deposited in the streams by glacial or hillslope processes). The possibility remains, however, that the gravel available for transport in steep streams may adjust its disposition within the existing channel in such a way that a consistent correlation exists between flow frequency and gravel transport. The goal of this paper is to investigate whether such a correlation exists.

---

1 The U.S. Department of Agriculture (USDA) prohibits discrimination in all its programs and activities on the basis of race, color, national origin, sex, religion, age, disability, political beliefs, sexual orientation, or marital or family status. (Not all prohibited bases apply to all programs.) Persons with disabilities who require alternative means for communication of program information (Braille, large print, audiotape, etc.) should contact USDA's TARGET Center at (202) 720-2600 (voice and TDD). To file a complaint of discrimination, write USDA, Director, Office of Civil Rights, Room, 326-W. Whitten Building, 1400 Independence Avenue, SW, Washington, D.C. 20250-9410 or call (202) 720-5964 (voice and TDD). USDA is an equal opportunity provider and employer.

Although the conditions and frequency of transport in steep channels may differ from those in alluvial channels with a milder slope, the motivation for identifying a consistent transporting flow frequency is the same. The primary objective is to estimate sediment yield, either for practical modern purposes or for understanding landscape evolution on a geological time scale. The practical applications range from engineering hydroelectric facilities to the ecological restoration of critical habitat.

MECHANICS OF GRAVEL ENTRAINMENT IN STEEP STREAMS

The dominant mechanism for gravel entrainment in steep boulder-bed channels is obstruction overtopping (Barta *et al*., in press). Simple empirical relationships using flow depth, *h*, obstruction height, *H*, channel width, *w*, and channel slope, *S*, have been developed from tracer particle studies to predict pocket gravel entrainment (Barta *et al.,* in press). In this paper I use one of these empirical relationships to estimate entrainment producing discharges.

This entrainment prediction relationship was developed from three years of flow and entrainment observations on five streams in the eastern Sierra Nevada, California (Table 1). Detailed descriptions, reach maps, and photographs of each stream can be found elsewhere (Barta *et al.,* in press) so only a brief description is provided here. The sites include a range of bed gradients and channel widths representative of steep boulder-bed channels. The bed slopes range from 2 to nearly 12% and channel widths range from 3 to 7 m. All sites are near gaging stations with at least 15 years of record. Median grain sizes for the pocket gravels are between 13 and 56 mm. Three of the study sites are unregulated; two study sites are downstream of run-of-river hydroelectric reservoirs. High flow events occur as a result of snowmelt or winter storms.

Table 1. Obstruction Heights and Gravel Entraining Discharges

Site Name	S Bed Slope (m/m)	$\tilde{H}$ Median Obstruction Height (m)	h_{ent} Gravel Entraining Flow Depth (m)	Q_{ent} Gravel Entraining Discharge (m^3/s)	Q_{bf} Bankfull Discharge (m^3/s)
Blackwood Creek	0.020	0.40	0.35	0.95	4.0
General Creek	0.035	0.50	0.40	2.50	2.8
Bishop Creek above Power Plant 3	0.050	0.54	0.38	1.90	5.5
Bishop Creek above Power Plant 2	0.057	0.78	0.51	2.10	5.0
Horton Creek	0.116	1.09	0.33	0.75	1.0

An empirical relationship that reliably defines a pocket gravel entrainment threshold is used here because it was not practical to be at each stream at the exact moment that gravel was entrained. Rather, a range of discharges higher and lower than the gravel entraining discharge were observed. A fuller explanation of the development of this empirical entrainment relationship can be found in Barta and others (in press) and is expressed as:

$$h^*_c = 0.8 - \left(\frac{\tilde{H}}{w} \right)^{1+S} \qquad (1)$$

where h^*_c is the critical obstruction submergence (h/H) for gravel entrainment, $\tilde{H}$ is the median obstruction height, w is the bankfull channel width, and S is the bed slope. Because obstruction overtopping is the dominant mechanism in pocket gravel entrainment, I expect that as h^*_c approaches unity (0.8 in Equation 1) then mobilization of the pocket gravels occurs by flow cascading over the obstruction. The second term accounts for the influence of obstruction size relative to channel width, the greater transverse flow in the bank region (implicitly with w in $\tilde{H}/w$), and the greater influence of larger and more frequent steps with increasing channel gradient (S).

Estimating the entraining discharge (Q_{ent} in Table 1) using Equation 1 requires the median height of the obstructions, bed slope, and a flow depth-discharge rating curve. The median height of flow obstructions is determined by measuring the height of all obstructions adjacent to gravel pockets in the reach. A depth-discharge

rating curve may be easily developed from the stage-discharge rating curve and geometry of one or more stream cross sections (Barta and Wilcock, in preparation).

FLOW FREQUENCY ANALYSIS

The objective of the flow frequency analysis was simply to relate the discharge that is associated with gravel entrainment to historical flow frequencies and measures of the channel morphology. For historical flow frequencies, the recurrence interval from peak flow analysis, the exceedence probability from a flow duration curve of daily mean flows, and a multiple of the average annual mean daily flow were identified. To relate to channel morphology, gravel entraining flows were evaluated as a proportion of bankfull discharge.

The objective of the flow frequency analysis was simply to relate the discharge that is associated with gravel entrainment to historical flow frequencies and measures of the channel morphology. For historical flow frequencies, the recurrence interval from peak flow analysis, the exceedence probability from a flow duration curve of daily mean flows, and a multiple of the average annual mean daily flow were identified. To relate to channel morphology, gravel entraining flows were evaluated as a proportion of bankfull discharge.

All streams had at least one stream gage but the gages varied in their proximity to the flow and entrainment observation reaches so adjustments to the gage records were necessary for some sites. At Blackwood Creek the gage was within the study reach so no corrections were necessary. In all cases except Bishop Creek, these adjustments were relatively simple. Peak and mean daily flows at General and Horton Creeks were adjusted according to the following equation:

$$Q_u = Q_g \left(A_u / A_g \right)^{0.8} \qquad (2)$$

where Q_u is the discharge at the ungaged site, Q_g is the discharge at the gaged site, A_u is the drainage area for the ungaged site, A_g is the drainage area for the gaged site, and the exponent 0.8 was recommended for peak flow adjustments in eastern Sierra streams by Blakemore and others (1995). Only the higher discharge portion of the flow duration curve is capable of mobilizing gravel so I used the same correction for mean daily flow. Thus, although errors in discharge adjustment may be greater at low flows, these flows are unlikely to move gravel and their ordering is unchanged, so it will not substantially bias the results.

The two study sites on Bishop Creek required the greatest adjustment of gage records because of the storage reservoirs and ungaged inflow between gages. A consultant to the reservoir operators recently completed a comprehensive analysis to estimate discharge throughout the Bishop Creek drainage for both regulated and natural conditions (Simons *et al.*, 1990) and I used their flow frequency estimates. Separate analyses were done for mean daily flows and annual peak flows. The mean daily flow analysis was based on the principle of continuity where the total of all ungaged flow was computed as the differences between all recorded inflows and outflows under current regulated conditions. Timing was ignored because, given the small size and steepness of the basin, sufficiently accurate estimates of daily flows were expected without considering timing. Ungaged flow was distributed based upon drainage area and an assumed annual unit runoff identical to similar and adjacent gaged areas.

The natural flow sequence of mean daily flows that would occur in the absence of reservoirs and diversions was computed by eliminating the effects of reservoirs and diversion from the computed regulated flow history. These effects were eliminated using a simple storage equation:

$$I - O = dS / dt \qquad (3)$$

where I is the inflow rate, O is the outflow rate (including an evaporation correction), and dS/dt is the change in storage with respect to time. Because this is done for the entire storage system beginning at the headwaters, the inflow (I) is equivalent to the natural (unregulated) mean daily flows. Annual peak flow frequency curves for regulated conditions were developed from three gages in the Bishop Creek drainage with a fifteen year period of record and interpolated for intermediate sites. No adjustments were made for regional skew because the recorded flows are strongly influenced by flow regulation.

Peak Flow Analysis

Peak flow analysis was done following the guidelines established in the Water Resources Council Bulletin 17B (1981) where sufficient historical flow records were available. This is the most widely used approach to developing flood frequency curves in North America and is incorporated in software developed by the U.S. Geological Survey (PEAKFQ) and used for this analysis. This procedure requires at least 10 years of annual instantaneous peak flow data.

Peak flow analysis can be done with either a series of annual-maximum floods or with a partial-duration series that includes all independent peak floods over a threshold discharge. Analysis using annual-maximum peaks provides estimates of the probability of an annual-maximum flood exceeding a computed value and it' s inverse, the probable annual-maximum recurrence interval. The partial-duration series estimates the average frequency of occurrence between floods of a given size without regard to their relationship to the year. The differences in return intervals between annual-maximum and partial-duration series are negligible for periods of 10 year and longer; the utility of the partial duration series thus is for more frequent events, whose actual return intervals may be overestimated with the annual maximum series. For computational ease, a relationship exists between annual-maximum return intervals and partial-duration return intervals as defined below in Equation 4 (Stedinger *et al.,* 1993).

$$T_p = -\frac{1}{\ln(1-1/T_a)} \qquad (4)$$

where T_p is the average return interval for the partial-duration series and T_a is the average return interval for the annual-maximum series. I computed the annual-maximum return interval using the U.S. Geological Survey' s PEAKFQ software (Kirby, 1981) and then found the partial-duration return intervals using Equation 4.

For Blackwood and General Creek at least 10 years of peak flow data was available and used for the analysis. The records for the stream gage on Horton Creek only include mean daily flows and not instantaneous peaks. For Bishop Creek, I had computed peak flows for both natural and regulated conditions for three locations in the Bishop Creek drainage but not directly for the study reaches.

An alternative method of estimating the annual flood frequency when gaged instantaneous peak discharges are not available is to use a regional regression equation. I have used the regional regression equations developed by Blackmore and others (1995) for the Eastern Sierra to estimate the discharge of the 2, 5, 10, 25, 50, and 100 year floods for all sites. Flood frequency curves are shown in Figure 1.

Flow Duration Curves and Mean Annual Flow

Mean annual flow was computed using the arithmetic average of gaged mean daily flow. The period of record ranged from 13 to 33 years for the study streams. For the Bishop Creek sites there is a mean annual flow for regulated conditions (actual) and for unaltered natural flows. The values for natural flows are based upon an adjustment of the regulated flows using Equation 3 as discussed earlier (Simons *et al.,* 1990). Flow duration curves based upon the mean daily flows are plotted for all sites on Figure 2.

Bankfull Flow

Bankfull discharge (Q_{bf}) is widely used as a parameter to describe both flow magnitude and channel morphology. This widespread use is the reason I attempt to relate gravel entrainment to Q_{bf} here. Conceptually, Q_{bf} is the flow that just fills the channel to the tops of the banks (Williams, 1978). Despite this conceptual simplicity, precisely defining or determining the Q_{bf} for a channel cross section or stream reach has proven to be difficult, especially for headwater channels with poorly defined banks. For this reason, at least ten more specific definitions and methods for determining Q_{bf} can be found in the geomorphic literature (see Williams, 1978, for a concise review and evaluation). The estimate of Q_{bf} follows recommendations made by Williams (1978) to first identify the elevation of the floodplain profile and then read the discharge from a section with a known stage-discharge relationship. These estimate of Q_{bf} are listed in Table 1.

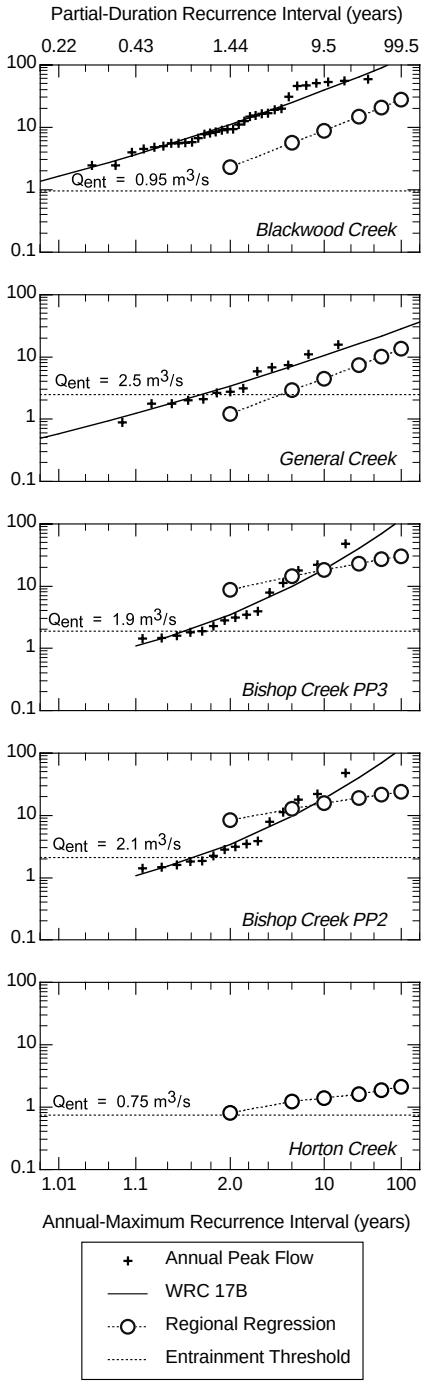

Figure 1. Peak-flow frequency curves for study streams. Flood frequency curves were developed following the recommendations of the Water Resources Council (1981) where sufficient data were available. Regional regression estimates of flood frequency were computed using the methods of Blakemore and others (1995). Entrainment threshold (Q_{ent}) shown for reference.

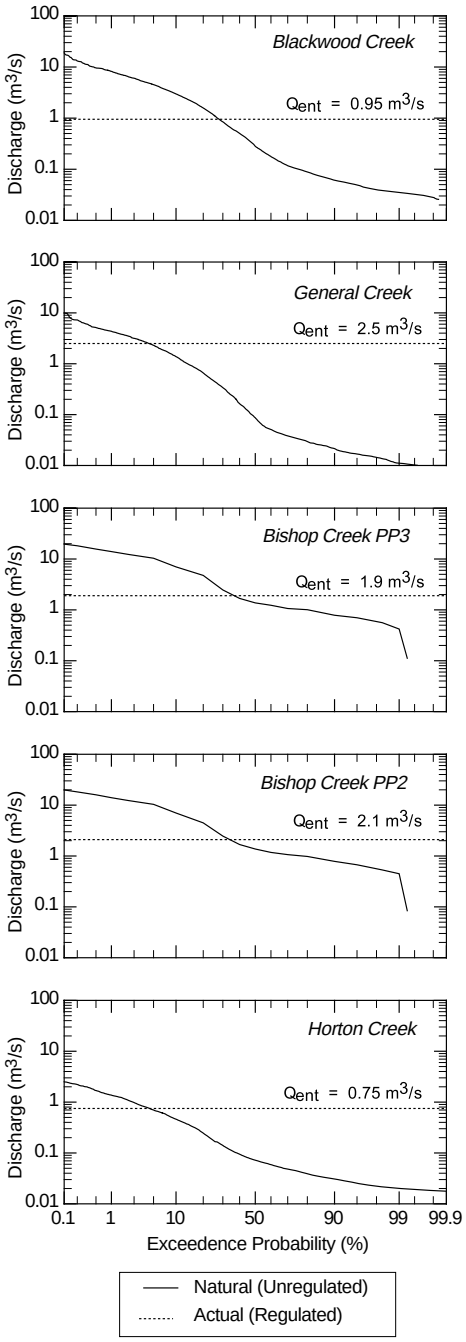

Figure 2. Flow duration curves of mean daily discharge for study reaches. Solid curves are for natural flow conditions (i.e. no flow regulation). For the Bishop Creek sites, a dashed line shows the flow duration curve for regulated conditions. Entrainment threshold (Q_{ent}) shown for reference.

RESULTS AND DISCUSSION

A primary objective of this study was to determine the frequency of gravel entrainment in steep streams. This information is summarized in Figure 3. The results suggest that the entrainment of gravels in steep streams occurs at a frequency similar to that in lower gradient alluvial channels (Andrews, 1984). Annual maximum recurrence intervals range from 1 to 4 years (depending upon stream and whether historical data or regional regression is used). Corresponding partial duration intervals range from 0.14 to 3.5 years.

Gravels were in streams unaffected by regulation were mobilized at flows that were exceed from 15 (Q_{15}) to 26 % (Q_{26}) of the time. For the regulated sites (both on Bishop Creek), gravels were mobilized at Q_{35} to Q_{36} of the natural flow and Q_4 to Q_8 of the current regulated flow regime. Gravel was mobilized at one site (Blackwood Creek) at flows less than the mean annual discharge (Q_{ma}) but more typically the gravel entraining flows were 3 to 10 times Q_{ma}. Gravel entraining flows ranged from 24 to 89 % of bankfull flow. Other criteria for bankfull would have yielded different results.

Sediment transport in steep streams tends to be more episodic than in lower gradient streams (Costa, 1974; Grant *et al.*, 1990). Explanations for this transport behavior include the coarseness of the available sediment and the relative flashiness of the streamflow hydrology in small basins with little storage. The term "effective" or "dominant" discharge is commonly used to designate that flow that moves the most sediment over the long term (Wolman and Miller, 1960). Whereas, many researchers (Emmett, 1975; Pickup and Warner, 1976) have reported that the effective discharge in lowland streams occurs with an average return interval of 1.5 years, Pitlick (1988) found the recurrence interval for the effective discharge approaches 75 years for channels with gradients exceeding 2 percent. Thus, higher magnitude less-frequent events appear to play a larger role in shaping the morphology and bed composition of headwater areas perhaps adjusting the channel elements to maximize flow resistance (Abrahams *et al*, 1995). Although the effective discharge that moves the bed and shapes the channel may occur less frequently in steep headwater channels, pocket gravel entrainment appears to be adjusted to flows of a similar frequency to bankfull flows in alluvial channels.

While direct measurement of gravel entrainment (e.g. tracer particles, scour chains) is the most accurate method for estimating the discharge necessary for pocket gravel entrainment, it is expensive and may require several water years of observations. If appropriate empirical relationships that relate flow depth and obstruction geometry to gravel entrainment exist for a given type of stream, then a reliable estimate of stream discharge necessary to entrain pocket gravels may be determined. Because these empirical entrainment relationships are postulated based on the physical understanding of the dominant hydraulic mechanisms driving entrainment (primarily, obstruction overtopping), these relationships should be useful across climatic and geomorphic regions as long as the channel morphologies are similar.

Estimates of steep stream gravel entrainment discharges from flow frequency or proportion of bankfull flow are likely to be less accurate than either direct observation of gravel entrainment or a sediment mechanics driven empirical relationship. This does not mean that an estimate based upon flow frequency or bankfull flow does not have great utility. A flow that is exceeded about 20% of the time or recurs about every 1.5 years (using an annual series) appears to be a good predictor for the streams examined here but requires additional testing in different environments.

ACKNOWLEDGEMENTS

Portions of this work were supported by funding to The Johns Hopkins University by the Southern California Edison Company [Purchase Order No. C1070905]. I thank Brian McArdell and Conor Shea for field assistance and helpful discussions. Matt Kondolf inspired this investigation and I thank him for assistance with site selection, logistical assistance, and critical guidance. James Clayton and Jack King provided helpful discussions, suggestions and encouragement. Additional field assistance was provided by Janet Parrish, Jennifer Gilson, and Caroline Barta. Helpful comments on an earlier draft by Peter Wilcock, Sandra Ryan-Burkett and Richard Woodsmith greatly improved this manuscript.

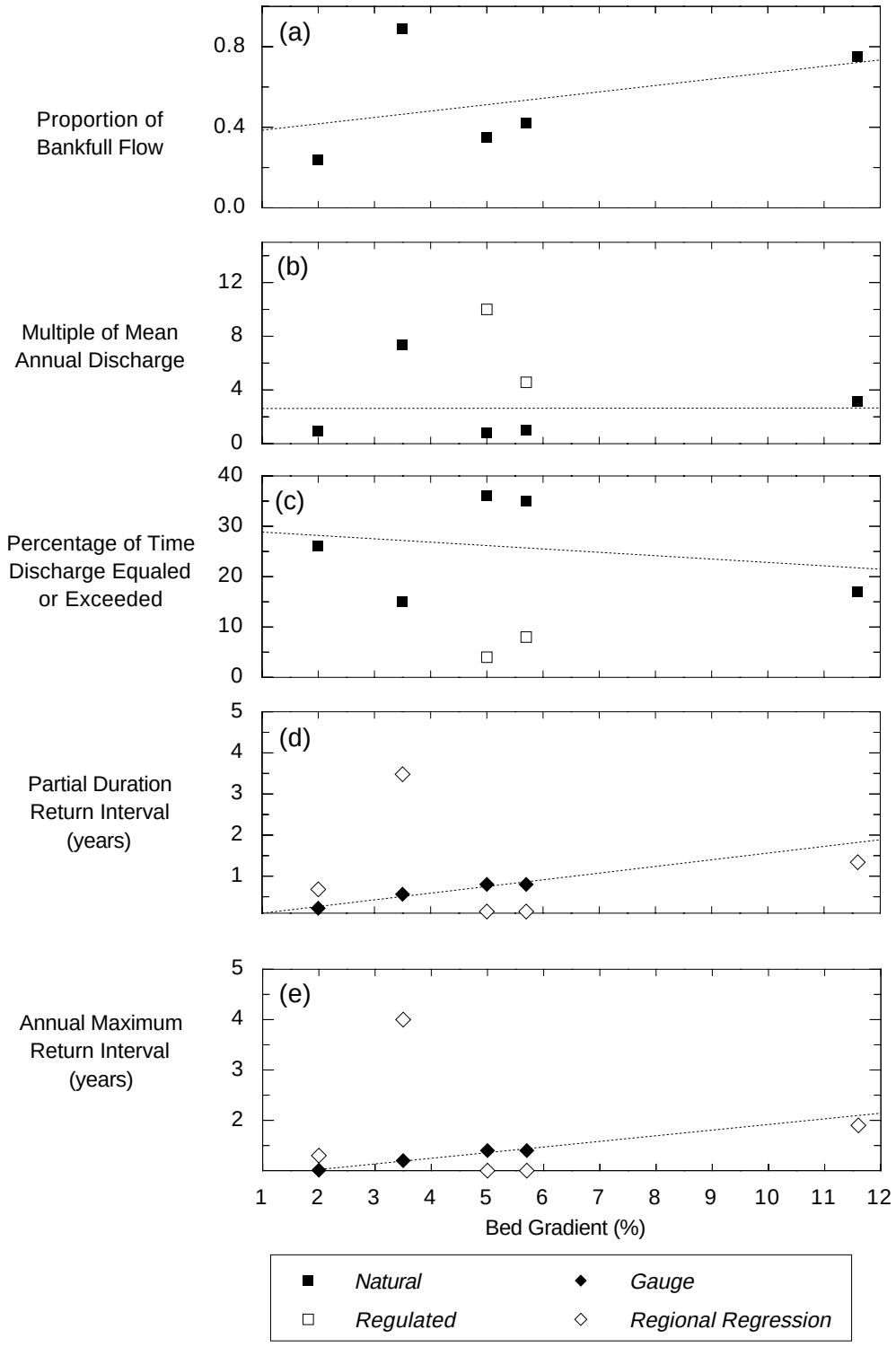

Figure 3. Gravel entraining flows versus stream gradient with flow plotted as: (a) a proportion of bankfull flow, (b) a multiple of mean annual discharge, (c) the percentage of time that Q_{ent} is equaled or exceeded, (d) the partial duration recurrence interval, and (e) the annual maximum recurrence interval. A regression line has been fit and is shown in each plot. Only gauge data and unregulated flows were considered in fitting the lines.

REFERENCES

Abrahams, A.D., Li, G. and Atkinson, J.F., 1995, Step-pool streams: adjustment to maximum flow resistance. Water Resources Research, 31(10), 2593-2602.

Andrews, E.D., 1984, Bed-material entrainment and hydraulic geometry of gravel-bed rivers in Colorado. Bulletin of the Geological Society of America, 95, 371-378.

Barta, A.F., Wilcock, P.R., and Shea, C.C.C., 1994, The transport of gravels in boulder-bed streams. In: Hydraulic Engineering ' 94, Proceedings of the Hydraulic Division, American Society of Civil Engineers, 780-784.

Barta, A.F., Wilcock, P.R., Shea, C.C.C., and Kondolf, G.M., in press, Gravel deposits and entrainment in boulder-bed channels. Water Resources Research.

Barta, A.F., and Wilcock, P.R., in preparation, Gravel entraining flows in steep streams. To be submitted to the Journal of the American Water Resources Association.

Blakemore, E.T., Hjalmarson, H.W., and Waltemeyer, S.D., 1995, Methods for estimating magnitude and frequency of floods in the Southwestern United States. U.S. Geological Survey Water-Supply Paper 2433.

Costa, J.E., 1974, Stratigraphic, morphologic, and pelagic evidence of large floods in humid environments. Geology, 2, 301-303.

Emmett, W.M., 1975, The channels and waters of the Upper Salmon River area, Idaho. U.S. Geological Survey Professional Paper 870-A.

Furbish, D.J., 1993, Flow structure in a bouldery mountain stream with complex bed topography. Water Resources Research, 29(7), 2249-2263.

Grant, G.E., Swanson, F.J., and Wolman, M.G., 1990, Pattern and origin of stepped-bed morphology in high gradient streams, Western Cascades, Oregon. Bulletin of the Geological Society of America, 102, 340-352.

Kirby, W.H., 1981, Annual flood frequency analysis using U.S. Water Resources Council guidelines (program J407): U.S. Geological Survey Open-File Report 79-1336-I, WATSTORE User's Guide, v. 4, chap. I, sec. C, 56 pp.

Kondolf, G.M., Cada, G.F., Sale, M.J., and Felando, T. 1991, Distribution and stability of potential salmonid spawning gravels in steep boulder-bed streams of the Eastern Sierra Nevada. Transactions of the American Fisheries Society, 120, 177-186.

Leopold, L.B., and Maddock, T, 1953, The hydraulic geometry of stream channels and some physiographic implications. U.S. Geological Survey Professional Paper 252.

Mackin, J.H., 1948, Concept of the graded river. Bulletin of the Geological Society of America, 59, 463-512.

Parker, G., 1979, Hydraulic geometry of active gravel rivers. Journal of the Hydraulics Division, American Society of Civil Engineers, 105(HY9), 1185-1201.

Pickup, G., 1976, Adjustment of stream-channel shape to hydrologic regime. Journal of Hydrology, 30, 365-373.

Pickup, G. and Warner, R.F., 1976, Effects of hydrologic regime on magnitude and frequency of dominant discharge. Journal of Hydrology, 29, 51-75.

Pitlick, J., 1988, Response of coarse bed rivers to large floods in Colorado and California. Ph.D. dissertation, Colorado State University, Ft. Collins, CO. 137 pp.

Simons, Li and Associates, 1990, Evaluation of stream channel processes and the growth of riparian vegetation, Bishop Creek, California. Report prepared for the Southern California Edison Company in 2 volumes.

Stedinger, J.R., Vogel, R.M., and Foufoula-Georgiou, E., 1993, Frequency analysis of extreme events. In: Handbook of Hydrology (Chap. 18) edited by D.R. Maidment, McGraw-Hill.

Water Resources Council, 1981, Guidelines for determining flood-flow frequency, Bulletin 17B of the Hydrology Committee of the U.S. Water Resources Council. Washington, DC.

Williams, G.P., 1978, Bank-full discharge of rivers. Water Resources Research, 14(6): 1141-1154.

Wolman, M.G. and Leopold, L.B., 1957, River flood plains: some observations on their formation. U.S. Geological Survey Professional Paper 282-C.

Wolman, M.G., and Miller, J.P., 1960, Magnitude and frequency of forces in geomorphic processes. Journal of Geology, 69, 54-74.

Woodyer, K.D., 1968, Bankfull frequency in rivers. Journal of Hydrology, 6, 114-142.

A DYNAMIC PROCESS FOR ASSESSING THE IMPACTS OF GRAVEL MINING AND LAND USE CHANGES ON THE SAN LUIS REY RIVER, CA

Vernon Finney, Watershed Planning Services Geologist, USDA, Natural Resources Conservation Service, 430 G St., #4164, Rm. 246, Davis, CA. 95616-4164, Phone – (530) 792-5665, Fax – (530) 792-5794, vern.finney@ca.usda.gov**,** vfinney@mother.com**,** http://www.mother.com/~vfinney

Abstract

The purpose of this paper is to describe a tool that can be used by regulators and gravel miners to assess the impacts of proposed sand/gravel mining on streambed stability. In order for the results of this tool to attain public, environmental, and regulatory acceptability, these and other special interest groups should be encouraged to participate in data acquisition and analyses.

The proposed tool defined here as a Dynamic Sediment Modeling and Analysis Process (DSMAP) will provide methodology for determining quantities of stream sand/gravel that can be mined without disrupting streambed stability. It will allow for sediment production predictions, as well as the potential for adverse impacts from sediment mining, based on current and proposed land use and conservation (or management) practices. End products will include sediment budgets and streambed profiles (1000 feet) of selected streams, showing either aggradation (streambed deposition) or degradation (channel erosion or incision).

The end product should allow the county, other interested parties, and representatives of the sand/gravel mining industry to agree to rates of sand/gravel mining at specific locations that will minimize the risk of adverse impacts to the environment such as degradation at bridge footings, etc. The models AnnAGNPS (Darden et Herring 1998) and CONCEPTS (Langendoen 2000) will be linked and their outputs linked to Sediment Budget spreadsheets.

KEYWORDS
Modeling, sediment routing, sediment budgets, AnnAGNPS, CONCEPTS, AGNPS98, sand – gravel mining

INTRODUCTION

The purpose of this paper is to describe a tool that will allow regulators and gravel miners to access the impacts of proposed sand/gravel mining on streambed stability. In order for the results of this tool to attain public, environmental, and regulatory acceptability, these and other special interest groups should be encouraged to participate in data acquisition necessary to use the tool, Dynamic Sediment Modeling and Analysis Process (DSMAP), described in this paper.

Description of the San Luis Rey River Watershed

The San Luis Rey River Basin lies east of the City of Oceanside in the northwestern part of San Diego County, California. The total drainage area of the watershed is 560 square miles. The basin is about 50 miles long and 16 miles wide, and is divided into two hydrologic units by Henshaw Dam. The area above the dam is 206 square miles and the drainage area below the dam, 354 square miles. (COE, 1977).

The San Luis Rey River is unusual for Southern California because it is mostly unchannelized. However, cumulative impacts to the floodplain and watershed of the San Luis Rey River appear to be degrading its environmental value. The San Diego County Water Authority has

documented an increased rate of bed erosion in the central reaches of the river attributable to numerous sand-mining operations (Chang 1991, Micheli 1991).

Sand and gravel mining

The San Luis Rey River provides the San Diego region with a major source of sand and gravel or aggregate. The river contains particularly valuable deposits of high quality sand. Sand mined from the San Luis Rey is used by the construction industry for a variety of concrete and asphalt applications. Multiple sand mining operations have been active on the river since the 1960s. During the housing construction boom of the 1980s, the rate of sand removal accelerated. While sand may be produced from other aggregate sources, the bed of the San Luis Rey provides a source that requires little processing.

Three sand and gravel companies (Marron Brothers, Fenton, and Conrock) are currently mining within the river material suitable for Portland cement concrete (PCC) aggregate. The Conrock Company also mines material from an alluvial fan deposit along the San Luis Rey River northeast of the town of Pala (CDCDMG, 1982).

Significance of fire events

Fire-flood events are calculated into watershed sediment budgets. As much as 253,000 pounds per acre of debris have been measured on burned plots in the Sierra Nevada foothills (Rowe 1941). DeBano, L.F. 1979 gives a comprehensive discussion of the effects of fires on soil properties and subsequent erosion.

The areal extent of fires in the San Luis Rey watershed have been mapped by decades, commencing with a 1910 coverage (CDF, 2000). Figure 1 displays the mapped coverage from 1970 through 1999 (CDF, 2000).

Large and intense fires can lead to accelerated erosion and resultant massive sediment production. In many cases, resulting sediment deposits are also likely to be high in fine sediments (clay, silt, fine sand) and require stream reworking for hundreds of years to make them economically viable for sand/gravel mining. One potential source of sand/gravel that can be released (sediment yield) to streams during fire-flood events is deposits of dry ravel. These infrequent releases (sediment yields) can be significant sources of sand and gravel delivered to upland streams. Dry ravel itself takes decades to accumulate on upland landscapes and, in addition, the frequency of fire-flood events has to be considered in accounting for this source of sand/gravel.

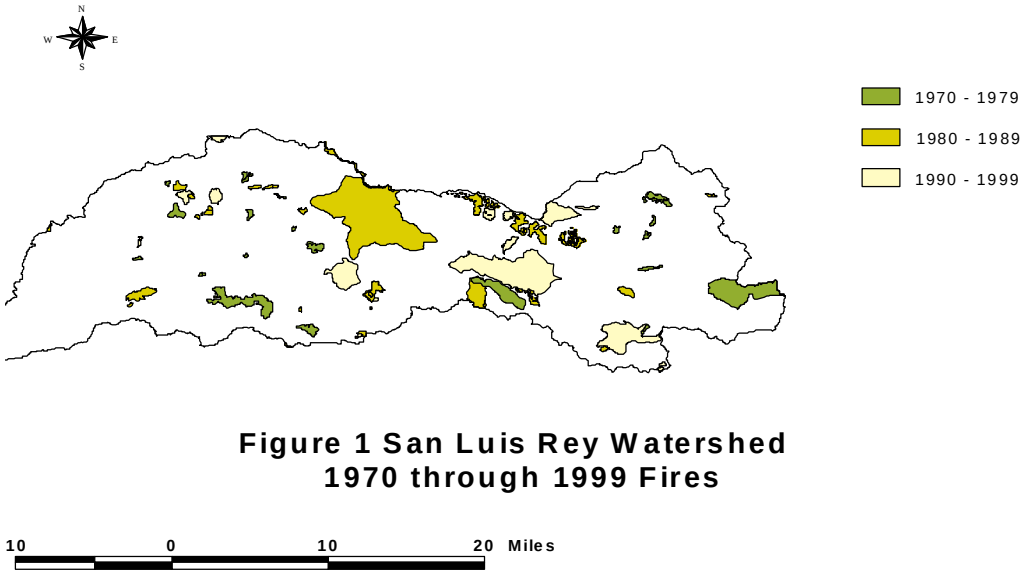

Figure 1 San Luis Rey Watershed 1970 through 1999 Fires

The effects of geology, landuse, and land management on sediment

The paramount geologic consideration is the geologic time scale itself. The time it took to create the present minable deposits appears to be overlooked. Although the present stream system appears to be replenishing mined deposits, the sources of this replenishment is primarily from upstream channel/flood plain alluvium (Qal) and Holocene stream terrace deposits (Qt). While some replenishment continues to occur from the uplands, the time to replenish the present sand deposits would require an equivalent time scale (10,000+ years) and similar climatic conditions.

Although the upland Mesozoic (66 to 225 million age) granitic rocks (Gr), Lindavista Formation (Qln), San Diego Formation (Tsd), Pomerado Conglomerate (Tp), and Stadium conglomerate (Tst) rocks are potential sources of sand/gravel deposits, they are not a significant source of river and terrace minable sand/gravel deposits in the short term (<100 years).

Changes in land use and poor stewardship can lead to accelerated erosion, which can lead to massive sediment production. Resulting sediment deposits are typically comprised of large amounts of fine sediments making them cost ineffective as sources of sand/gravel.

DESCRIPTION OF THE DYNAMIC SEDIMENT MODELING AND ANALYSIS PROCESS

The Dynamic Sediment Modeling and Analysis Process (DSMAP) provides a methodology for estimating quantities of stream sand/gravel that can be mined without disrupting streambed stability. It will calculate sediment production predictions, as well as assess streambed erosion, for current and proposed land use. End products will include sediment budgets and streambed profiles (1000 feet) of selected streams, showing either aggradation (streambed deposition) or degradation (channel erosion or incision). The use of spreadsheets to calculate deposition or erosion by stream reach is illustrated in the McCormick/Saeltzer Dam Sediment Transport

Report (NRCS1997). This report can be viewed on the home page: http://www.mother.com/~vfinney

These end products will provide the county, other interested parties, and representatives of the sand/gravel mining industry with an unbiased basis for determining sand/gravel mining at specific locations with minimal risk to the environment.

The flow chart below (Figure 2) displays the linkages required to build the DSMAP. The models AnnAGNPS (Darden et al, 1998) and CONCEPTS (Langendoen, 2000) are linked and their outputs linked to Sediment Budget spreadsheets. Detailed descriptions of TOPAGNPS, AnnAGNPS and CONCEPTS, models included in the AGNPS98 suite of models are available at the WEBPAGE: http://www.sedlab.olemiss.edu/AGNPS98/Concepts98.html

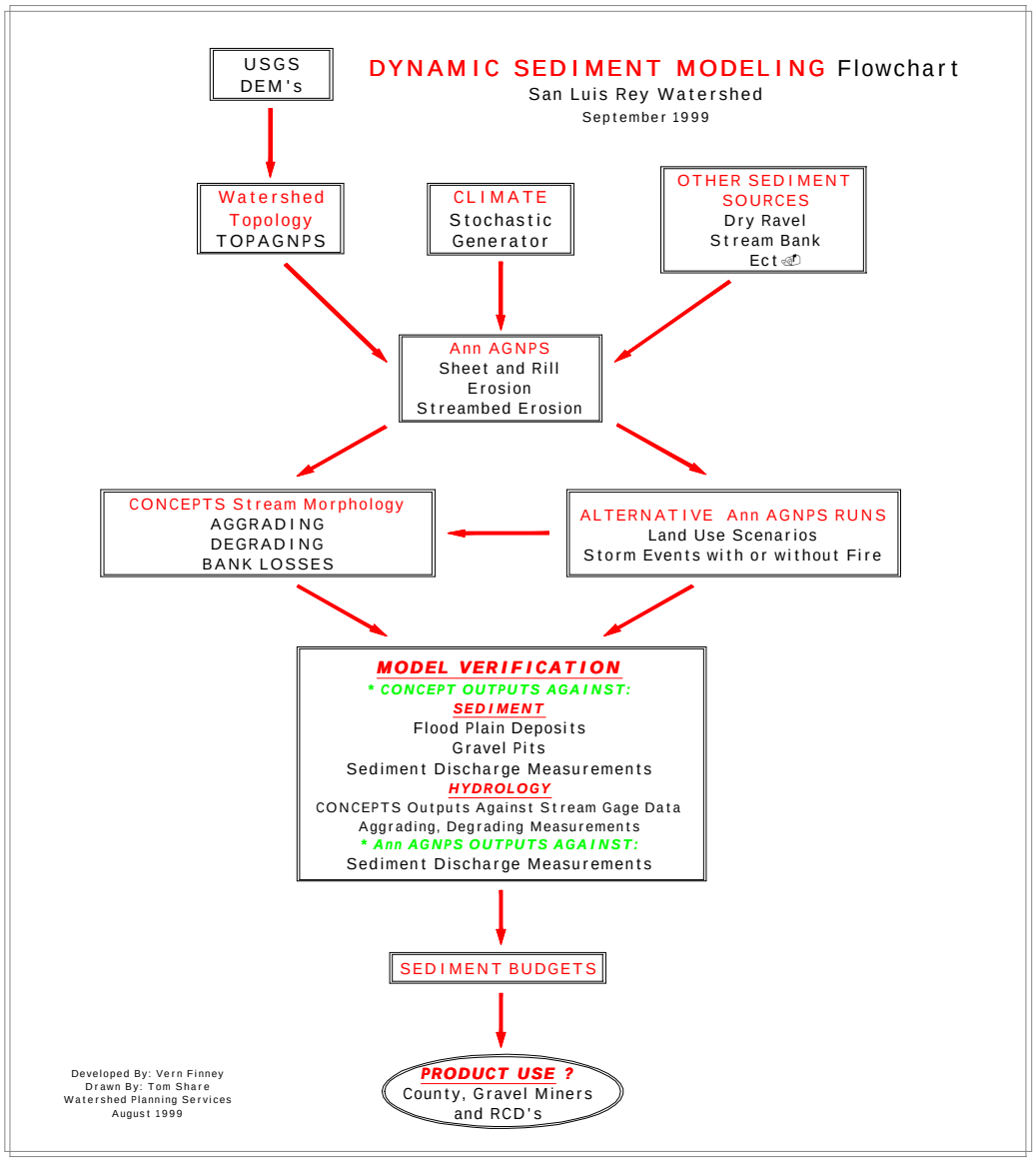

Figure 2 Flow chart of steps

Hydrology

Basic hydraulic parameters will need to be measured in the field as input to the AnnAGNPS (Darden et al, 1998) and CONCEPTS (Langendoen, 2000) models. These parameters include channel cross-sections, stream gradient, wetted perimeters, hydraulic radii, etc. AnnAGNPS will be downloaded into the dynamic stream morphology model CONCEPTS. Pre-and post-dam scenarios will be run to determine the impact of upstream dams on in-stream sand/gravel replenishment.

Sediment budgets will be sufficiently robust to assess the effects of variable water discharges and changes in land use and land use practices. Sediment budgets will be linked to models facilitating evaluation of scenarios. The validity of sediment budgets thus hinges on model validation.

Assumptions of sediment budgets (sources and sinks)

A primary assumption in developing a sediment budget is that all sources, sinks (entrainment), and remobilization can be accounted for. Even more frustrating is estimating the time release of sediment from sediment sources. The interaction of models and spreadsheets will allow for an unbiased accounting of some sources and remobilization. However, there is no way to predict the influx of sediment generated by dry raveling and released into the watersheds streams by fire-flood events. Nor is there any way to predict the occurrence of fire-flood events and the production of sediment from other sources than dry raveling. Thus, these occurrences can only be accounted for in maximum possible sediment loading to the streams and displayed in maximum possible sediment yield budgets.

DATA REQUIREMENTS for AnnAGNPS

Land Use Coverage

The AnnAGNPS model (Darden et al, 1998) uses land use to calculate sheet and rill erosion and to determine the runoff curve number used to calculate overland water flow. Land use coverage from GIS allows for easy updating, allowing dynamic calculations of sheet and rill erosion. Sheet and rill erosion is a significant source of fine sediment in the stream systems. Land use coverage will be digitized from aerial photos. The local Farm Service Agency (FSA) office has delineated crop fields on aerial photos. The polygon size of the AnnAGNPS model cells will be determined based on the accuracy needed to display land use and soil polygons.

Soils Coverage

Soil coverage provides the AnnAGNPS model (Darden et al, 1998) with the input variables soil texture and the sheet and rill soil erodibility "K" factor. The soil coverage should also be useful in the identification of sediment sinks. The status of the soil survey for San Diego County is "in need of updating". This survey will be digitized as a soil coverage, the minimum polygon size being approximately 500 by 500 feet. This coverage can be replaced with an updated soil survey.

DEM

Thirty meter resolution, 1:24,000 scale digital elevation data from 7.5-minute quads covering the watershed area will be downloaded from the USGS WEB SITE

(http://edcwww.cr.usgs.gov/doc/edchome/ndcdb/ndcdb.html). The model TOPAGNPS (Darden et al 1998) uses this data to determine watershed topography and the flow paths of water. The watershed area is covered by twenty-two USGS 1:24,000 7.5-minute quadrangles.

OTHER SEDIMENT SOURCE DATA

AnnAGNPS (Darden et al, 1998) only models sheet and rill erosion and some channel erosion. However, the model does allow input of other sediment sources and provides sediment routing through the watershed to the watershed outlet. All field locations will be geo-referenced with a Geographic Positioning System (GPS) and the inventory points displayed on an existing coverage. To aid in quantifying other erosion sources such as dry ravel, stream bank erosion, flood plain scour, landslides, etc., the fire-flood linear regression debris equations of Scott and Williams (1978) and the COE (1992) will be run to estimate other sediment source inputs to the model AnnAGNPS.

DATA for CONCEPTS

In addition to the data needed for AnnAGNPS (Darden et al, 1998), the model CONCEPTS (Langendoen, 2000) needs grain-size analyses of streambed and streambank samples and in situ stream bank measurements of shear stress. Existing cross-sections will be updated and used where possible. In general, the entire flood plain from immediately below Lake Henshaw to the Pacific Ocean will be surveyed (valley and channel cross-sections) at an interval of approximately 1000 feet. Also, cross-sections will be surveyed 100 feet above and 100 feet below all road crossings. In total, including existing cross-sections, there will be approximately 250 cross sections.

NEW DATA

- Streambed and streambank samples for grain-size analyses
  American Society For Testing And Materials (ASTM) Standards: C 136 Test Method for Sieve Analysis of Fine and Coarse Aggregates and C 117 – 95 Standard Test Method for Materials Finer than 75-µm (No 200) Sieve in Mineral Aggregates by Washing will be used for grain size analyses of stream bed and stream bank samples.
- Stream bank measurements for shear stress
- Use of GPS (Global Positioning System)

1. GPS will be used for locating all field data collection points.
2. GPS will be related to other digital maps (i.e. soils, land use).

- Use of GIS (Geographic Information System)
  GIS will be useful in data synthesis. The principal usage of GIS in this process is preparing input data for the model TopAGNPS. DEM data downloaded from the USGS web site in STDS format is to be converted to a USGS DEM format file. Using ARCINFO, an Arc lattice (grid) is created and the quads merged into a single grid using the GRIS function MOSAIC. UTM coordinates are determined for the four corners of a rectangle and a rectangle containing the watershed area cut from the merged grid. The DEM grid is then converted to an ASCII file using the ARCINFO command Arc> GRIDASCII <in_grid>

<out_ascii_file>. A DNMCNT.INP file is prepared from this ASCII file, reformatted to AGNPS DEDNM.INP format and input to DEDNM.EXE

- Creation of 2D- and perhaps 3D-maps of the San Luis Rey River and Watershed to illustrate model results

MODEL VERIFICATION
Water and Sediment Discharge Measurements

The calculated water and sediment discharges from the models AnnAGNPS-CONCEPTS will be compared to water and sediment discharge measurements. Inquiries will be made of the county, US Corp of Engineers (COE), and the United States Geological Survey to locate and secure existing water and sediment discharge measurements. If insufficient data exists to characterize water and sediment discharges from the watershed, a contract should be let to characterize the watershed' s water discharge to sediment discharge relationships.

Sediment Deposition

Gravel Mining Volumetric Measurements

Gravel mining maps can be used to determine volumes and rates of deposition that can be compared to in-stream deposition calculations from CONCEPTS. Gravel mining maps will be collected. These maps should contain pre-mining elevations and projected elevations of mining. The gravel mining plans should also contain grain-size analyses of pre-mined materials. Surveys will be made to determine post-mining elevations. This data will allow calculation of post-mining sediment in-filling that can be compared to CONCEPTS sediment deposition calculations.

Cs-137 Volumetric Measurements

The presence of Cs-137 in sediment indicates deposition since the initiation of bomb tests, circa 1954 (McHenry et al 1973, 1975; Ritchie and McHenry, 1978; Finney, 1983). A number of discharge events since circa 1917 have resulted in significant deposition in the lower reaches of San Luis Rey. A sampling grid should be laid out to determine the location of core samples. The core samples in conjunction with the Cs-137 analyses will allow volumetric calculations of deposition prior to 1954, 1954 to 1964, and 1964 to present. Valley cross-sections will be surveyed to determine the grid, and digitized on one existing coverage. In addition, cores will be logged, and representative samples for grain-size analysis taken and analyzed. These historical deposition rates and volumes will be compared to depositional volumes calculated by CONCEPTS.

ACKNOWLEDGEMENTS

The author wishes to thank the conceptual and editorial reviewers of DSMAP and this paper. These reviewers are: Jerry Bernard, NRCS National Geologist, Washington, D.C.; and from Davis, California, Julia Grim, NRCS State Geologist; Patricia Grover, NRCS Watershed Planning Administrative Assistant; Robyn Myers, NRCS Watershed Planning Landscape Ecologist; Madalene Ransom, NRCS Watershed Planning Economist; and Robin White, NRCS West Regional Technical Team Geologist.

REFERENCES

CDCDMG, 1982. Mineral Land Classification: Aggregate Materials In The Western San Diego County Production-Consumption Region. California Department Of Conservation Division Of Mines And Geology (CDCDMG), Special Report 153, 28 pp., plus maps.

CDF, 2000. Personal Communication and Transmittal. Mark Rosenberg, Research Program Specialist, California Department of Forestry and Fire Protection, Sacramento, CA. Phone: (916) 227-2658.

COE, 1977. San Luis Rey River, Design Memorandum No. 1, Hydrology. Prepared by: U.S. Army Engineer District, San Francisco for U.S. Army Engineer District, Los Angeles Corps Of Engineers.

COE, 1992. Debris Method. Los Angeles District Method For Prediction Of Debris Yield. U.S. Army Corps of Engineers, Los Angeles District, Los Angeles, California, 55 pp., plus Appendices.

Chang, H, 1991, Assessment Of Sand And Gravel Mining Impacts On San Luis Rey River Aqueduct Crossings. Prepared for: San Diego County Water Authority, Nolte and Associates.

Darden, R. and G. Herring, 1998, AGNPS 98 Input Data Preparation Model, User' s Guide, Version 1. USDA-ARS, National Sedimentation Laboratory, 598 McElroy Drive, Oxford, MS 38655.

DeBano, L.F, 1979, Effects Of Fire On Soil Properties. Rocky Mountain and Range Experiment Station, Tempe, Arizona, California Forest Soils, Division of Agriculture, University of California, # 4094, The Regents of the University of California, Pp. 109 to 117.

Finney, V.L., 1983, Soil Loss-Sediment Yield to Silver Lake, Missouri. Bulletin of the Association of Engineering Geologists, Vol. XX, No. 4, pp. 405-409.

Langendoen, E. J., 2000, CONCEPTS - Conservational Channel Evolution and Pollutant Transport System, Stream Corridor Version 1.0, Research Report (submitted for approval). USDA, ARS National Sedimentation Laboratory, Oxford, Mississippi, July 2000.

Lisa, M., 1991, River And Watershed Planning: The San Luis Rey River Case Study. Prepared for: U.S.E.P.A. Wetlands Research Program, Corvalis, Oregon, U.C. Berkeley Environmental Planning.

McHenry, J.R.; Ritchie, J.L.; and Gill, A.C., 1973, Accumulation of fallout cesium-137 in soils and sediments in selected watersheds: Water Resources Research, Vol. 9, No. 3, pp. 676-686.

McHenry, J.R.; Ritchie, J.C.; and May, J., 1975, Recent sedimentation rates in the Lower Mississippi River Valley: Lake Verret-Lake Palourte, Louisiana. In Proceedings, Mississippi Water Resources Conference: Water Resources Research Institute, Mississippi State University, Mississippi State, MS, pp. 13-23.

NRCS,1997. McCormick/Saeltzer Dam Sediment Transport, unpublished. USDA, Natural Resources Conservation Service, 430 G St., #4164, Davis, CA. 95616-4164, 17pp and two appendixes.

Ritchie, J.C., and McHenry, J.R. 1978, Fallout Cesium-137 in cultivated and non-cultivated North Central United States watersheds. Journal of Environmental Quality, Vol. 7, No. 1, pp. 40-44.

SLRWC (San Luis Rey Watershed Council), 1998, The San Luis Rey Watershed: A Framework for Management. Prepared by: The San Luis Rey Watershed Council.

Scott, K.M. and Williams, R.P., 1978, Erosion and Sediment Yields in the Transverse Ranges, Southern California. Geological Survey Professional Paper 1030. U.S. Government Printing Office, Washington, D.C., 38 pp.

HEADCUT ANALYSIS DUE TO SAN GORGONIO RIVER LEFT OVERBANK SAND AND GRAVEL MINING

H. M. Hu, Ph.D., WEST Consultants, Inc., CA; Craig Phillips, R.C.E., Robertson's Ready Mix, CA; and Brian Doeing, P.E., WEST Consultants, Inc., CA

Abstract: Floodplain mining activities are common practices in arid areas. However, channel and overbank responses to overbank excavation may endanger property and structures in the vicinity of the mining operation. Adequate hydraulic, erosion, and sedimentation analysis are usually required for developing an acceptable mining plan. This paper describes a qualitative evaluation of a case study related to the headcut formation associated with a proposed sand and gravel mining pit on the left overbank of the San Gorgonio River south of the I-10 freeway in the Banning area, Riverside County, California.

INTRODUCTION

A sand and gravel mining pit is proposed on the left overbank of the San Gorgonio River south of the I-10 freeway in the Banning area, Riverside County, California. Figure 1 shows the project site map. The study reach extends from 205 feet upstream of the I-10 freeway bridge to the downstream confluence with Smith Creek. The approximate horizontal dimensions of the pit are 2,400 feet long by 850 feet wide, while the maximum depth is 230 feet. A new levee is proposed to protect the mining operation from the 100-year flood and also contain the 500-year superflood. However, in the event of high flows and levee failure, at the upstream boundary of the mining pit, the increase of the energy slope, flow velocity, and sediment transport capacity will initiate bank sloughing upstream of the pit. If a headcut associated with levee failure propagates upstream, it may endanger the railroad bridge (about 1,900 feet along the channel upstream of the pit) and the Interstate 10 freeway bridge (about 2,200 feet upstream of the pit). A detailed headcut analysis is therefore necessary to address the magnitude of the headcutting and the potential impact on the bridges upstream. This paper provides a qualitative evaluation procedure for estimating the maximum headcut distance and depth.

PHYSICAL PROCESSES OF HEADCUT

The extent of the headcut induced by sand and gravel mining is a function of volume and depth of the gravel pit, location of the pit, bed material size, flood discharge, and sediment inflow rates and volume. For a floodplain mining pit, low flows are generally not of concern. Flood flows will not be of concern until they spill overbank into the pit laterally or from upstream. While overbank flows are filling a floodplain gravel pit, the headcutting and erosion continue to propagate upstream. However, once the floodplain pit is filled, it will constitute only a pool or slackwater area on the floodplain and the headcutting generally ceases.

METHODS OF HEADCUT ANALYSIS

In this study, for the purpose of a qualitative evaluation, no detailed sediment transport modeling is conducted. The analysis is based on other relevant and applicable study results and

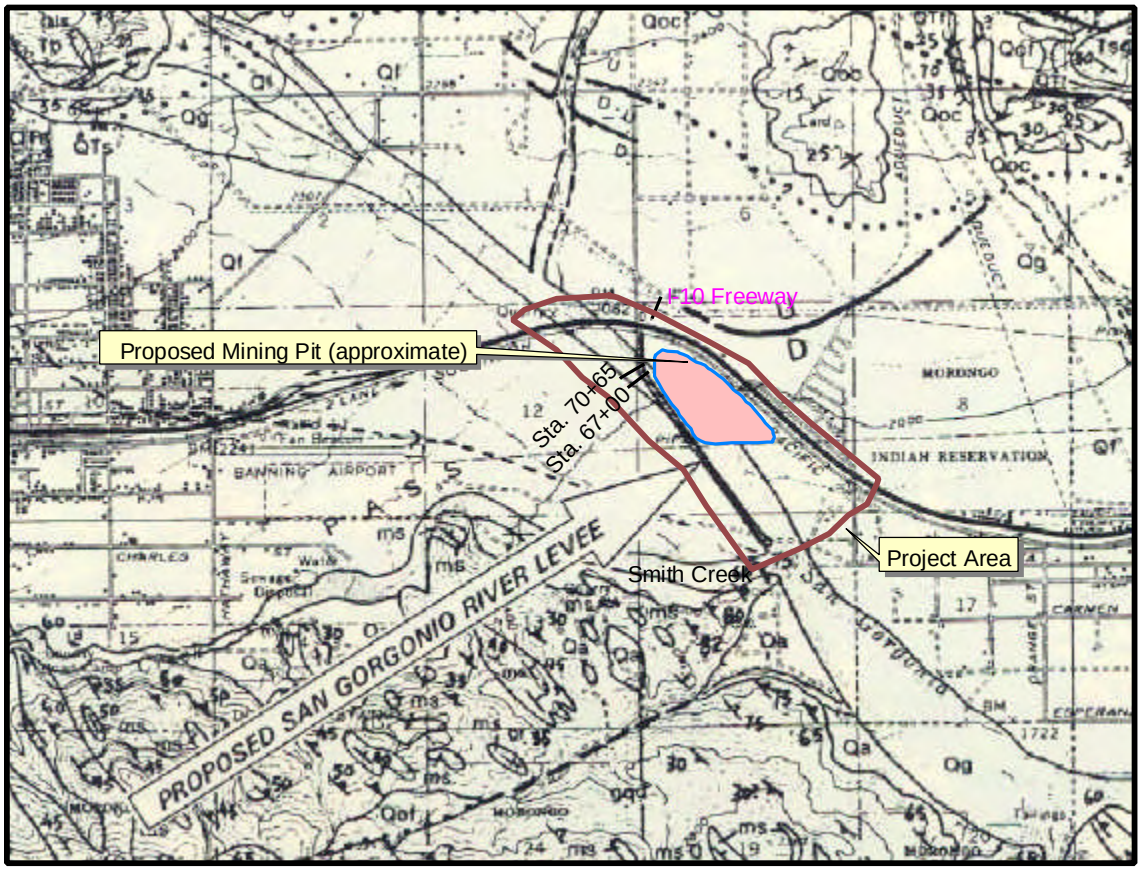

Figure 1. Project Site Map (Base Map By: A.R. Brown, 1982)

engineering practices related to headcutting induced from a mining pit. The following studies were found to provide valuable background and methods for headcut analysis:

(1) Anderson-Nichols assisted by Colorado State University conducted physical modeling for analyzing the impact of instream gravel mining on the adequacy of the Salt River channelization project and for developing the guidelines to implement proper control of those mining operations to avoid adverse impacts (Roberts, B. R., Horn, D. R., and Chen, Y. H., 1980). The experimental results show that the upstream migration along the channel thalweg through the process of headcutting is a function of pit depth and volume. The maximum headcutting depth usually occurs during the initial stages of the hydrograph when water starts to enter the pit. The headcutting action stops when the gravel pit is filled with water and the newly cut channel aggrades slightly during the remainder of the flood. The results also indicate that headcutting depth and distance vary strongly with pit depth.

(2) Simons, Li & Associates, Inc. (SLA, 1982), developed a guideline for the engineering analysis of sand and gravel mining. SLA modified and utilized the water and sediment routing method developed by Simons and Li (1979) to analyze erosion and deposition problems associated with instream or floodplain mining operation. The model was applied to predict the

headcutting profile induced by the instream mining operations in San Juan Creek and Bell Canyon of Orange County, California, as well as in Rillito Creek of Tucson, Arizona. Model predictions were found to be in good agreement with the measured values for the gravel pit in San Juan Creek. Similar studies were also conducted for the proposed Columbia pit for sand and gravel mining in the Santa Cruz River floodplain, Pima County, Arizona. The study also shows that the pit depth significantly influences the severity of the headcut effect. In the study, the 100-year flood hydrograph for the proposed pit and the associated headcut distance and headcut depth were presented graphically for different pit depths up to 30 feet. The analysis reveals that headcutting should practically cease after the drown-out time. To provide a factor of safety, a 1.5 multiplier to get the ultimate headcutting distance was recommended.

(3) Cotton and Ottozawa-Chatupron (1990), in their paper, described the analysis procedure developed for the Arizona Department of Transportation for the estimation of short-term longitudinal channel response due to instream mining. The procedure was developed using a simulation model formulated specifically for the hydraulic conditions typical of mined river reaches in Arizona. The model was calibrated using data from mined river reaches in sand bed and gravel bed channels throughout Arizona. Simulations were then conducted to create several synthetic data sets from which general dimensionless relations were developed. Formulas for the maximum depth and distance of scour upstream and downstream of an instream excavation for a flood hydrograph could then be determined and applied. In their paper, the regression equations for the case of a sand bed channel with a sediment gradation of D_{50} = 1 mm were presented. From the model simulations, limiting conditions for scour were found for headcutting. Headcutting is limited to no more than half the excavated depth due to deposition immediately downstream of the pit brink.

(4) W. J. McKeever, Inc., provided an estimated headcutting profile for the proposed mining pit in the study area. The profile was determined using a slope twice the natural ground slope down to half the pit depth. Thus, the maximum headcutting depth is also half the pit depth. The available headcutting profiles from Anderson-Nichols and SLA for different conditions were analyzed. All the maximum headcutting depths are found to be less than but close to half the mining pit depth. However, the slope of the headcutting profile is much larger than the slope determined using the rule-of-thumb above. Therefore, the headcutting profile calculated using this engineering rule-of-thumb might provide the limiting envelope for the extent of headcut migration.

In order to test the applicability of the regression equations presented by Cotton and Ottozawa-Chatupron (1990), hereafter referred to as “regression equations”, the equations were applied to calculate the maximum headcutting distance and depth using the data of SLA. The computed results were then compared to the values obtained using the SLA model. The comparisons show that the values of headcutting distance using the regression equations are generally 3.5-4.5 times the SLA values. This is probably because the available regression equations were developed for a sand bed channel and an instream mining pit. If these regression equations are used to predict the headcutting magnitude induced by the floodplain sand and gravel mining operation, the results may be over-predictive and conservative.

HYDROLOGIC CONDITION

Figure 2 shows the 100-year and 500-year discharge hydrographs downstream of Southern Pacific Railroad (S.P.R.R.) Bridge. The hydrographs were developed by transforming the available hydrograph on downstream Smith Creek based on the peak discharge factor and the drainage area ratio. The hydrographs indicate that floods are usually of the Aflash@ type, reaching their peak within a few hours, and then subsiding just as quickly. The major floods would rise from the streambed to extreme flood peak in about 5 to 6 hours from the beginning of rainfall.

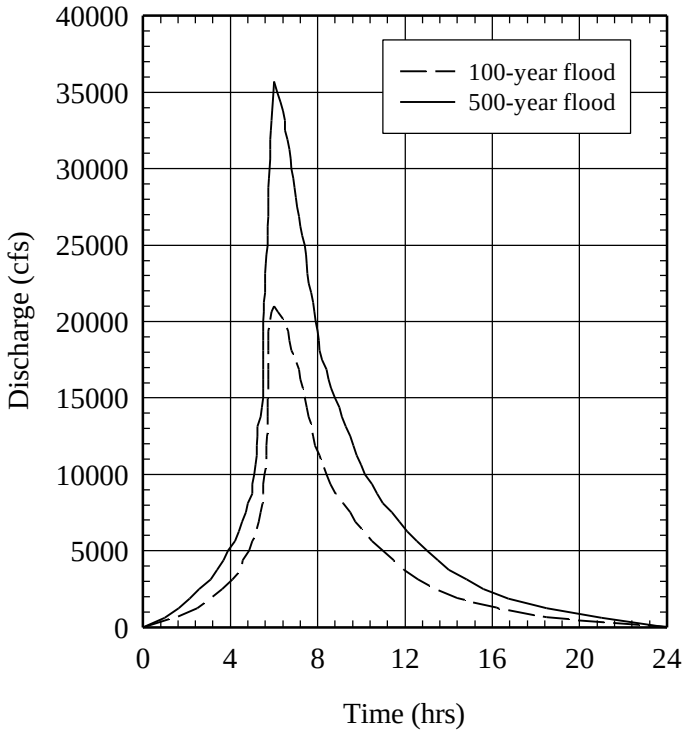

Figure 2. Discharge Hydrographs for the Study Reach at the S.P.R.R. Bridge

As described previously, the volume of inflow entering the mining pit plays an important role in developing the headcutting profile. A HEC-RAS model developed for the levee analysis was used to determine the hydrograph of the flow into the pit.

In the event of levee failure, split flow develops at the location where the levee fails. The levee assumed to be breached at the same location as in the 1969 flood, which breached the existing earthen dike at a location approximately 1,500 feet downstream of the Southern Pacific Railroad bridge where high flows impinged on the dike between the two cross-sections at stations 70+65 and 67+00 as shown in Figure 1. It is also assumed that the split flow on the left overbank enters

the mining pit from the upstream boundary of the pit. This assumption is conservative since flow entering from upstream yields maximum headcutting distance and depth.
In HEC-RAS, the left overbank was treated as a separate channel. Two cross sections were used in the overbank. The HEC-RAS program treats the flow region where split flow develops as a junction. Since the HEC-RAS program, Version 2.2, does not have the split flow option and the amount of flow going to each reach is unknown, a trial and error process was used to obtain the correct flow distribution. After an initial estimation of flow diversion at the junction, the program was run to compute the energies and water surfaces at all locations around the junction. The energy at main channel station 67+00 and the upstream cross section in the overflow reach was then compared. The flow was re-distributed until the resulting energies at these two cross sections were equal.

Table 1 shows the computed flow going to the left overbank for the 100- and 500-year floods. In the computations, the continuous hydrographs shown in Figure 2 were transformed as a sequence of discrete steady flows, each having a specified duration. At a particular discharge, the HEC-RAS model was used to get the flow distribution. The calculation shows that when the discharge upstream of the junction is larger than 5,270 cfs, overflow to the left bank begins and flow starts to split into the mining pit.

Table 1. Flow split into the mining pit.

100-year flood				500-year flood			
Duration (hrs)	Storm Time (hrs)	Discharge from upstream (cfs)	Discharge going to pit (cfs)	Duration (hrs)	Storm Time (hrs)	Discharge from upstream (cfs)	Discharge going to pit (cfs)
4.0	4.0	1,210	0	4.0	4.0	1,950	0
1.5	5.5	4,725	0	1.5	5.5	8,700	1,520
1.0	6.5	21,000	6,550	1.0	6.5	35,700	12,380
1.0	7.5	15,000	3,970	1.0	7.5	25,600	8,340
1.5	9.0	11,500	2,490	1.5	9.0	17,000	4,870
3.0	12.0	5,280	0	3.0	12.0	9,877	1,910
12.0	24.0	1,150	0	12.0	24.0	1,915	0

HEADCUT ANALYSIS

The methods described in the previous section were used to estimate the range of maximum headcutting distance and depth. The following sections describe the detailed computations.

Regression Equations: The calculations using the regression equations need the dimensions of the mining pit and the hydrograph of inflow entering the pit. The volume of the proposed mining pit which can be filled with water was estimated to be about 4.06×10^8 cubic feet. The estimation was based on the project plan sheet. The proposed excavated pit bottom slopes in the downstream direction. The top elevation at the most downstream brink of the pit is about 1,950 feet, which is 200 feet above the pit bottom. Considering the sloping effect of the pit bottom, the

flow split into the pit may only rise up to about 200 feet above the pit bottom since the flow will leave the pit at the downstream brink. Therefore, the limits of an area representing the surface area up to the elevation that the filling flow may reach, was sketched. The numerical areas of the surface and bottom areas were then estimated by using a digital planimeter. The volume of the effective pit was approximately computed using the formula for calculating the volume of a frustum of a pyramid. In the headcut analysis, the following dimensions of pit were used: 2,400 feet long, 736 feet wide, and 230 feet deep to represent the calculated volume.

The regression equations were applied to determine the variation of headcut distance and depth with time. First, the 100-year flood discharges were applied to get the maximum headcut distance and depth. However, since the volume and depth of the existing pit are so large, the 100-year flood can only fill 13% of the pit volume. If a second sequential 100-year storm follows to hit the study area, the headcutting effect of the first 100-year flood will continue. Therefore, the headcutting distance and depth shown are the impact of a sequence of 100-year floods. In this case, after the second 100-year flood, the water still only fills 25% of the pit volume. To be conservative, the full flow upstream the junction was applied for the computation. At any given time, the flow rate splitting into the pit equals the discharge from the upstream minus 5,270 cfs at which flow split starts to develop.

One single 500-year superflood was also used to estimate the maximum headcut distance and depth. Table 2 shows the results for different flow conditions. According to the recommendation of SLA, a safety factor of 1.5 to get the final headcut distance was applied. The maximum headcutting depth is about 115 feet which is half the pit depth. The maximum headcutting distance is about 834 feet. It should be pointed out that, according to the sensitivity analysis, both the discharge and duration affect the value of headcut distance. For example, if the duration of 500-year peak flow is widened from 1 hour to 2 hours, the headcut distance will correspondingly increase to 1,054 feet.

Table 2. Headcut distance and depth for different flow conditions.

Descriptions of Flow Conditions	Percentage of Pit Volume filled (%)	Headcut Distance (ft)	Headcut Depth (ft)
First 100-year flood, split flow only	13	230	24
Second 100-year flood, split flow only	25	359	46
First 100-year flood, full flow	31	449	63
Second 100-year flood, full flow	62	772	106
Single 500-year flood, split flow only	32	408	53
Single 500-year flood, full flow	77	834	115

SLA Method: By examining Figures 20.18a and 20.18c in SLA's book (SLA, 1982) showing the effect of pit depth ranging from 5 feet to 30 feet on headcut distance and headcut depth, headcut dimensions are found to be linearly related to the pit depth. The curve was linearly extrapolated to the pit depth of 230 feet. The obtained headcut distance and depth are 830 feet and 43 feet, respectively. Although there might exist some uncertainties for this linear extrapolation, the extrapolated values still provide an estimate of the headcutting magnitude.

Rule-of-Thumb: The channel bed slope between the bridges and the proposed mining pit is about 3%. Applying the rule-of-thumb, the maximum headcutting depth will be 115 feet and the headcutting distance will be about 1,200 feet.

SUMMARY AND DISCUSSIONS

Based on the calculations, the range of the headcut depth is from 24 feet to 115 feet, while headcut distance ranges from 230 feet to 1,200 feet. It should be noted that the current analyses imply some uncertainties, such as the inflow hydrograph, the location of levee failure, and the accuracy of the estimating method. Also, no credit was given to the armored concrete layer that protects the streambed below the railroad bridge because no design information was available for this feature. However, the results show, given the most conservative assumptions for the analysis, and considering the rule of thumb which may represent the maximum envelope of headcut distance, that headcut migration does not reach the railroad bridge or I-10 freeway.

REFERENCES

Cotton, G.K. and Ottozawa-Chatupron, V. (1990), *Longitudinal Channel Response due to In-Stream Mining*, in Proceedings of the 1990 National Conference on Hydraulic Engineering, Edited by Howard H. Chang and Joseph C. Hill, San Diego, CA.

Roberts, B.R., Horn, D.R., and Chen, Y.H. (November 1980), *Impact of Gravel Mining on the Proposed Salt River Channelization Project*, Prepared for U.S. Army Corps of Engineers, Sacramento, CA.

Simons, Li & Associates, Inc. (1982), *Engineering Analysis of Fluvial Systems*, Fort Collins, CO.

Simons, D.B. and Li, R.M. (1979), *Erosion and Sedimentation Analysis of San Juan Creek near Conrock Gravel Pit, Orange County, CA*, Prepared for Dames & Moore, Denver, CO.

H.M. Hu, WEST Consultants, Inc. 11848 Bernardo Plaza Court, Suite 140-B, San Diego, CA 92128-2418; Tel: 858-487-9378; Fax: 858-487-9448; E-mail: hhu@westconsultants.com

ASSESSING THE GEOMORPHIC EFFECTS OF INSTREAM GRAVEL MINING ON THE MAD RIVER, HUMBOLDT COUNTY, CALIFORNIA

By Kevin Knuuti, P.E., Hydraulic Engineer, U.S. Army Corps of Engineers, San Francisco, California

Abstract: Approximately 100,000,000 cubic yards (140,000,000 tons) of gravel are mined each year in California, the large majority being mined from riverbeds and floodplains. Gravel mining in the Mad River has been an ongoing business since the 1800s and has caused varying degrees of controversy throughout much of this century. Various individuals and agencies assert that gravel mining is causing riverbed degradation and riverbank erosion. Others counter that the mining is preventing bed aggradation and is thus providing a flood control benefit. Questions concerning the effects of gravel mining on the geomorphology of the Mad River have not been clearly answered.

In 1994, Humboldt County, gravel mining companies, and environmental interest groups established a committee to review gravel-mining practices and to study the effects of gravel mining on the lower Mad River. The committee estimates the lower Mad River can support a mean annual extraction of 150,000 to 200,000 cubic yards (210,000 to 280,000 tons) of bed material per year. Gravel miners contend the river can support more than twice that amount with no adverse morphological consequences. In 1999, the U.S. Army Corps of Engineers began studying the lower Mad River in relation to past and current gravel-mining practices. The study's goal is to assess the geomorphic effects of instream gravel mining on the lower Mad River and to recommend, if necessary, what additional work is needed to quantify those effects and ensure the stability of the channel.

Assessing the effects of riverbed gravel mining on channel evolution is a complicated task. Erosion and deposition are directly related to channel width and slope variation and are affected by stream power, bed load, and effective (dominant) discharge. Natural channels tend to evolve toward a state of equilibrium that may be distorted by the artificial removal of bed material. This paper examines available data in an attempt to quantify the factors associated with a stable lower Mad River channel and to assess the effects that gravel mining has had on channel morphology.

INTRODUCTION

The geology and land use practices in northwestern California result in rivers with extremely high sediment loads. Humboldt County is especially susceptible to these conditions, with a result being that the Mad River is one of the highest sediment producers (5,000 tons per square mile per year) in the world (California, 1982).

The topography of Humboldt County is characterized by deep V-shaped canyons that have resulted from complex folding and faulting and periodic tectonic uplift. The geology is primarily made up of the Franciscan assemblage, which is mostly grawacke, siltstone, shale, and conglomerate, with some altered volcanic and metamorphic rocks. These rocks are highly susceptible to weathering and, given the high annual rainfall (40 to 70 inches per year) and the steep terrain of the area, erode rapidly.

The forests of Humboldt County are dominated by Redwoods (*Sequoia sempervirens*) and Douglas Fir (*Pseudotsuga menziesii*). After a local railroad was established in 1892, the timber industry in the area expanded. Activities such as clear cutting, log skidding, and road building resulted in massive erosion and severe sediment problems in the lower Mad River. The river, which had been straightened in some areas to reduce flooding and to improve fishing, began to aggrade. The readily available sediment supply, combined with the increasing population and development in the area, led to the establishment of the local gravel-mining industry.

Currently, several gravel-mining companies operate on the lower Mad River. Their primary means of mining is to "level skim" the gravel bars in the river during the low flow periods that accompany the dry summer season. If done properly, by extracting the excess sediment the river deposits on its bed each year, the gravel mining industry can help maintain the river in a stable condition with no aggradation or degradation of the bed. Determining the optimum average annual extraction volume for this condition, however, is not simple. In a preliminary attempt to quantify the sustainable yield of gravel the lower Mad River can supply, the U.S. Army Corps of Engineers (Corps) is currently reviewing a variety of available data. The available data includes historic aerial photographs, bedload and stream flow measurements, and channel cross sections.

PROCEDURE

General: The purpose of this analysis was to examine available data and information and to determine the sustainable extraction yield, for gravel mining, from the Mad River. The analysis was also to look at what effects, if any, recent gravel-mining practices have had on the morphology of the lower Mad River. To accomplish this, we divided the analysis into two parts: analytical methods and historical information (photographs and cross-sectional surveys).

Available Data: In 1970, as part of a water supply project, the Corps surveyed thirty cross sections along a thirteen-mile stretch of the lower Mad River that covered the entire area in which the gravel miners currently operate. We intended to compare those 1970 cross sections to cross sections from this year but, at the time of writing this paper, the results from the new survey were not available (because of the absence of new survey data for the original thirty cross sections, we consider the information in this paper to be preliminary). In addition to the Corps cross sections, the California Department of Transportation (CALTRANS) and the Humboldt Bay Municipal Water District (HBMWD) each have river cross sections that they have surveyed. CALTRANS measures bridge cross sections in the study area at Highway (Hwy) 101 and Hwy 299, at a frequency of approximately once every ten years, and has survey information for these two bridges dating back approximately fifty years. HBMWD collects groundwater from beneath the Mad River with a series of Raney collectors and has cross section surveys for the portion of the lower Mad River in which it operates its collectors.

Federal, state, and local government agencies have taken a variety of aerial photographs of the lower Mad River. We have compiled a collection of aerial photographs, covering the entire project area, that date from the 1940s to the present.

In the early 1970s, the Corps worked with the U.S. Geological Survey (USGS) to measure bed load in the Mad River. The USGS collected bedload and associated discharge measurements at

three different stream gauging stations along the lower portion of the river (Arcata, Blue Lake, and Kneeland). The USGS also has a record of average daily stream flow and suspended sediment concentration at the Arcata gauge that is over fifty years in duration and shorter duration stream flow information at the Blue Lake and Kneeland gauges.

ANALYSIS

General: Any systematic changes to the Mad River's boundary conditions could result in instability in the river system. Modifications such as increasing the sediment load (a result of logging practices and local geology), decreasing the sediment load (a result of gravel mining), changing the channel slope (a result of certain gravel mining techniques), or changing the flow in the river (a result of extraction for water supply purposes) all have effects. Generally, these effects can be described using Lane's proportionality relationship (Lane, 1955):

$$Q_s D \sim Q_w S$$

where Q_s is the bed material load, D is the sediment size, Q_w is the water discharge, and S is the channel slope. Using this relationship, we can predict the effects a change in one of the variables would have on a stable river (see Table 1). The effects can differ for the areas immediately near, upstream, and downstream from the change. Typically, however, a change in the bed material load will have an effect that migrates downstream while a change in the channel bed level or slope will have an effect that migrates upstream (Hey, forthcoming). With these relationships in mind, we examined available data and information on the Mad River to determine what effects gravel mining might be having on the morphology of the river.

Action	Immediate result	Downstream Effect	Upstream Effect
Increased upland erosion (due to logging and other land use practices)	Increased sediment load in the river causes aggradation in area of increased erosion	Increased sediment load causes channel aggradation to progress downstream from deposition area	Decreased slope may result in channel aggradation progressing upstream from deposition area
Gravel mining (level skimming of the bars)	Channel is overwidened and slope may be decreased, area becomes a sediment trap (increased deposition)	Decreased sediment load in the river causes channel degradation to progress downstream from mining area, increased bank height could lead to instability and increased erosion	Increased slope at upstream end of mining area may cause channel degradation to progress upstream (headcutting), increased bank height could lead to instability and increased erosion

Table 1 – Predicted effects of land use practices on a stable river

Analytical Methods:

Geomorphic Features and Hydraulic Geometry: Analyzing the current stability of the Mad River using geomorphic features and hydraulic geometry is, at best, difficult. To use this approach, it is best to have a stable reach of river to use for comparison with the reaches being

examined. The middle and upper portions of the Mad River are tightly confined by steep, mountainous terrain. The lower Mad River, however, flows through a much wider valley with a gentle slope, allowing room for the river to meander. This entire lower portion of the Mad River was the subject of our analysis. The middle and upper portions of the Mad River are not similar enough to the lower Mad River for direct comparisons in terms of planform or hydraulic geometry. Additionally, the lower Mad River is no longer in regime, since its outlet was moved over 100-years ago and since it now receives such an abnormally high influx of sediment from local erosion and loses such a large amount of transportable sediment to gravel mining. Despite this, we examined possible relationships for geomorphic features and hydraulic geometry.

We began by measuring radii of curvature for meander bends and comparing them to meander wavelengths. We compared the relationship of these values for the lower Mad River to the relationship described by Leopold (equation 1)(Leopold, 1964) and found Leopold's relationship to consistently underpredict the wavelength of meanders on the lower Mad River.

$$L = 4.7\, r_m^{0.98} \quad (1)$$

We next calculated hydraulic geometry relationships at the three gauging stations on the lower Mad River by using the USGS data (9-207 forms) from the stations. We estimated effective discharge at two of the gauging stations (Arcata and Kneeland) by integrating the bedload transport curves with the discharge frequency curves for those stations. We used the effective discharge, along with the hydraulic geometry relationships, to determine the channel depth, width, and cross-sectional area for the effective discharge. We compared these values to the relationships between channel dimensions and meander bend radii described by Williams (Williams, 1986). Our comparison indicated that the river is much wider and shallower in the areas where the gravel miners operate than it is throughout the rest of the river. Our comparison also indicated that the river is much wider and shallower, in those same areas, than Williams' relationships predict.

Sediment Transport Analysis: In the early 1970s, the Corps and the USGS collected bedload samples for a variety of flows at the gauging stations on the lower Mad River. From this data, we developed bedload transport curves for the Arcata and Kneeland stations. Kneeland and Blue Lake each had only five data points. With the Blue Lake data being so clustered, with no obvious relationship, we did not feel it was appropriate to define a transport curve for that gauge. The Kneeland data and the Arcata data were consistent enough (despite the variability in the Arcata data at higher flows) that we thought we could approximate a relationship between bedload transport and river flow at those locations (see Figure 1). We also examined the particle size distributions for samples of bedload and of bed material (which should be more representative of bed material load). Our comparison of bedload and bed material particle sizes showed them to be very similar, incicating that there may not be a significant portion of suspended bed material load in the system and that bedload by itself may be a reasonable approximation for calculations of channel forming sediment transport.

Using the bedload transport and flow duration curves for Kneeland and Arcata, we estimated the average annual sediment transport into our study reach (Kneeland data) and out of our study reach (Arcata data). The difference between these two values was the amount of sediment that is

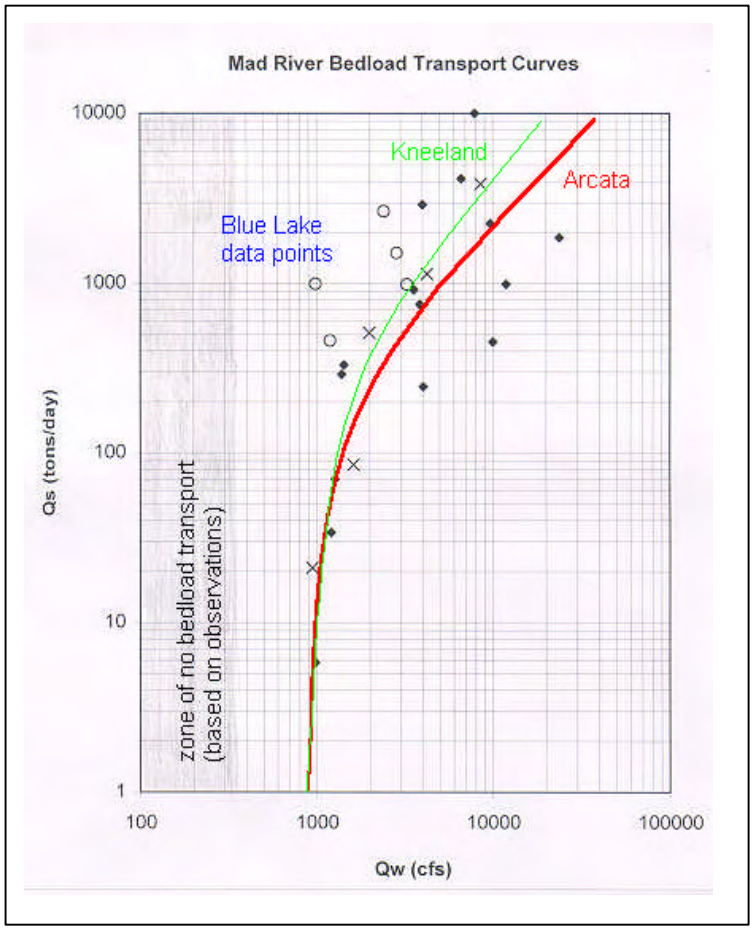

Figure 1 – Mad River bedload transport curves

stored in or lost from the study reach. As a comparison, we also calculated sediment transport rates using sediment transport equations. To determine appropriate equations, we plotted several different equations on our plot of measured bedload transport data. The equations we considered included Meyer, Peter and Muller; Ackers and White; Yang, 1984; and Brownlie. All of these equations predicted higher sediment transport values than were measured during bedload sampling, but this was not unexpected. The equation by Ackers and White showed the closest relationship to the measured bedload data so we calculated annual sediment transport into and out of the study reach using that equation. Our calculated values are summarized in Table 2.

Analysis Method	Study Area Input	Study Area Output	Study Area Storage
Bedload rating curves	152,000 tons/year	81,000 tons/year	71,000 tons/year
Ackers and White	251,000 tons/year	106,000 tons/year	145,000 tons/year

Table 2 – Calculated sediment budget for study area

Due to the limited amount of bedload data, and the scatter shown in that data, we considered the possibility of using suspended sediment data to predict bedload or bed material load transport.

We had no suspended sediment data for Kneeland or Blue Lake, but were able to compare our bedload data from Arcata to the suspended sediment data from Arcata. Despite the fact that bedload or bed material load can often be estimated from suspended sediment load, we were not able to identify any relationship between the two using the data we had for the Arcata gauge.

Historical Information: Assessing historical information was the major portion of our study. We began by examining historical aerial photographs of the river and comparing channel widths, meander arc radii, meander wavelengths, and sinuosity for each set of photographs. We also considered the following general relationships, as described by Simons (Simons, 1992):

$$S \sim Q_s \qquad \text{and} \qquad s \sim 1/Q_s$$

where S represents channel slope, s represents sinuosity, and Q_s represents bed material load. Our review of aerial photographs indicated that the sinuosity of the lower Mad River has increased very slightly from 1.28 in 1954 to 1.30 in 1999. This represents an increased length of approximately 1,300 feet over the 68,640-feet long study section. This increased sinuosity and decreased channel slope are possible effects of a decrease in bed material load transport.

The principle portion of our analysis was supposed to be a comparison of thirty channel cross sections, surveyed in 1970 and 1999. The Corps completed the 1970 cross sections as part of a hydraulic study of the lower Mad River and the 1999 cross sections were to be surveyed in the same locations for analysis in this study. At the time of writing this paper, however, the thirty new cross sections were not yet available. Instead, we were only able to compare channel cross sections at two bridge locations, at the Arcata gauging station, and at three other locations in the HBMWD area upstream from the bridges. Of these five cross sections, Hwy 101 is closest to the river mouth, Hwy 299 is approximately 13,000 feet upstream, the Arcata gauge is a few hundred feet upstream from Hwy 299, and the HBMWD cross sections are spread over a 9,000-feet long reach upstream from Hwy 299. The bridge cross sections showed steady bed degradation from approximately 1960 until approximately 1990. The Hwy 299 cross section showed the greatest average degradation, approximately 12 feet or 0.4 feet of degradation per year (see Figure 2). During the same period, the Hwy 101 cross section showed an average of 8 feet of degradation (0.25 feet per year) and the Arcata gauge showed an average of 5.8 feet of degradation (0.18 feet per year). The HBMWD cross sections indicated a slower, but still obvious, rate of degradation, approximately 4.5 feet of degradation for the same period of time (0.15 feet per year). Using similar channel cross sections and plan view areas, Lehre estimated the volume of material lost from the river bed (due to degradation) to be approximately 185,000 cubic yards (259,000 tons) per year from 1962 to 1992 (Lehre, 1993).

Two other sources of historical information we had available were the records of Sweazy Dam and of gravel mining activity. Sweazy Dam was built in 1938 between the Blue Lake and Kneeland gauges. The dam had an impoundment area of 3,000 acre-feet that was completely filled with sediment by 1960. This record gave us a reliable estimate of approximately 215,000 cubic yards per year (301,000 tons per year) of bed material load being transported into our study area. Gravel mining records indicated a minimum average extraction rate of 380,000 cubic yards per year (532,000 tons per year) from 1952 to 1992. Since regulated in 1992, the average

extraction rate has decreased to approximately 260,000 cubic yards per year (364,000 tons per year).

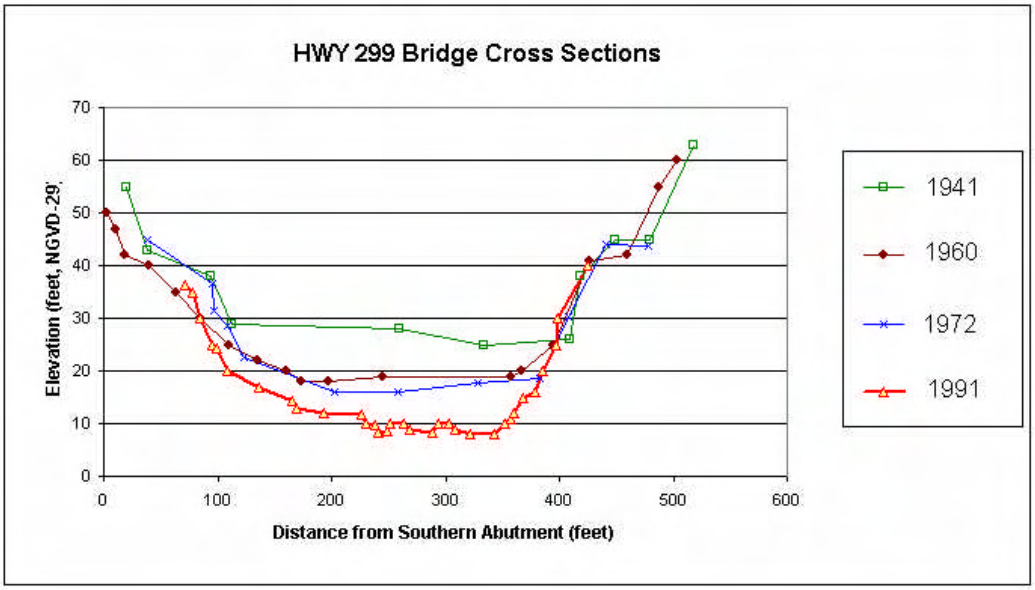

Figure 2 – Highway 299 Channel Cross Section

CONCLUSIONS

Our analysis of geomorphic features and hydraulic geometry showed the lower Mad River to be meandering with a shorter wavelength than might be expected and to be slowly increasing in sinuosity. Our analysis of these relationships also indicated that the river has several extensive sections (primarily where the gravel operators mine) where the channel is much wider and shallower than other sections of the river and much wider and shallower than would be expected in a stable system. While we did not place much emphasis on the results of the meander radius of curvature to meander wavelength relationship we did consider the channel's high width:depth ratio to be significant. The extremely high width:depth ratio in sections of the lower Mad River is a primary result of gravel mining techniques. By level skimming the bars that the river builds each year, the gravel mining prevents the river from stabilizing itself. The disproportionate width:depth ratio may also adversely affect fish habitat in the river by reducing habitat diversity and possibly increasing water temperature.

Using the sediment transport curves and equations to quantify the effects of gravel mining on the river is also difficult. The Blue Lake gauge data is essentially useless (in terms of defining a relationship from it), the Kneeland gauge data is suspect (since it only contains five points), and the Arcata gauge information is quite variable. Sediment transport equations may be extremely unreliable if they are not applied to conditions similar to those from which they were derived. Still, we were able to compare estimated sediment transport rates as determined by transport curves and equations. For our study area of the lower Mad River, the transport rates calculated with the curves and equations were relatively close and certainly on the same order of magnitude. We compared those rates with the estimated transport rate as determined at Sweazy

Dam as well as with the estimated volume of gravel lost from the river bed due to degradation and found the results quite compatible (see Table 3).

Study Area Input (tons/year)	Study Area Output (tons/year)	Study Area Storage (tons/year)	Average Gravel Extraction (tons/year)	Study Area Storage (tons/year)	Volume of Bed Degradation (tons/year)
Bedload rating curve 152,000	Bedload rating curve 81,000	71,000 (stored)	Mining records 532,000	461,000 (loss)	Lehre's estimate 259,000
Ackers and White 251,000	Ackers and White 106,000	145,000 (stored)	Mining records 532,000	387,000 (loss)	Lehre's estimate 259,000
Sweazy Dam value 301,000	Bedload rating curve 81,000	220,000 (stored)	Mining records 532,000	312,000 (loss)	Lehre's estimate 259,000
Sweazy Dam value 301,000	Ackers and White 106,000	195,000 (stored)	Mining records 532,000	337,000 (loss)	Lehre's estimate 259,000

Table 3 – Lower Mad River sediment budget results (1960-1992)

All of these results compare reasonably well with Lehre's estimate of bed material volume loss during the period from 1960 to 1992. With the uncertainty of the sediment budget and mining extraction values, however, and with their annual variability, we cannot specify one volume for gravel extraction that would be an acceptable sustainable yield for the study area. Rather, we can specify a range of acceptable annual extraction values (100,000 to 200,000 tons/year, for example) from which regulatory officials may select a value based on the river flows during the previous winter and the results of regular channel cross section surveys.

Given the uncertainty associated with the sediment budget calculations, we feel that the most reliable means of regulating gravel mining in the lower Mad River is through the use of annually surveyed channel cross sections. We anticipate being able to specify cross section locations for future annual surveys after we receive and analyze the most recent set of survey data for the cross sections the Corps originally surveyed in 1970.

REFERENCES

California Department of Water Resources, 1982. Mad River Watershed Erosion Investigation.

Hey, Richard, forthcoming, Pre-Design Stability Assessments for River Restoration.

Lehre, Andre, 1993, Final PEIR on Gravel Removal from the Lower Mad River.

Leopold, Luna B., M. Gordon Wolman, and John P. Miller, 1964, Fluvial Processes in Geomorphology. Toronto: General Publishing.

Simons, Daryl B., and Faut Senturk, 1992, Sediment Transport Technology. Littleton, CO: Water Resources Publications.

Williams, G., 1986, River Meanders and Channel Size. Journal of Hydrology, Vol 88, 147-164.

HISTORIC PATTERNS OF SEDIMENTATION IN THE ATCHAFALAYA BASIN FLOODWAY SYSTEM

[1]Lamar F. Hale, LSU Agricultural Center, Baton Rouge, LA; [2]Nancy Powell, USACE, New Orleans, LA; [3]Michael G. Waldon, U.S.Dept. Of Int., Boynton Beach, FL, [4]C. Fredrick Bryan, USGS, Reston, VA

[1]Louisiana Cooperative Fish & Wildlife Unit, 124 Forestry, Wildlife and Fisheries, Louisiana State University, Baton Rouge, LA 70803, 225-342-4681; lhale@agctr.lsu.edu
[2]U.S.C.O.E., Hydrologic Eng. Section, CMVN-ED-HH, New Orleans, LA 70160-0267, 504-862-2449; Nancy.J.Powell@mvn02.usace.army.mil
[3]A.R.M. Loxahatchee Wildlife Refuge, 10216 Lee Rd., Boynton Beach, FL 33437-4796, 561-732-3684; waldon@members.asce.org
[4]Louisiana Cooperative Fish & Wildlife Unit, 124 Forestry, Wildlife and Fisheries, Louisiana State University, Baton Rouge, LA 70803, 225-388-4184; cbryan@lsuvm.sncc.lsu.edu

Abstract: Less than 100 years ago, Grand Lake, also known as Lake Chetimaches, was a major feature of the Atchafalaya Basin. Today, because of lake sedimentation and succession, accelerated by construction of features of the Corps of Engineers' Mississippi River and Tributaries flood control system, only small remnants of the lake remain within the Atchafalaya Basin Floodway System. The Corps of Engineers has surveyed historical topographic data since 1917. These data present a dynamic picture of how sediments have filled Grand Lake. To better define the processes and trends underlying the sedimentation observed in the Grand Lake area, a simple accretion model has been developed. This model assumes that annual accretion is proportional to annual volumetric water discharge and increases asymptotically toward a maximum as average water depth increases. This paper presents the historic topographic data, the accretion model development and projections, and some conclusions as to future sedimentation rates in the Grand Lake area.

INTRODUCTION

The present 3496.5 km^2 (1350 mi^2) Atchafalaya Basin Floodway that lies between the East and West Floodway Protection Levees has been termed America's Greatest River Swamp (United States Fish and Wildlife Service 1978). The Atchafalaya Basin extends inland 201 km (125 mi) and is roughly 24 km (15 mi) wide. Subsidence and the development of distributary channels (Tye and Coleman 1989a, Tye and Coleman 1989b) drive long-term patterns of sediment deposition in the Atchafalaya Basin. Grand Lake, the large lake which formed at the lower end of the Basin, primarily discharges through two outlets, the Lower Atchafalaya River at Morgan City, and the Wax Lake Outlet artificial channel, completed in 1942. In recent decades sedimentation has filled most of the area of Grand Lake (Fig. 1).

The Flood Control Act of 1928 authorized the Mississippi River and Tributaries Flood Control Plan and developed the plan to utilize the Atchafalaya Basin as a floodway to reduce flood stages in the Lower Mississippi River. Today, the Atchafalaya Basin serves multiple uses. The principal role, and arguably the most valuable role, of the Atchafalaya Basin Floodway system is to convey one half of the 85,000 $m^3 s^{-1}$ (3,000,000 cubic feet per second, cfs) design flood of the Mississippi River and Tributaries Flood Control Plan. During such conditions the Atchafalaya Basin conveys half of the total Mississippi River Basin flood discharge to the Gulf. To insure use as a floodway, the federal government has purchased flowage easements on property within the Basin and regulates development that might interfere with floodway operation. Other important uses of the Atchafalaya Basin include fishery production, sport and non-sport wildlife production, tourism, recreation, agriculture and silviculture.

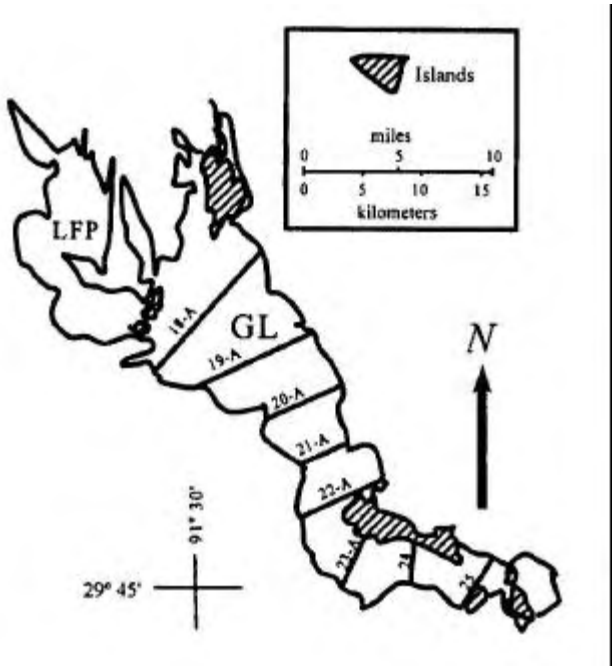

Fig. 1. Grand Lake (GL) and Lake Fausse Point (LFP) shorelines as mapped in 1917. Locations of the 8 Rangelines examined in this study are shown (18-A, 19-A, 20-A, 21-A, 22-A, 23-A, 24 and 25).

During the early 1930's, the route of the Atchafalaya River through the Atchafalaya Basin was altered. Originally, the major flow of the Atchafalaya River turned sharply eastward near Butte La Rose and followed a course that was in part outside the current East Atchafalaya Basin Protection Levee. Before the 1930's, the Atchafalaya River channel did not pass through Grand Lake. Flow through Grand Lake was limited to discharge through a web of small distributaries and overland flows during flood events. In the early 1930's the main Atchafalaya River channel was rerouted to flow through Grand Lake. Although this new channel may have improved channel capacity and created an efficient hydraulic connection to the newly constructed Wax Lake Outlet, it also promoted succession of Grand Lake through the increased deposition of sediments.

In the nineteenth century Grand Lake, also called Lake Chitimaches, was a dominant feature of the Atchafalaya Basin covering approximately 15% of the present day Basin. Today, only small shallow remnants of the lake exist within the protection levees of the Floodway. This rapid reduction of Lake Volume is similar to that documented in some man-made reservoirs which have filled in less than 25 years (Chanson and James 1998). Protected from sediment load of the Atchafalaya, an arm of the former lake has been preserved as Lake Fausse Point (Tye and Coleman 1989a), located to the west of the West Atchafalaya Basin Protection Levee. The rapid disappearance of Grand Lake has heightened concern about succession and loss of other features within the Basin. While sedimentation and delta growth are most often considered desirable processes in the Atchafalaya Bay, sedimentation and associated succession are commonly considered undesirable within the Atchafalaya Basin. This paper focuses on changes in Grand Lake, documented in USCE, New

Orleans records of the eight rangelines (upstream to downstream 18-A, 19-A, 20-A, 21-A, 22-A, 23-A, 24 and 25) which cross this lake.

METHODS AND MATERIALS

In order to identify changes in the capacity of the Atchafalaya Basin to convey flood discharges, the U.S. Army Corps of Engineers has surveyed elevations along transects, termed rangelines, at irregular intervals beginning in 1916. Data from these surveys were obtained from the New Orleans District Office of the Corps of Engineers as large format graphs of elevation plotted against distance along the rangeline. Rangeline data for the entire Atchafalaya Basin for all years were digitized and registered into a three-dimensional georeferenced Intergraph Microstation GIS database. In this 3-d database, the rangelines can be analyzed from many different aspects.

Average elevations were measured using the Microstation polygon area function. A horizontal base line of arbitrary elevation was constructed directly below each rangeline. Vertical lines were then erected from this baseline connecting to the rangeline under consideration at its endpoints or the inner levee toe, and at the main river channel banks. The area of the resulting polygon (or polygons if a section of the main channel crossed the rangeline) was then divided by the total length of the baseline under the polygon to determine the average elevation of the rangelines above the baseline elevation excluding the levees and main Atchafalaya River Channel. These elevations were imported into a spreadsheet for further analysis.

RESULTS

Data from 79 rangeline surveys of Grand Lake in 23 different years over the period from 1916 to 1988 were available for this study. Because of budget and logistical considerations, all eight rangelines were surveyed in only one (1974) of these 23 years. As a reference, the Corps of Engineers Butte La Rose gage (03120) is located at river mile 64.8, the Six Mile Lake gage (03645) is located at river mile 105.2, and the gage at Morgan City (03780) is located at river mile 117.7.

Over the entire period of observation the bottom surface elevation sloped toward the Gulf. In the earliest observations in 1917, the minimum elevation was -3.19 m at rangeline 25 near river mile 110. By 1980 this downstream elevation had risen to -0.34 m, an average rate of accretion of 4.5-cm yr^{-1}. From 1917 to 1941 accretion rate at this rangeline was 4.2-cm yr^{-1}, and from 1941 to 1980 accretion rate was 4.7-cm yr^{-1}, an increase of 12%. At the upstream rangeline, 18-A, at river mile 85, elevation rose from -1.07 m in 1917, to 0.09 m in 1940, to 0.93 m in 1978. This corresponds to an accretion rate of 3.3-cm yr^{-1} over 1917 to 1978, a rate of 5.0 from 1917 to 1940 and a rate of 2.2-cm yr^{-1} from 1940 to 1978. Thus, at the upstream rangeline accretion rate dropped 56 percent in the later period.

Overall average accretion rate for all rangelines over the entire period of study was 3.6-cm $yr^{-1.}$ This is an unusually high rate of accretion. Referring to canals and wetlands, Dortch (1996) show that typical accretion rates are more than an order of magnitude below the values determined here. The high rate of accretion observed in Grand Lake may be attributed to the high-suspended sediment concentration of the Atchfalaya River, the very large flow passing through the lake, and the initial lake depth.

To provide comparative water surface elevations, stage data from three Atchafalaya River Stage gages were analyzed. Lines of water surface elevation, termed flowlines, at three different discharge

values were derived from published stage and discharge data for the 1974 calendar year. Elevations at Butte La Rose, Six Mile Lake, and Morgan City were determined for three Atchafalaya River discharges measured at Simmesport. Flowlines for 3000, 4000, and 6000 $m^3 s^{-1}$ (106,141, and 212 thousand cfs) were determined. These discharges represent approximately the 25, 40, and 60% flow duration (i.e. percent of days that the flow is not exceeded) since the Old River Control Structure began operation (Wells and Demas, 1977).

MODEL DEVELOPMENT

In order to overcome variability in data, a simple empirical model of annual accretion was developed and compared to the given values. Sedimentation and accretion models are most commonly based on an assumed particle settling velocity determined through calibration or using Stoke′s Law (Cerco and Cole 1995, Dortch 1996). Applications of these models require at a minimum, knowledge of water velocities and depths; these were unavailable for Grand Lake. In consideration of this limitation, the model developed here is empirical and is based on observed trends and asymptotic reasoning. Annual change in average elevation was modeled as:

$$r_t = E_{t-1} = \frac{E_o - E_{t-1}}{K + E_o - E_{t-1}} = r_{\max}$$

$$r_{\max} = r_o Q_t^a$$

where r_t is the annual accretion rate over year t (m yr^{-1}). E_t is average rangeline elevation AMSL (m) at the end of year t. E_o is the equilibrium (maximum) accretion elevation (m). r_{max} is the maximum accretion rate (m yr^{-1}). Q_t is river annual calendar-year average volumetric discharge ($m^3 s^{-1}$). K is the distance (m) below E_o at which accretion rate is reduced to half r_{max}, and r_o and a are constants.

For Grand Lake these parameters were estimated through a visual calibration to the observed values. An optimal value of the exponent "a" was found to be near unity, and a value of 1 was accepted as the calibrated value. The parameter r_o was determined to be 1.803 s m^{-2} yr^{-1} through calibration. For these parameter selections, the average value of r_{max} for the period from 1934 to 1990 is 9.95-cm yr^{-1}. The parameter K was found, through calibration, to be 0.4 m at all rangelines. The maximum accretion elevation, E_o, was found to depend on the rangeline location, and generally decreased from upstream to downstream locations. For the rangelines 18-A, 19-A, 20-A, 21-A, 22-A, 23-A, 24, and 25, the value of E_o was estimated to be 0.9, 0.8, 0.5, 0.4, 0.35, 0.2, 0.1, and 0.1 m, respectively.

Because the spatial pattern of flows through the Atchafalaya Basin was radically changed in the 1930's, the calibrated model was initiated in 1934. Initial values were input for 1934, and subsequent years were then calculated on an Excel spreadsheet using the parameters cited above. Calculated values were in close agreement (Fig. 2) with the observations listed above.

One goal of this study is to provide a more generalized method for projecting accretion that may be particularly useful in planning river diversions for habitat restoration. It is therefore further conjectured that r_{max} can re belated to annual average suspended sediment concentration, c_a and water application rate (discharge per unit area inundated), q_t, by:

$$r_{\max} = r * q_t \frac{C_a}{l}$$

where: r* is a dimensionless constant which may be expressed as a percentage, λ is surfical sediment bulk density, the dry weight of bottom sediments per unit accreted volume (dg l^{-1}), and the value of q^t is commensurable with precipitation rate and other area-specific intensive parameters, and may be most conveniently reported as m yr^{-1}, and

$$q_t = \frac{Q}{A}$$

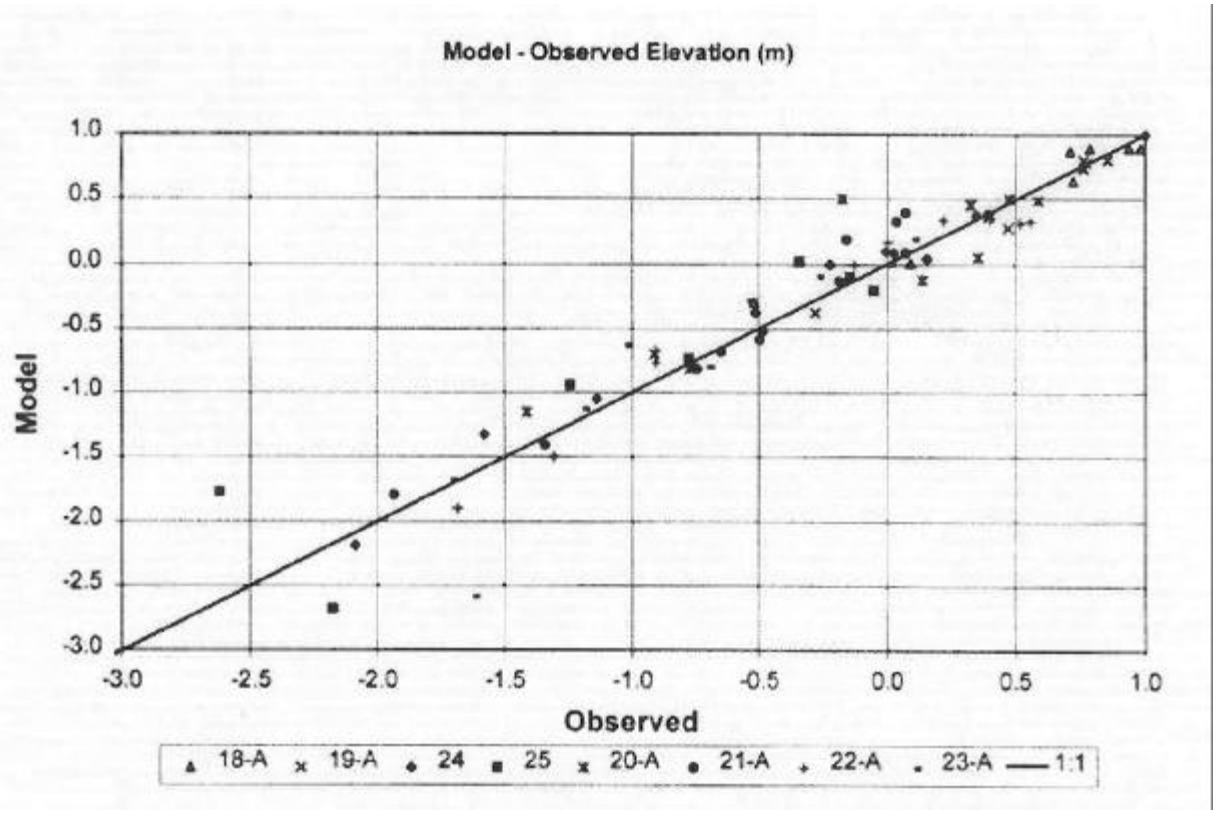

Fig. 2. Comparison of model and observed average rangeline elevations. Solid line is line of perfect fit (1:1 slope).

The parameter r* can be interpreted as the fraction of the suspended sediment which is removed from the water column in the process of accretion and is related to trapping efficiency defined in other sedimentation studies (Strand and Pemberton 1982; Salas and Shin 1999). Solving Equations 2 and 3 gives:

$$r^* = r_o A l / C_a$$

Using parameter values available from the literature, the value of r* can be roughly estimated. Over the period 1964 through 1974, Atchafalaya River suspended sediment concentration averaged 460 mg l^{-1} (Wells and Demas 1977). Although suspended sediment concentrations in the Mississippi River have declined since the middle of this century (Dardeau and Causey 1990), a constant value is used here for analysis in order to simplify computation, and because very roughly half of the suspended sediment of the Atchafalaya River is supplied by the Red River (Mossa 1990) which is not known to have declined in suspended sediment concentration prior to the relatively recent navigation improvements. Dendy and Champion (1969) have compiled bottom surficial sediment densities for a

large number of North American lakes. A typical value of 1.12 kg 1^{-1} (70 lbs ft^{-3}) is used here. Combining these values with the original area of Grand Lake provides an estimate of 49% for r*. This estimate may be further compared to the peak percent of load removal projected in the model. Wells and Demas (1977) report that the average suspended sediment load passing Simmesport is 86 x 10^6 t yr^{-1} (260,000 td^{-1}). The peak modeled annual accretion rate (Fig.3) is 38 x 10^6 m^3, which, using 1.12 t m^{-3}, converts to 43 x 10^6 t yr^{-1}, or 50% of the average suspended sediment load. Average annual accretion projected by the model for 1965 through 1971 is 11.8 x 10^6-m^3 yr^{-1}. This would correspond to an annual removal of 13.2 x 10^6 t. Wells and Demas (1977) report that although data are limited, it is estimated that over this period approximately 75% of the suspended sediment load at Simmesport were transported through the two outlets. They also report that net scour of the Basin was observed during the floods of 1973, 1974, and 1975.

DISCUSSION AND CONCLUSIONS

Accretion in Grand Lake peaked around 1950, and has generally diminished since that time (Fig. 3). Sedimentation and succession of Grand Lake will continue in isolated areas, but at a greatly reduced rate. In the future, sedimentation will likely focus on the remaining low-lying areas of the former lake as upper rangelines equilibrate at a mean elevation of <1 m. During the disappearance of deep open water, the river channel extended itself through its growing floodplain. Development of a more efficient channel must, to some degree, reduce the sediment load flowing over the elevated floodplain, and affect final equilibrium elevation. Succession is approaching a final equilibrium condition with a typical channel, natural levee, and flood plain morphology. Today, the rate of sediment trapping in the former Grand Lake has greatly slowed or stopped, and Grand Lake is approaching an equilibrium surface elevation.

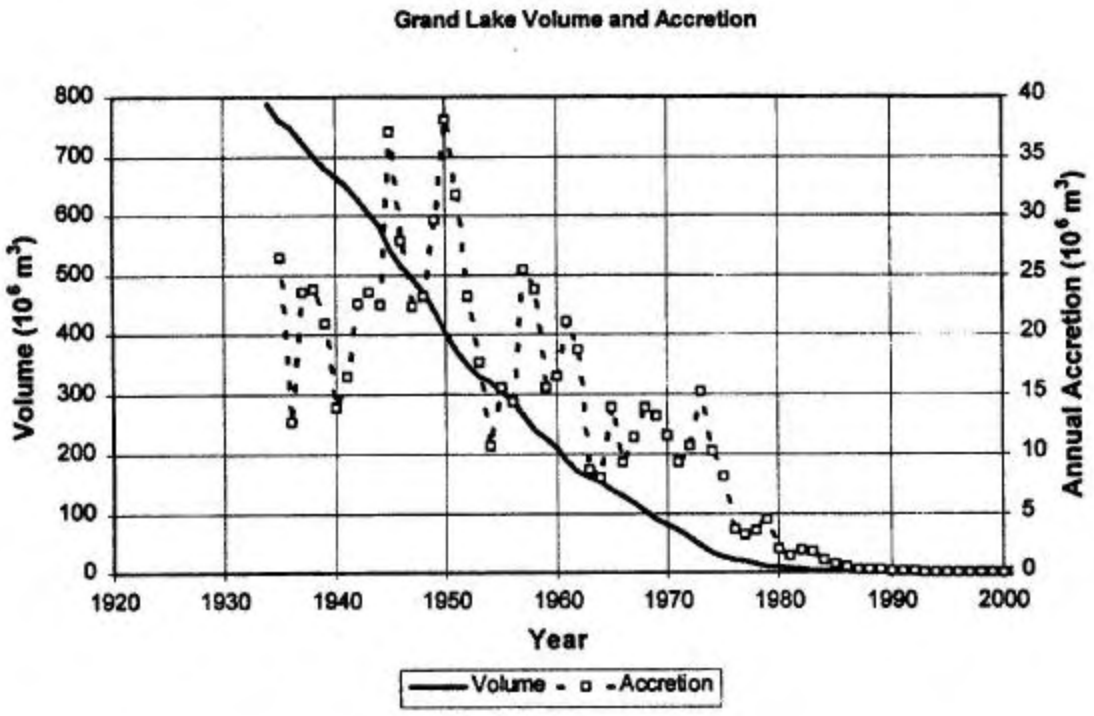

Fig. 3. Model projected Grand Lake volume (below equilibrium elevation) and annual accretion rate.

During the decades of the 1930's and 1940's a significant fraction, perhaps 20-40%, of the suspended sediment load entering the Atchafalaya Basin remained in the Basin and was unavailable for delta accretion in Atchafalaya Bay. Fisk (1952) projected that the Atchafalaya Basin would be filled with sediment by the early 1970's, and a new marine delta would then build in Atfchafalaya Bay (Tye and Coleman 1989b). Grand Lake has been effectively filled since the mid 1970's. Today, the sediment trapping efficiency of the lake has declined to near zero, and nearly all suspended sediment entering Grand Lake is delivered to Atchafalaya Bay. Similar succession patterns have been observed in man-made reservoirs (Lajczak 1996, Kern and Westrich 1997).

Patterns of sedimentation have been identified in this study. Accretion slows and finally stops as elevation approaches an equilibrium elevation. Areas of deep water accrete sediments more rapidly than shallow water bodies. Lakes also may preferentially fill with sediments from upstream to downstream segments. Expression of these patterns to the point that they can be identified and quantified depends on local hydraulic conditions and suspended sediment availability.

Accretion occurs preferentially in deep areas. This observation is consistent with observations and models of reservoir sedimentation (Strand and Pemberton 1982). In Grand Lake, we found that accretion slows to 33% of the maximum rate at a bottom elevation 0.2-m below the equilibrium elevation. For a depth of 2 m below the equilibrium elevation, sedimentation occurred at > 80% the maximum rate determined by suspended sediment load. Thus, the rate of sediment accretion is relatively uniform and higher in deeper waters.

The model developed here does not consider the longitudinal reduction of suspended sediment concentration that results from upstream accretion. Here this is appropriate because detention times are sufficiently short. In other situations it may be appropriate to consider upstream trapping and loss of suspended sediment by subdividing the study area into interconnected segments.

A better understanding is needed of the factors that determine the equilibrium surface elevation. It is likely that this elevation is related to some statistic (e.g. mean annual low water) of local water-surface elevation. Mechanisms that reduce observed accretion as the equilibrium elevation is approached include loss of sediment source, increased scour and erosion, and enhanced consolidation of higher elevation surfaces.

Preferential accretion in deep water may be one mechanism contributing to indirect land loss from excavation of canals in wetlands. In situations where suspended sediment supply is limited, sediments may preferentially settle in deep canals and therefore are unavailable to maintain surface elevations of surrounding wetlands.

The methodology reported here could provide a quantitative basis for projecting and analyzing river diversion projects that divert flow to open water. It may also provide a basis for design of accretion monitoring studies in these areas. These simple modeling techniques also may provide insight in interpretation of other wetland sedimentation studies using different data collection methodologies (Hupp and Morris 1990, Hupp et al. 1993).

Much information about sedimentation and accretion can be extracted from the Atchafalaya Basin rangeline data. Only the data concerning Grand Lake has been considered in this paper. We plan to continue examining these valuable records, and to extend the analysis to the entire Atchafalaya River Basin. Opinions and conclusions expressed in this paper are solely those of the authors.

LITERATURE CITED

Cerco,C.F.and Cole,T.M., 1995, User' s guide to the CE-QUAL-ICM three-dimensionaleutrophication model, release version 1.0. Technical Report EL-95-15, U.S. Army Engineer Waterways Experiment Station, Vicksburg, MS

Chanson,H. and James,P., 1998, Rapid Reservoir Sedimentation of Four Historic Thin Arch Dams in Australia. *Journal of Performance of Constructed Facilities, ASCE* 12:85-92.

Dardeau,E.A. and Causey,E.M., 1990, Downward trend in Mississippi River sediment loads. Potamology Program (P-1) Report 5, Environmental Laboratory, U.S. Army Engineer Waterways Experiment Station, Vicksburg, MS.

Dendy,F.E. and Champion,W.A., 1969, Summary of reservoir sediment deposition surveys made in the United States through 1965. Miscellaneous Publications No. 1143, reprinted as Appendix F in Water Quality Assessment: A Screening Procedure for Toxic and Conventional Pollutants - Part 2, U.S. Environmental Protection Agency, EPA-600/6-82-004b, U.S. Department of Agriculture.

Dortch,M.S., 1996, Removal of solids, nitrogen, and phosphorus in the Cache River Wetland. *Wetlands* 16:358-365.

Fisk,H.N., 1952, Geological investigation of the Atchafalaya Basin and the problem of the Mississippi River diversion, United States Army Waterways Experiment Station, Vicksburg, MS.

Hupp,C.R. and Morris,E.E., 1990, A dendrogeomorphic approach to measurement of sedimentation in a forested wetland, Black Swamp, Arkansas. *Wetlands* 10:107-124.

Hupp,C.R., Woodside,M.D. and Yanosky,T.M., 1993, Sediment and trance element trapping in a forested wetland, Chickahominy River, Virginia. *Wetlands* 13:95-104.

Kern,U. And Westrich,B., 1997, Sediment budget analysis for river reservoirs. *Water and Soil Pollution* 99:105-112.

Lajczak,A., 1996, Modeling the long-term course of not-flushed reservoir sedimentation and estimating the life of dams. *Earth Surface Processes and Landforms* 21:1091-1107.

Mossa,J. 1990. Discharge-Suspended Sediment Relationships in the Mississippi-Atchafalaya River System, Louisiana. Dissertation, Louisiana State University, Baton Rouge, LA

Strand,R.I. and Perberton,E.L., 1982, Reservoir Sedimentation Technical Guideline for Bureau of Reclamation. United States Department of Interior, Denver.

Tye,R.S. and Coleman,J.M., 1989a, Depositional processes and stratigraphy of fluvially dominated lacustrine deltas: Mississippi delta plain. *Journal of Sedimentary Petrology* 59:973-996.

Tye,R.S. and Coleman,J.M., 1989b, Evolution of Atchafalaya lacustrine deltas, south-central Louisiana. *Sedimentary Geology* 65:95-112.

United States Fish and Wildlife Service, 1978, The Atchafalaya: America' s greatest river swamp. Field Office, Lafayette, LA.

Wells,F.C. and Demas,C.R., 1977, Hydrology and Water Quality of the Atchafalaya River Basin. Water Resources Technical Report No. 14, United States Geological Survey, published by Louisiana Office of Public Works, Baton Rouge, LA.

STREAM MORPHOLOGICAL RESPONSE TO CLIMATE AND LAND USE IN THE MINNESOTA RIVER BASIN

J. Magner, Senior Hydrologist, Minnesota Pollution Control Agency, St. Paul, MN;
L. Steffen, Geologist, Natural Resources Conservation Service, Lincoln, NE

INTRODUCTION

Luna Leopold has said, "the river is the carpenter of its own edifice" (Leopold, 1994). Channel morphology is determined by the interaction of the opposing forces of gravity and resistance. Lane (1955) formulated this physical principle into a generalized relationship of $Q_s * D_{50} \propto Q * S$, known as the stable-channel balance equation. The sediment half of the equation, sediment load (Q_s) and particle size (D_{50}), represent the resistance or load factors. The runoff half, stream discharge (Q) and channel slope (S) represent the energy in the system. A stable-channel is one whose load and energy factors are in balance. Because these factors are interconnected, a change in one will cause channel adjustment. For example, a decrease in sediment load or an increase in stream discharge will cause an adjustment toward degradation, whereas, an increase in sediment size or decrease in stream slope will tip the scale toward aggradation. Womack and Schumm (1977) have documented the adjusting phenomena in Douglass Creek Valley of Western Colorado. Over a 79-year period, the channel degraded and aggraded to form six terraces. These changes were primarily a result of variable sediment loads. Emerson (1971) illustrated the response of channel slope due to channelization. Channelization produced steeper slope resulting in downcutting and subsequent bank erosion. Schumm et.al., (1984) have observed and described an evolutional pattern associated with channel adjustment. Bed resistance and nickpoint migration control downcutting, so as stream energy becomes laterally contained, the channel widens. When the incised channel banks become unstable they collapse into the overwidened bed to eventually form a new active floodplain within the old channel. The bankfull or channel-forming flow determines the morphology of this new channel. The channel-forming flow was defined by Wolman and Miller (1960) when they examined the relationship between sediment transport rate and flow frequency. They found that erosion and high sediment loads occurred with extreme floods. However, more frequent flows transported the greatest quantity of sediment over time. Dunne and Leopold, (1978) observed this flow frequency to occur between the 1-and 2-year recurrence interval, with the average being the 1.5-year event.

The work described above was foundational to developing river assessment methodology to define morphological health. These principles provide insight into why the Minnesota River and its tributaries have become environmentally stressed over the past century.

BACKGROUND

When the Des Moines Lobe of the Laurentide ice sheet retreated for the last time, a relatively flat terrain with variable-sized depressions remained throughout most of the Minnesota River basin. The Minnesota River valley (MRV) was carved by glacial river Warren when glacial lake Agassiz drained in a catastrophic event (Wright, 1972). This basin formation is rather unique compared to typical fluvial geomorphic processes. Most river basins are formed by much slower rates of denudation, where soil in the upland is eroded and deposited in the lowlands. This process is driven by elevation differences throughout a basin. Drainage networks evolve in a dynamic equilibrium with climate, stream morphology and geology over time until they reach a quasi-balance. Balanced basins are considered mature unless a change in climate, landscape or geology occurs.

After glacial river Warren carved the MRV, the tributaries that were previously connected to an incipient Minnesota River were not in equilibrium - these rivers needed to cut down and widen their channels to reach a new balance. We do not know how much time was required to achieve a new equilibrium, but we do know from early explorers (Featherstonhaugh, 1970) that some relatively stable degree of equilibrium was reached in the Minnesota River prior to plowing of the prairie. Magner and others (1993), along with Leach and Magner (1992) have documented changes in vegetation, land use management and hydrology which have systematically, over the last century, moved the Minnesota River away from it's historic state of equilibrium.

A thorough analysis of climate change was not conducted as part of this study. However, Mallawatantri and others (1996) applied a linear regression between logarithms of monthly average flow and the Palmer Drought Severity Index (PDSI) to model the influence of climate on discharge in the Minnesota River basin. They examined a twenty

six-year record (1968-1994) for the months of May, June, July and August. The largest flow increases occurred during the month of May. The authors concluded that a wetter climate accounted for flow increases. However, two-thirds of the flow increase in May was not due to climate but to changes in land management.

Records from twenty-seven weather stations throughout the study area were examined. Only five long-term records were found (1915 or 1932 to 1998). For these five stations, the average annual total precipitation from 1936 to 1955 was 27.26 inches and it was 29.56 inches for the period from 1979-1998. There was an increase of 8.4 percent between the two periods of time. It appears that a small percentage of the increase in flows at stream gages, between those two time periods, can be attributed to the increase in total precipitation.

METHODOLOGY

To evaluate stream morphology with respect to the bankfull stage, 35 non-regulated USGS gage stations with at least 20-25 years of record were selected (Figure 1) using sites identified in Lorenz et.al, (1997). After selecting a range of drainage areas throughout South-central and Southwestern Minnesota, station description sheets were obtained from the USGS office in Mounds View, Minnesota. Station description sheets were examined for the type of gage, channel control features and the datum reference. Flows associated with 1-to 2-year recurrence intervals were examined and a range of gage heights noted before collecting field data. An initial visit was made to each site to look for morphological evidence of the bankfull stage.

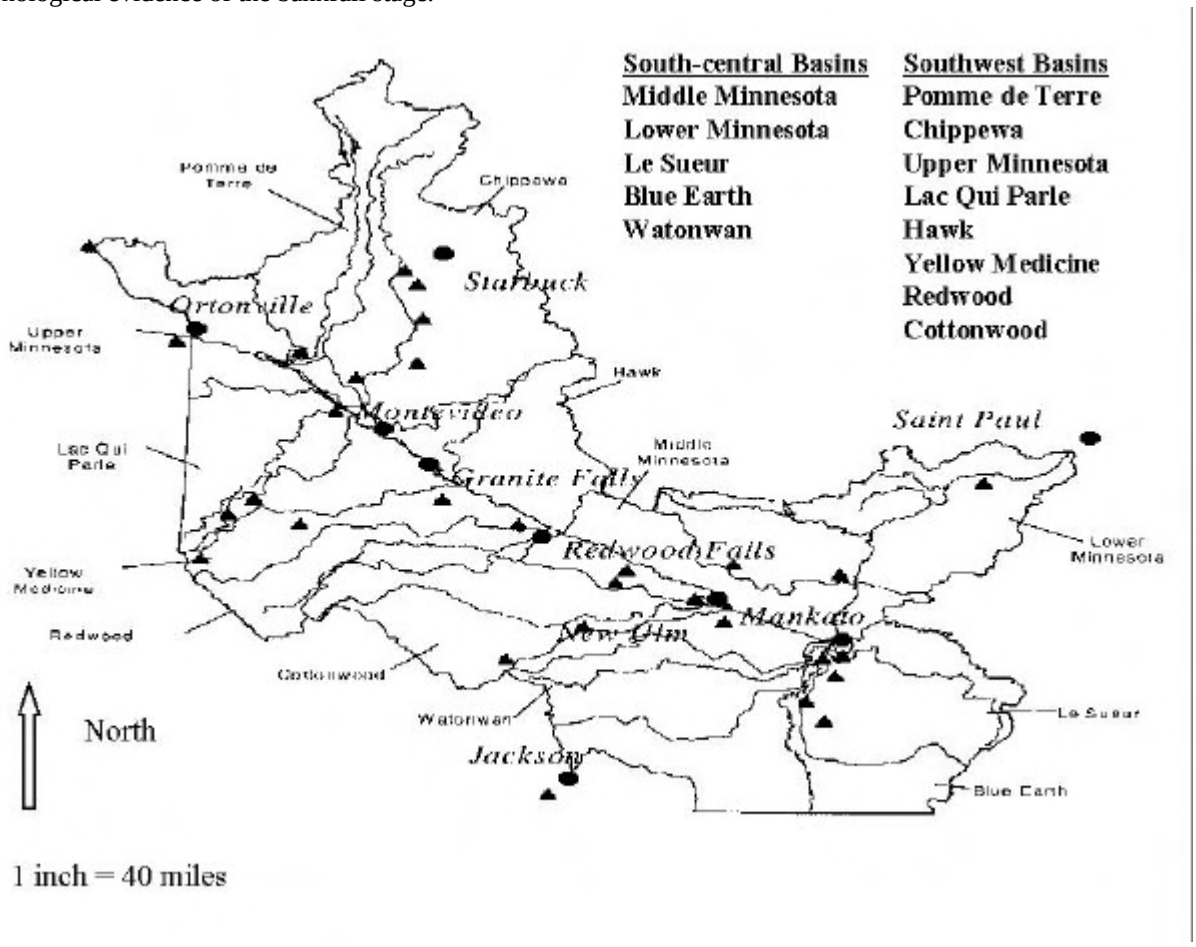

Figure 1. Stream gage sites in the Minnesota River Basin in Southwest and South-central Minnesota.

The approximate field elevation of the bankfull stage at a riffle was noted and compared to the gage height to insure that field observations were within the 1-to 2-year recurrence interval. At a riffle, the bankfull channel width and depth were measured to determine a cross-sectional area. These values, for 29 streams in the original data set, were plotted against drainage area on a log-log scale to form regional curves for South-central and Southwestern

Minnesota (Figure 2). This step was essential for visual calibration to correctly identify bankfull indicators across changes in scale. The regional curves were constructed across similar geomorphic, land-use and climatic regimes.

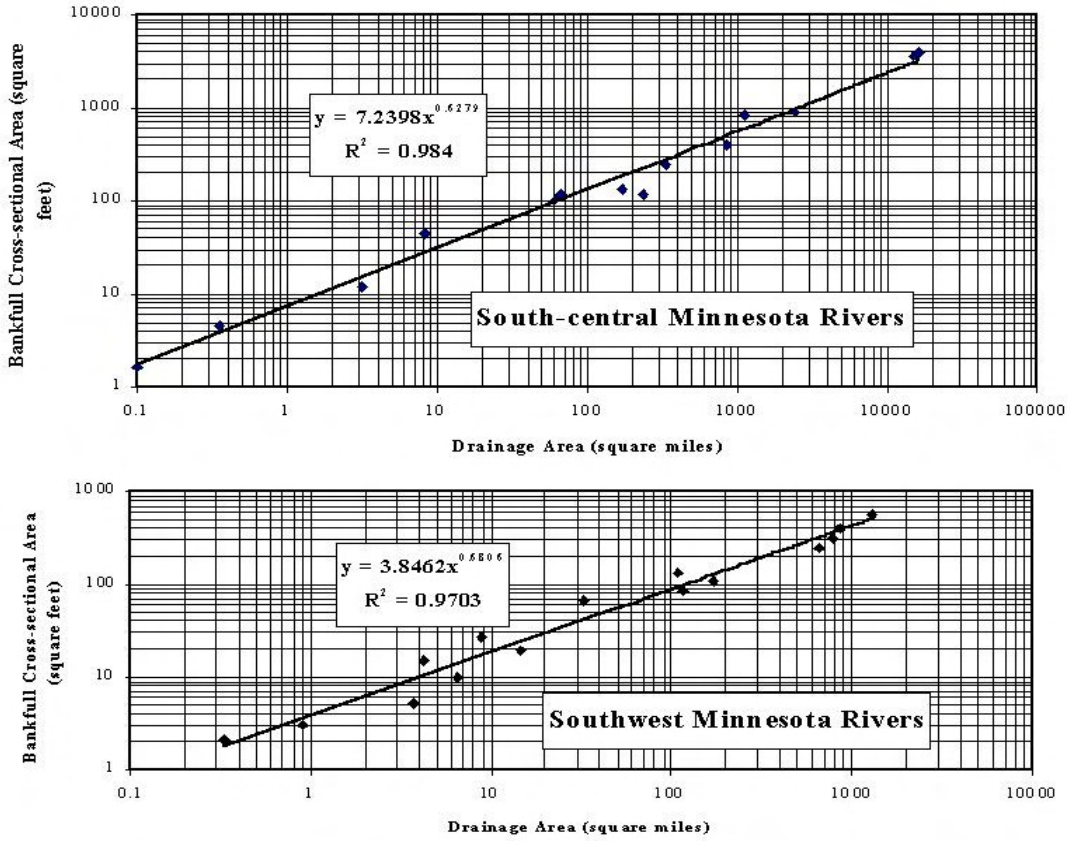

Figure 2. Regional curves of cross-sectional area for South-central and Southwestern Minnesota

Twenty-five of the initial stations were selected across a gradient of mean annual runoff; with 1.3-3 inches/year in Southwestern Minnesota to 4.5-4.9 inches/year in South-central Minnesota near Mankato. These sites were evaluated according to Rosgen's level II stream classification (Rosgen and Silvey, 1996) and Schumm's channel evolution model (Schumm et.al., 1984) to assess channel and bed stability (Table 1).

Table 1. Stream classification and detailed data for twenty-five selected sites across a mean annual runoff gradient from Southwestern to South-central Minnesota.

MN River Major Tributaries	Drainage Area	Cross-section Area	Mean Width	Mean Depth	Bankfull Discharge	W/D Ratio	Entenchment Ratio	Rosgen Class	Schumm Stage
Mean Ann RO = 1.3 - 3 in	(sq mi)	(sq ft)	(ft)	(ft)	(cfs)				
Yellow Medicine River									
NBYM trib nr Wilno	0.33	2.1	3	0.7	13	4.3	>2.2	E	I
NBYM trib nr Porter	3.7	5.2	4	1.3	74	3.1	>2.2	E	I
NBYM nr Ivanhoe	14.7	19	12	1.6	35	7.5	>2.2	E	II
SBYM River @ Minneota	115	85	47	1.8	300	26.0	<1.4	F	III/IV
Yellow Medicine R nr Granite	664	252	68	3.7	891	18.4	<1.4>2.2	F/C	V
Mean Ann RO = 2.4 - 3.3 in									

Chippewa River									
Outlet Crk trib nr Starbuck	0.6	3	2	1.2	8.4	1.7	>2.2	E	I
Hassel Creek nr Clontarf	7.2	14	10	1.4	39	7.1	>2.2	E	I
Spring Crk nr Montevideo	15.8	22	10	2.5	80	4.0	>2.2	E	V
Little Chippewa nr Starbuck	96	60	25	2.4	76	10.4	>2.2	E	I
Chippewa River nr Milan	1880	624	104	6	1340	17.3	<1.4>2.2	F/C	III/V
Shakopee Crk	308	200	74	3.5	450	21.1	<1.4	F	III
Mean Ann RO = 2.2 - 4.2 in Cottonwood/Little C. River									
Cottonwood trib nr Balaton	0.9	3	3	1	20	3.0	>2.2	E	I
Spring Crk trib nr Sleepy Eye	4.2	24	10	1.5	15	6.6	1.7	B	I/II
Spring Crk nr Sleepy Eye	33	150	28	2.3	65	12.2	>2.2<1.4	E/F	V/III
Cottonwood R @ Springfield	777	320	80	4	1100	20.0	<1.4	F	III
Cottonwood R @ New Ulm	1300	561	102	5.5	2600	18.5	>2.2	C	V
Little C. River nr Jeffers	10	17	10	1.7	100	5.9	<1.4	G	III
Little C. River nr Courtland	170	108	40	2.7	400	14.8	>2.2	C	V
Mean Ann RO = 4.5 - 4.9 in BER/LeSueur/Rush Rivers									
LeSueur Trib nr Mankato	0.1	1.6	2.7	0.6	10	4.5	<1.4	G	IV
Cobb R trib nr Beauford	8.2	45	15	3	98	5.0	<1.4	G/F	II/III
Maple R nr Rapidan	338	250	90	3.8	1900	23.7	1.4	B	IV
LeSueur R nr Rapidan	1110	851	115	7.4	3300	15.5	1.45	B/F	IV
Blue Earth R nr Rapidan	2410	900	150	6	4390	25.0	1.5	B/F	V
M. Br. Rush River nr Gaylord	67	207	52	4	400	13.0	<1.4	F	III

Stream flow records for thirteen rivers in South-central and Southwestern Minnesota were examined to determine if annual peak flows changed over time (Table 2). The first nine rivers represent Southwestern Minnesota. Rivers with USGS stream gaging stations with long-term records (>60 years) were selected. Peak flows for each gage were downloaded from the USGS web site. These files were edited to create data input files for the U. S. Army Corps of Engineers, Flood Frequency Analysis (FFA) software (COE 1992). FFA calculates the annual peak flows for the 1.01- to 500-year return periods using the Bulletin #17B procedure (USDI 1982). The 1.5-year event is not printed in the output table so a log-probability scale graph of flow frequencies was used to determine that value.

Table 2. Stream gages used in analyzing changes in annual peak flows.

Gage Number	Location	Drainage Area (mi^2)	Period of Record
05291000	Whetstone R nr Big Stone City, SD	389	1910-12, 1919, 1931-98
05292000	Minnesota R nr Ortonville, MN	1,160	1938-98
05294000	Pomme de Terre R nr Appleton, MN	905	1931-98
05300000	Lac Qui Parle R nr Lac Qui Parle, MN	960	1911-14, 1931-98
05304500	Chippewa R nr Milan, MN	1,880	1937-98
05311000	Minnesota R @ Montevideo, MN	6,180	1910-98
05313500	Yell. Medicine R nr Granite Falls, MN	664	1919, 1931-98
05316500	Redwood R nr Redwood Falls, MN	629	1910-14, 1931-98
05317000	Cottonwood R nr New Ulm, MN	1,300	1910-13, 1931-98
05320000	Blue Earth R nr Rapidan	2,430	1910, 912-46, 1948, 1950-98
05325000	Minnesota R @ Mankato	14,900	1881, 1903-98
05330000	Minnesota R nr Jordan	16,200	1935-98
05476000	Des Moines R @ Jackson, MN	1,250	1909-13, 1931-98

The stream flow record for each river was divided into two, 20-year time periods. The first time period, defined as "old" was from 1936-1955. The year 1955 was selected as a limit for old because most major drainage ditches were

constructed by this date. However, adequate field drainage, i.e. subsurface tile, was just beginning. The introduction of laser technology in the early 1980's accelerated the pace of field drainage development.

The second period, 1979-1998, defined as the "new" period, represents a time of more adequate field drainage. These periods also were selected based on the common years of flow measurements for each gage. The 20-year time periods also provided statistically significant values for the most frequent annual peak flows, the 1.01-, 1.5- and 2.0-year events. The 1936-1955 period for the Blue Earth River only has 18 years of record. This same period for the Chippewa River and Yellow Medicine River gage sites only have 19 years of record. The Blue Earth River near Rapidan, is regulated, however, the data from this station is of importance to South-central Minnesota. The Des Moines River at Jackson, Minnesota is outside of the Minnesota River basin boundary. It was added because soils, landscape, land-use and drainage development in that basin were similar to the other basins in Southwestern Minnesota. The percent of change was calculated between the "old" and "new" periods. To normalize between periods, the annual peak flows were divided by drainage area for each gaging station and the average percent change was also calculated.

RESULTS

The regional curves developed for Southwestern and South-central Minnesota show a close fit to the data. The R^2 for drainage area versus bankfull discharge, cross-sectional area, mean width and mean depth in South-central Minnesota are 0.97, 0.94, 0.98, and 0.87, respectively. Similarly, the R^2 values are 0.93, 0.97, 0.96, and 0.81 in Southwest Minnesota. Table 1 shows the detailed data for the twenty-five selected sites across a mean annual runoff gradient from Southwestern to South-central Minnesota. Table 1 also provides the Rosgen stream classification and the Schumm channel stage. At some gage stations, two values are given to reflect differences in the channel above and below the bridge or culvert. The smaller western tributaries showed fewer disturbances as evidenced by E channels at stage I. Streams with larger drainage areas were typically incised as evidenced by F channels in a disturbed or recovering evolutionary stage. Drainage ditches, more prevalent in South-central Minnesota, were classified as B if they were stable and G if they were unstable. Most were unstable and evolved to a stage III, evidenced by undercut bank toes with rotational slumps.

Drainage ditches with larger drainage areas in cohesive soils were classified similar to Southwestern rivers as unstable F's and stage III's. However, gage stations located in the Paleozoic bedrock of South-central Minnesota tended to have evolved stage IV or V channels and met the criteria for a stable B or moderately entrenched channel or a stable C which is a slightly entrenched channel.

The changes in the 1.01-, 1.5- and 2-year peak-flow frequency analysis, for the gage stations described above, are presented in Tables 3, 4, and 5. Data for the Minnesota River at Ortonville and Montevideo were not used in determining the averages in Tables 4 and 5 due to flow regulation at those sites. The average results indicate changes of 68.1%, 46.4% and 43.7% for the 1.01-, 1.5- and 2-year recurrence intervals, respectively. Any changes greater than plus or minus ten percent are assumed to be significant. Twenty-six of the thirty-three events examined show significant changes. Table 5 compares the normalized values of average peak flows per square mile of drainage area, with 54.7%, 37.6% and 36.2% for the 1.01-, 1.5- and 2-year recurrence intervals, respectively. The increases in peak flows, though lower than those shown in Table 4, are still significant. The changes are typically greatest for the 1.01-year peak flows and become less as the recurrence interval decreases. Changes between the 1.5-year and 2-year recurrence intervals were nearly the same, whereas, the 1.01-year recurrence interval showed a one-and-a-half times greater change than the less frequent flows. The Cottonwood, Lac Qui Parle and Pomme de Terre Rivers showed some decreases in peak flows between the old and new periods. However, when normalized by drainage area, the decreases were nearly negligible.

Table 3. Changes in peak flows from the 1936-1955 to the 1979-1998 time period.

Stream Gage Site	Annual Peak Flow Frequencies (cfs)			Annual Peak Flow Frequencies (cfsm)		
	1.01-yr	1.5-yr	2.0-yr	1.01-yr	1.5-yr	2.0-yr
Whetstone R old	96	940	1490	0.25	2.42	3.83
new	105	1240	2040	0.27	3.19	5.24
Minn R, Ortonville old	80	500	725	0.07	0.43	0.63
new	102	870	1360	0.09	0.75	1.17
Pomme de Terre R old	115	645	921	0.13	0.71	1.02
new	73	630	985	0.08	0.70	1.09
Lac Qui Parle R old	216	1510	2270	0.23	1.57	2.36
new	208	1550	2330	0.22	1.61	2.43
Chippewa R old	144	1020	1530	0.08	0.54	0.81
new	533	2510	3460	0.28	1.34	1.84
Minn R, Montevideo old	343	2510	3760	0.06	0.41	0.61
new	537	4200	6380	0.09	0.68	1.03
Yellow Medicine R old	239	1260	1780	0.36	1.90	2.68
new	248	1500	2150	0.37	2.26	3.24
Redwood R old	146	900	1300	0.23	1.43	2.07
new	346	1810	2530	0.55	2.88	4.02
Cottonwood R old	737	3140	4220	0.57	2.42	3.25
new	552	3570	5210	0.42	2.75	4.01
Blue Earth R old	978	5300	7480	0.40	2.18	3.08
new	2990	7450	9000	1.23	3.07	3.70
Minn R, Mankato old	2640	12000	16300	0.18	0.81	1.09
new	4470	18900	25100	0.30	1.27	1.68
Minn R, Jordan old	2440	12100	16800	0.15	0.75	1.04
new	4290	19500	26300	0.26	1.20	1.62
Des Moines R old	295	1480	2040	0.24	1.18	1.63
new	424	2050	2830	0.34	1.64	2.26

Table 4. Percent change in peak flows from the 1936-1955 to the 1979-1998 time period.

Stream Gage Site	Old to New Percent Change Annual Peak Flows		
	1.01-yr	1.5-yr	2.0-yr
Whetstone R	9.4	31.9	36.9
Pomme de Terre R	(36.5)	(2.3)	6.9
Lac Qui Parle R	(3.7)	2.6	2.6
Chippewa R	270.1	146.1	126.1
Yellow Medicine R	3.8	19.0	20.8
Redwood R	137.0	101.1	94.6
Cottonwood R	(25.1)	13.7	23.5
Blue Earth R	205.7	40.6	20.3
Minnesota R, Mankato	69.3	57.5	54.0
Minnesota R, Jordan	75.8	61.2	56.5
Des Moines R	43.7	38.5	38.7
Average	68.1	46.4	43.7

Table 5. Percent increase in annual peak flows normalized by dividing peak flows by the drainage area for each gage site.

Scenario	Annual Peak Flows/Drainage Area (cfsm)		
	1.01-year	1.5-year	2.0-year
Average for 11 rivers (1936-1955)	0.25	1.45	2.08
Average for 11 rivers (1979-1998)	0.39	1.99	2.83
Percent change from old to new (11 rivers)	54.7	37.6	36.2

DISCUSSION

In Southwestern Minnesota, small drainage-area channel slopes tend to be steeper than similar channel slopes in South-central Minnesota. These differences reflect the glacial history and subsequent topographic differences of the regions. The Des Moines Lobe in South-central Minnesota is a flat ground moraine with glacial lake bed features, whereas lateral and end moraine landscapes dominate in Southwestern Minnesota. Because of terrain and climate in many upland portions of Southwestern Minnesota, tile development has likely been less extensive compared to the upland portions of South-central Minnesota. As drainage areas become larger (> 20 square miles) in the Southwest, and flow moves from the more rolling areas of the moraines to the flatter lake bed, ditch and tile densities become similar to the South-central region.

Small tributaries near Mankato have been partially channelized and tile-line outlets have been added over the past three decades. Even the constructed channels have adjusted because the contributing drainage area has progressively increased over time. The best visual evidence of channel adjustments are hanging roots from trees less than 30 or 40 years old and road culverts that have a 2 or 3 foot drop on the downgradient side. At several gage stations, the upgradient side of the culvert appeared stable (E or C in Stage I or V), whereas nickpoint migration moved the downgradient stream reach toward an unstable G or F (Stage II or III). Spring Creek near Montevideo showed more advanced channel evolution with an E channel at stage V below the road culvert.

The larger drainage areas (> 100 square miles) appear to have integrated the cumulative drainage impact. Downcutting by the Minnesota River likely initiated nickpoint migration up the tributaries. As the tributaries of the Yellow Medicine, Chippewa, Cottonwood, Rush and Blue Earth Rivers experienced head cutting, channels incised and laterally confined stream energy, resulting in F stream types at stage III. Little Cottonwood River near Courtland is an exception because channel reconstruction created an active floodplain.

The Pomme de Terre basin drains sandy soils derived from outwash, whereas other basins analysed drain clayey, glacial till-derived soils. Many prairie lakes in the Lac Qui Parle basin were drained by the mid-fifties. A large flow diversion was also constructed upstream of this gage. These situations may explain why peak flows decreased or increased only slightly between the time periods for the Pomme de Terre and Lac Qui Parle gages. The Redwood basin contains many potholes with heavy clay soils. In the last quarter-century, open-tile surface drains have been installed throughout the lower Redwood basin. It is not known why the change in the Cottonwood basin runoff peaks were so low, although less open-tile surface drains occur in the lower Cottonwood basin compared to the Redwood basin. The large increase in the 1.01-year peak flows for the Chippewa, Blue Earth and Redwood basins may be related to millions of linear feet of subsurface tile added to portions of these watersheds. A large portion of the Blue Earth basin was covered by glacial lake Minnesota. This region is extremely flat compared to the other basins examined. The flat terrain necessitated the increased density of subsurface tile lines. The large increases in the Chippewa River peak flows may be caused by flood control work in Shakopee Creek. The channel was straightened and widened during 1961 to 1968. The Shakopee Creek basin is relatively flat, and noncontributing micro-depressions likely became contributing areas between the old and new time periods.

In conclusion, the evidence suggests that the bankfull discharge (1- to 2-year peak flow) has generally increased throughout the Minnesota River basin. Climate and land-use management influenced the increase in frequent peak flows. Agricultural drainage has increased stream density, improved channel conveyance and added previous noncontributing drainage areas. Increases in bankfull discharge have resulted in channel incision, which disconnects the channel from the active floodplain. The resultant loss of the active floodplain has destabilized riparian vegetation, habitat and the riparian corridor's ability to buffer environmental stress. Subsequent channel adjustments following incision have resulted in land loss and increased sediment loads in the unstable channels. Some of the

increased sediment loads were deposited in downstream, widened reaches, but silts and clays were transported further downstream as an increased suspended sediment load.

REFERENCES

Dunne, T. and L. B., Leopold. 1978. Water in Environmental Planning. W. H. Freeman and Company, San Francisco, CA: 818 pp.

Emerson, J. W. 1971. Channelization: A case study. *Science 172:325-326.*

Featherstonhaugh, G.W., 1970. A Canoe Voyage Up the Minnay Sotor. Vol. 1, reprint edition, Minnesota Historical Society, St. Paul, MN 55101

Lane, E. W. 1955. The importance of fluvial morphology in hydraulic engineering, ASCE, *Proceedings 81, paper 745:1-17.*

Leach, J. and J. Magner. 1992. Wetland Drainage Impacts within the Minnesota River Basin. *Currents 2:3-10.*

Leopold, L. B. 1994. "A View Of The River". Harvard University Press, Cambridge, MA: 298 pp.

Lorenz, D.L., G.H. Carlson, and C.A. Sanocki. 1997. Techniques for Estimating Peak Flow on Small Streams in Minnesota. WRI report 97-4249. USGS Mounds View, MN 55112

Magner, J.A., G.D. Johnson, and T.J. Larson, 1993. The Minnesota River Basin: Environmental Impacts of Basin-wide Drainage. *In Eckstein and Zaporozec (Ed),* Industrial and Agricultural Impacts of the Hydrologic Environment. Vol. 5, p. 147-162, Water Environment Federation, Alexandria, VA. 22314

Mallawatantri, A., D. J. Mulla, and M. Seeley, 1996. Sediment Reductions in the Minnesota River from Improved Land Management Practices. Unpuplished report, Department of Soil, Water and Climate, University of Minnesota, St. Paul, MN 55108

Rosgen, D. L., and H. L. Silvey. 1996. Applied River Morphology. Wildland Hydrology, Pagosa Springs, CO 81147

Schumm, S. A., M. D. Harvey and C. C. Watson. 1984. Incised Channels - Morphology, Dynamics and Control. Water Resources Publications, Littleton, CO 80161: 200 pp.

U.S. Army Corps of Engineers, 1992, Flood Frequency Analysis Software, Version 3.0, Hydrologic Engineering Center, Davis, CA.

U. S. Department of the Interior, 1982, Guidelines for Determining Flood Flow Frequency, Bulletin #17B, United States Geological Survey, Office of Water Data Coordinator, Interagency Advisory Committee on Water Data, Hydrology Subcommittee, 182 pp.

Wolman, M. G., and J. P. Miller, 1960. Magnitude and Frequency of forces in geomorphic processes. *Journal of Geology 68:54-74.*

Womack, W. R., and S. A. Schumm. 1977. Terraces of Douglass Creek, Northwestern Colorado: An example of episodic erosion. *Geology 5:72-76.*

Wright, H.E., 1972. Quaternary History of Minnesota. *In P.K. Sims and G.B. Morey (Ed),* Geology of Minnesota: A Centennial Volume. p.515-546, Minnesota Geological Survey, University of Minnesota. St. Paul, MN 55105

AUTHORS

Joseph Magner; Minnesota Pollution Control Agency, 520 Lafayette Road, St. Paul, MN 55155-4194; PH (651) 296-9268; FAX (651)297-2343; email: joseph.magner@pca.state.mn.us

Lyle Steffen, Natural Resources Conservation Service, National Soil Survey Center, 100 Centennial Mall, N, Rm 152, Lincoln, NE 68508-3866; PH (402)437-4010; FAX (402)437-5336; email lyle.steffen@usda.gov

TIRTAHARAPAN® SYSTEM

DISSOLVED, SUSPENDED AND BED LOAD SEDIMENT LOGGER

by PROF DRS DIRK DE HOOP

1 PREFACE

I often say that when you can measure what you are speaking about, and express it in numbers, you know something about it; but when you cannot express it in numbers, your knowledge is of a meagre and unsatisfactory kind; it may be the beginning of knowledge, but you have scarcely, in your thoughts, advanced to the stage of Science, whatever the matter may be, (Lord Kelvin, 1824-1907).

Scope of the problem

Since the mid-thirties land degradation has become a major element of concern. Rapid population growth stimulated the settlement of vulnerable and marginal lands. Together with deforestation and the opening up of catchments through the expansion of road networks, river basins have been subjected to increased environmental pressures.

Off-site effects of soil degradation, such as the sedimentation of reservoirs have so far been less well documented or mapped.

With greater appreciation of the economic impact of erosion and sediment, there is an increasing requirement for a greater understanding of quantities and sources of sediment, the processes invoked in its detachment and transport and its movement through the system (Walling, 1988).

With increased computer capabilities the development of numerical "model building" has also boomed. Numerical ground water and surface water models are now widely used to generate information. However information created in this manner should not be confused with hydrological field data. Information created through models, are thus, used to make up for the lack on hydrological field data, collected particularly in the developing countries. This in spite of the fact that modelling, without enough data, will not satisfy at all. As we stated before, numerical models require huge amounts of data over many years. Otherwise models will not approach real field situations.

From the environmental point of view, a cheap monitoring system will be essential in the very near future, to overcome environmental disasters in the developing countries, before or after artificial changes in the hydrologic systems.

See salinisation of irrigation schemes in Pakistan, Egypt, Thailand etc., water pollution in combination with suspended load, sediment transport etc., etc.

2 PHYSICAL PRINCIPLES AND JUSTIFICATION

2.1 Introduction

All calculations in the hydrology are based on the weight of the column of water, better defined as the negative value of the upward force. The weight of a water body is thus defined as the force of gravitational attraction exerted on the body by earth. This gravitational pull, however, is not merely one force exerted on the body as a whole (Sears 1950). Each small element of the body is attracted by earth, and hence the force which is called the weight of the body is in reality the resultant of all these small parallel forces. The direction of the gravitational force on each element of a body, is vertically down, so the direction of the resultant is also vertically down.

Stoke's law

When a viscous fluid flows past a sphere with streamline flow or when a sphere moves through a viscous fluid at rest, a friction force is exserted on the sphere. (A force is, of course, rexperienced by a body of any shape, but only for a sphere is the expression for the force readily calculable.
The friction force is given by

$$F = 6\pi\eta rv$$

where η is the viscosity of the fluid, r the radius of the sphere, and v the relative velocity of sphere and fluid.

Consequently the pressure near the sensor depends on three variables.

1. The height of the water table above the sensor,
2. The density or specific weight of the liquid
   (inc. the dissolved, suspended and bed load sediment,)
3. The atmospheric pressure.

The pressure near the sensor, which today can be measured with a high degree of accuracy and with high frequencies, is thus a function of the above three variables. If two of the variables are known the third one can be calculated.

2.2 A fluid system employing steady state flow

Bernoulli's Energy Equation states that, ignoring friction losses, from point to point in a fluid system employing steady state flow, the total energy is the same at every point in the path of flow.

These energies are composed of Pressure Head, Velocity Head, and Elevation Head.

In other words, if there is a reduction in the energy of any form, there must be an equivalent increase in another.

The disturbing factor or noise by the measurement is the Velocity Head (Bernoulli's Energy Equation or expressed by Torricelli's Theorem, $v^2=2gh$, $h=v^2/2g$).

The existence and properties of the velocity-potential in the various cases that may arise, will appear as a consequence of the following definition.

The circulation in every 'infinitely small' circuit is assumed to be zero.

If the motion of any portion of a fluid mass be irrotational at any one instant it will under certain very general conditions, continue to be irrotational (Lamb, Kelvin).

As a consequence, the installation of the sensor in the bedding will partly avoid an influence of a velocity-potential.

2.3 Sediment, Suspended Load, Bed Load

Besides water level, rainfall, evaporation and temperature it is possible to directly measure (monitor), the sediment load (inc. bed load, sediment load, and dissolved sediments) as a part of the density of a water body. The negative value of the upward force (Pascal, Simon Stevin),is measured, and the specific gravity of clear water is known.

To keep the length of the water column constant, the difference in the negative value of the upward force of two measuring points in the vertical in a water body (top and bottom of the specific water column within the water body), will give an indication of the weight of a specific water column compared with the weight of a similar column of clear water.

The difference of the weights of the two columns, mentioned before will give a excess in weight that can be translated to sediment load etc. and the volume of water shipped by the particles. This is so because as, according to 'Archimedes principle', a body immersed in a fluid is buoyed up with a force equal to the weight of the displaced fluid. Hence again an equation with two unknown variables exists, i.e. the density of the particles and the fluid displacement.

The above principles translate into the following equations, from which the estimated error of measurement of the Tirtaharapan logger can be calculated.

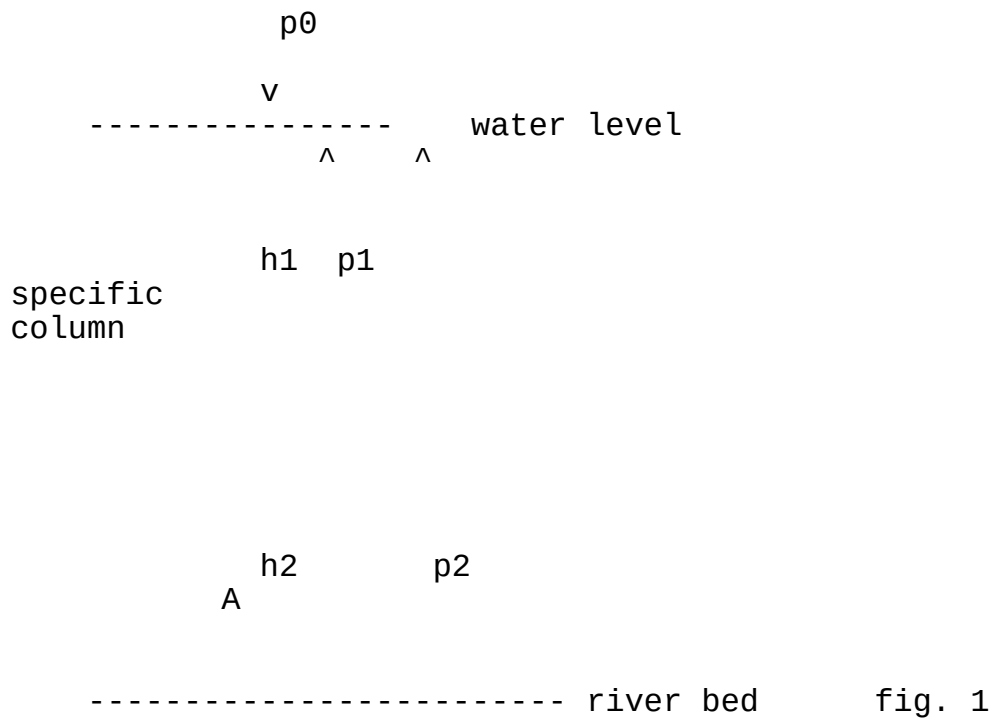

fig. 1

2.4 SEDIMENT LOAD

Pressure difference between h2 and h1

$(p2 + p0) - (p1 + p0) = Dc*g*(h2 - h1)$

$p2 - p1 = Dc*g*(h2 - h1)$ (1)

Dfl (Kg/M^3) = K * Dw = density fluid incl. dissolved sediment.
Dc (Kg/M^3) = weighted average density of the fluid column
incl. dissolved, suspended and bed load sediments.
Dw = density clear water
Ds = weighted average density sediment load
K = correction factor for dissolved load.
The condition is K=constant.
hc (M) = height specific column
hs (M) = height column sediment load
A (M^2) = cross section of the column
g = gravity (9.8 m/sec2)
p0 ($Kg/M*sec^2$) = atmospheric pressure
p1, p2 = fluid pressure on the respective depths h1, h2
M = Mass (Kg)
Ms = Mass of sediment (Kg)
Ws = weight of sediment (kg*m/sec2)

K*Dw = Dfl

h2-h1 = hc

p2-p1 = Dc*g*hc = X (X = pressure difference
= specific column) (2)

Dc*g*A*hc = K*Dw*g*A*hc + Ds*g*A*hs - K*Dw*g*A*hs (3)

We assume as a condition a specific column:
hc and A are fixed (condition II).

Dc*hc = K*Dw*hc - K*Dw*hs + Ds*hs (4)

because of the above condition (II),

hc = 1 M

Dc = K*Dw*(1 - hs) + Ds*hs (5)

If we assume dDc equals zero

dDc = 0 = -dhs*K*Dw + dhs*Ds + hs*dDs

then

dhs/hs = dDs/(K*Dw - Ds)

The weighted averages of the particle density, Ds, of soil mainly consisting of clay minerals and silt is in the order of 2.6(DON KIRKHAM,IOWA STATE UNIVERSITY, Handbook of Applied Hydrology, Chow).

If we assume arbitrarily boundaries for Ds resp. 2.4 and 2.8, the estimated error because of suspended load composition will be dhs/hs = 2.4 - 2.8/2.6 = .4/1.6 = 25 %

Creative network planning and to installation of the monitoring system in a river basin, plus a sampling programme, will be necessary.

In a strict sense, the error depends on the results of the sample programme and the proper installation, both spatially as constructionally, and is possibly smaller.

from (5) follows

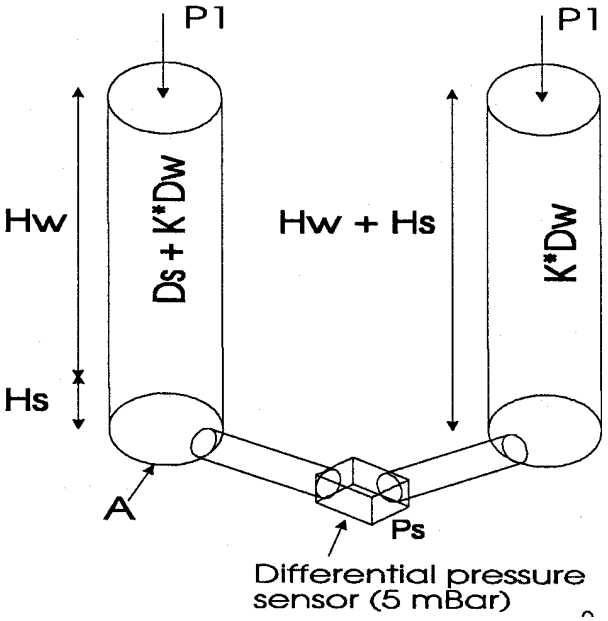

Dc*hc - K*Dw*hc = Ds*hs - K*Dw*hs

Dc*hc*g - K*Dw*hc*g = Ps = hs*g*(Ds - K*Dw) (6)

Ps = measured pressure difference
Ps * A = the weight of the volume of sediment/suspended load equal to the volume of the displaced fluid body

and hs becomes

hs = (Dc - K*Dw)/(Ds - K*Dw) (7)

K is constant, K*Dw=Dfl density of clear water inclusive solutions. Dfl had to be measured and taken as constant over a time period.

Ws = Ds * g * A * hs (8)

Ms = Ds * A * hs (9)

Ds = 2.6 (subject to results of sampling programme)
Dw = 1 (at 4 degrees C)
g = 9.8 m/Kg/s^2
Ps = measured difference (Kg/m*sec^2) (Pascal)

A = unit area (m^2) = 1

So the mass sediment (suspended sediment plus bed load is to be calculated by inserting hs in equation (9).
In case of K*Dw = Dw, K = 1

M = Ds * A * hs
A = 1 M^2
Ps = hs * g * (Ds - K*Dw) = 10 Pascal
hs = Ps/(g * (Ds - K*Dw)
hs = 10/(9.8 * (2.6 - 1)
hs = 10/(9.8 * 1.6) = 10/15.68 m
hs = .64 M sediment
M = 2.6 * 1 * .64
M = 1.7 Kg
because of condition II and (5)
hc = 1 M
Sediment content of the water body is 1.7 / 1000 = 0.0017 Kg/L
= 1.7 g/L

If A = unit area = 1 M^2 and hc = o.99 M
Sediment content of the water body will be 1.7/990 = 1.72 g/l
A percent error in the measurement of the size of the specific column will give 1.2 percent error sediment content or an error of 20 mg/l.

In order to realise a specific water column in a water body, a special sensor for sediment load is required.

Proposed installation of sediment logger.

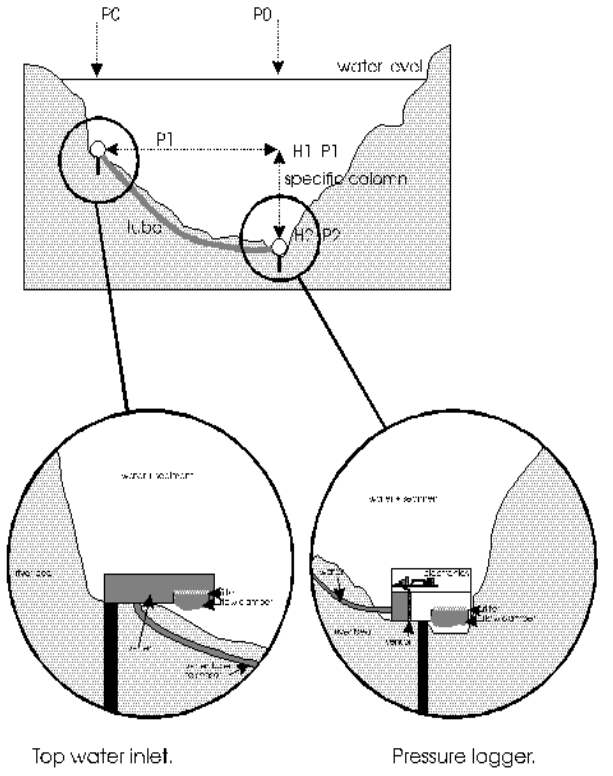

A wet/wet pressure transducer with on one end (upper end) a tube filled with water free of suspended load and sediment. On the bottom of the tube the upward force is built up by the liquid column of clear local water and solutions, the water column above the tube and the atmospheric column. On other side of the sensor, the upward force is built up by the water column, with suspended load, sediment, solutions(disolved matter) and the atmospheric column.

This is not a new approach but a very old dream of ARCHIMEDES (287-212 BC). It is new, because, thanks to our technical advances, it is now possible to measure economically, where until recently, it was impossible to measure at all with automatic recorders. In order to realise the economics one has to compare labour costs, installation costs and instrumentation.

3.0 CONCLUSIONS AND RECOMMENDATIONS

The present state of sediment concentration measurement practices has given rise to major errors of several hundred of percent (Walling 1984, Meijerink 1977). Infrequent, untimely and poor standards of concentration measurements, very high labour, transport and laboratory costs etc. are the main causes for these failures. With respect to sediment/suspended load concentration measurements, the proposed Tirtaharapan system is properly developed and tested under qualified laboratory conditions (August, 1993). With respect to the tests the Tirtaharapan Sediment/Suspended Load Logger is expected to measure with an accuracy in the order magnitude of +/- 50 ppm or less under field conditions, mostly depending upon an appropriate installation. The noise due to the velocity-potential is of a greater importance than sensor accuracy itself in BSL.

The field of application for the Tirtaharapan sediment logger can typically be found in rivers with sediment concentration ranges of 200 ppm. and upwards, as can be seen from Sedimentation Concentration Data published by Mahmood (1987).

REFERENCES

Bogen J., Walling D.E., Day T.J., Erosion and Sediment Transport Monitoring Programmes in River Basins, IAHS Publicatition No.210

Dirk de Hoop, Loggers for Water and Rainfall, ITC journal 1985-1

D.de Hoop, Rainlog and Preslog: Novel tools for in situ measurements, ISPRS, Symposium on Remote Sensing for Resources Development and Environmental Management/Enschede/ August 1986).

Dirk de Hoop, Tirtaharapan Water level and Rainfall Logger System, "Joint Seminar on Watershed Research and Management", 1989, Bogor and Balikpapan, Indonesia, pp.181-205.

Dirk de Hoop, Sediment, Suspended Load, Bed Load, August 23, 1993

Dirk de Hoop, The Tirtaharapan Sediment Logger, THE CONTROL OF RESERVOIR SEDIMENTATION, Anex VI, 1994

Sir Horace Lamb, Hydrodynamics, Dover Publications, New York, Six edition, 1932, originally published in 1879.

Dorpzicht, Geesteren(Gld), The Netherlands, 09 October 2000.

STATISTICAL MODELING OF LANDSLIDE HAZARD USING GIS

By Peter V. Gorsevski, Department of Forest Resources College of Natural Resources – University of Idaho; Randy B. Foltz, U.S. Forest Service, Rocky Mountain Research Station, Moscow, Idaho; Paul E. Gessler, Department of Forest Resources College of Natural Resources – University of Idaho; and Terrance W. Cundy, Potlatch Corporation, Lewiston, Idaho

Abstract: A model for spatial prediction of landslide hazard was applied to a watershed affected by landslide events that occurred during the winter of 1995-96, following heavy rains, and snowmelt. Digital elevation data with 22.86 m x 22.86 m resolution was used for deriving topographic attributes used for modeling. The model is based on the combination of logistic regression and principal component analysis (PCA) of road related landslides and assumes that the meteorologic factors which caused failures in the past will cause failures in the future. This model was intended to provide forest land managers with additional information on landslide hazards associated with roads. The advantage of the model is that it allows rapid assessment of spatial correlation of the topographic attributes on large areas. A Geographic Information Systems derived map using the principal component analysis model delineates areas with relatively high probabilities of failure in the basin.

INTRODUCTION

Forest roads play a key role in the vitality of any managed forest area. These roads provide access to the forest for multiple purposes including timber harvesting, recreation and fire suppression. Without forest roads, millions of acres of forest lands are unreachable. Beside providing many positive benefits, roads can have negative impacts as well. Concern about erosion and landslide failure from roads is high especially in highly dissected mountainous topography such as the Clearwater Basin in Idaho. Damage from landslides is a critical issue concerning fish habitat and water quality. Concerns about landslide failure have created a need for developing quantitative hazard models and prediction of landslide hazard.

In the literature there are various approaches for developing quantitative hazard models for prediction of landslide hazard (Carrera et al., 1991; Montgomery and Dietrich, 1994; Mark and Ellen, 1995, Gorsevski et al. 2000a, Gorsevski et al. 2000b). They are mostly based on the combination of Geographic Information Systems (GIS) and either an infinite slope stability model (Montgomery and Dietrich, 1994; Wu and Sidle, 1995; Okimura and Ichikawa, 1995) or statistical models, which link environmental attributes based on spatial correlation (Carrera et al., 1991, 1995; Chung et. al., 1995, 1999; Mark and Ellen, 1995; Chung and Fabbri, 1999).

Multivariate methods combined with GIS have been applied since the early 1980s (Carrera et al., 1983, 1991, 1992, 1995). The strategy of sampling in these applications was based either on a large-grid basis or in morphometric units. In either case the presence or absence of landslides were represented in a binary manner. All attributes believed to be relevant were sampled. These data sets were used to construct a model by applying multiple regression or deterministic analysis.

More recently Gorsevski et al. (2000a) applied logistic regression for spatial prediction of landslide hazard. A Receiver Operator Characteristic curve (Williams et al., 1999) was used to assist in the interpretation of the logistic regression results.

The approach taken in this paper uses a high resolution digital elevation model (DEM), a combination of logistic regression and Principal Component Analysis (PCA), and GIS. The DEM provides a representation of the topography of the study area and allows topographic attributes to be determined. The logistic regression analysis models the probability that an individual grid pixel will contain a landslide. The PCA identifies the most significant topographic variables that influence its occurrence. Although interpretation of the most significant topographic variables is difficult when PCA is applied, it can help to better screen the data and transform a set of correlated variables into a new set of uncorrelated variables called principal components. The principle components are also used for locating and identifying abnormalities in the data, and to check assumptions that may be required for certain statistical analysis to be valid. The principle components are used directly into the model for a backward elimination logistic regression. A table was derived from the logistic regression showing the classification of the landslides hazard. The classification table can be used as a tool for deciding a proper thresholds for hazard classification.

Although there are several solutions for categorizing ranges of probabilities, for this study area we used a scatterplot derived from the results of the logistic regression. The scatterplot shows a range of different outcomes based on the correctly identified landslides and non-landslide pixels from the classification table. From the scatterplot or the classification table we chose the influential point, which is the optimal combination for maximizing the correctly identified pixels from both groups. Departing from this influential point in one direction would classify better one of the binary groups, and misclassify in the other direction. Errors in one direction might be more serious than errors in the other direction. Managers can choose the level of risk they are prepared to accept based on the scatterplot or the classification table.

METHODS

In this paper we focused on the 85.9 km^2 Silver Creek watershed (Figure1) located northwest of Headquarters, Idaho in the North Fork of the Clearwater River Basin. The topography is highly dissected with elevations ranging from 485 m to 1635 m and slopes vary between 0 and 48 degrees. Precipitation averages about 980 mm annually. The density of roads is 5.5 km of road per square kilometer. A total of 81 road related landslides were inventoried by both photo interpretation and field inventory. The landslide triggering mechanism in the winter of 1995-96 was a combination of heavy rains and snowmelt.

DEM data with 22.86 m x 22.86 m resolution was used for deriving the topographic attributes. The original data for developing the DEM was collected on 38.1 x 76.2 m grid, then resampled to 22.86 m x 22.86 m. Topographic attributes included slope, elevation, aspect, profile curvature (slope profile curvature of a surface at each pixel center), tangent curvature (curvature of line formed by intersection of surface with plane normal to flow line), plan curvature (contour curvature), flow path (distance from watershed divide to the point of interest), and contributing

area. The topographic attributes were generated from a DEM using TAPES-G software (Gallant et al., 1996). The parent material coverage was supplied by Potlatch Corporation.

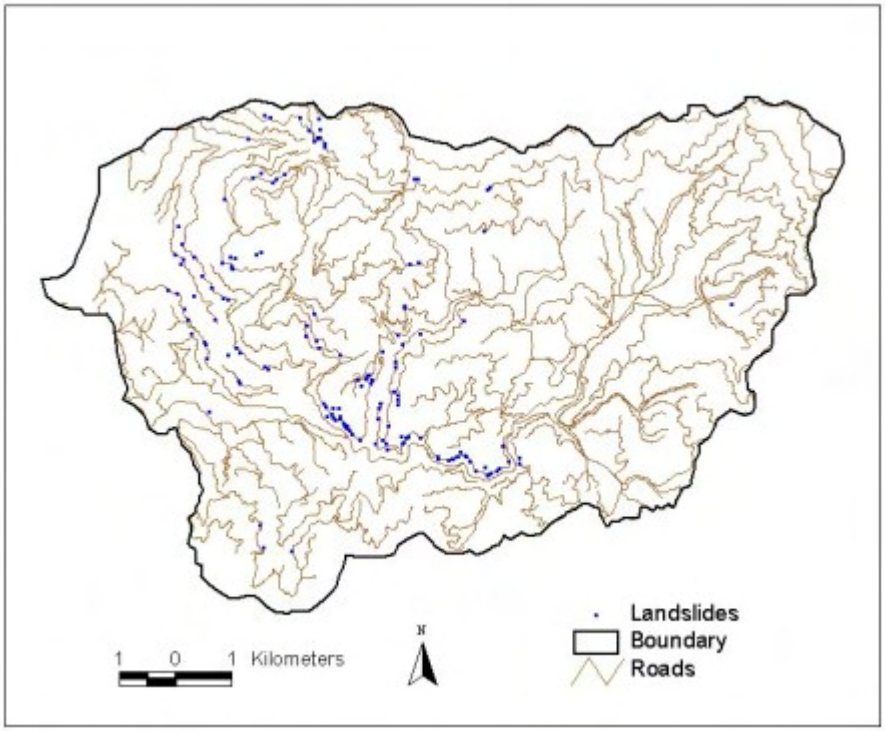

Figure 1. Distribution of Landslides and Road Network Over the Silver Creek Watershed

The topographic attributes of 15 percent of the roaded, non-landslide pixels in the watershed (24,372) were randomly sampled. All of the road-containing landslide pixels (81) were selected. These data sets were combined for further analysis.

PCA were used to screen the combined data, to produce a smaller set of uncorrelated variables, to determine the dimensionality of the space in which the data fall, and to determine the number of principal components to be used. The dimensionality of the space in which the data lies was decided by scree plot and accounting of at least 80% of the total variability in the original topographic attributes. Following the PCA, logistic regression with a backward elimination procedure was applied to the principal components. Backward elimination procedure helped to remove those principal components that were not statistically significant. After the logistic regression equation was derived, intermediate maps were generated for each of the principle components to assist in deriving the final landslide hazard map using the logistic regression equation.

RESULTS

A total of 25 original topographic attributes were reduced to 15 new, uncorrelated variables (principal components) by applying PCA. The backward elimination procedure used with the logistic regression produced six variables that were statistically significant at 95% significance level. The backward elimination method resulted in the equation shown in Table 1.

Log (p/(1-p)) = -7.0732 – PRIN1 * 1.0975 - PRIN2 * 0.6742 + PRIN3 * 0.2430 - PRIN4 * 0.3946 - PRIN5 * 0.5033 – PRIN6 * 0.5839

p – probability of landslide hazard
PRIN1 – first principle component (slope and schist)
PRIN2 – second principle component (elevation and basalt)
PRIN3 – third principle component (east and northeast)
PRIN4 – fourth principle component (south, southeast and quartzite)
PRIN5 – fifth principle component (northeast, north, granite and quartzite)
PRIN6 – sixth principle component (north, gneiss, quartzite, and alluvium)

Table 1. Logistic Regression Equation for Predicting Landslide Hazard

Interpreting the principle components with high confidence is difficult. Upon examination of the normalized eigenvectors, the elements with the largest absolute value suggested that the first principal component (PRIN1) in the logistic regression has a strong relationship with slope and the parent material schist. The variables that tend to have strong relationship with the second principal component (PRIN2) are elevation and the parent material basalt. The variables that tend to have strong relationship with the third principal component (PRIN3) are the east and northeast aspect. The fourth principal component (PRIN4) has a strong relationship with south and southeast aspect and quartzite parent material. The fifth principal component (PRIN5) has a strong relationship with northeast and north aspect and granite and quartzite parent material. Finally, the sixth principal component (PRIN6) has a strong relationship with north aspect and the following parent materials gneiss, quartzite, and alluvium. Except for the third principal component (PRIN3) variable, all other variables in the logistic regression have negative coefficients. When interpreting the logit coefficients, caution should be taken, because the logit model assumes a nonlinear relationship between the probability and the explanatory variables (Allison, 1999). For example, the estimated coefficient for the second principle component (PRIN2) is –0.6742. If our interpretation that the second principal component (PRIN2) have strong relationship with elevation and basalt is correct, then the risk of landslide hazard decreases with higher elevation for basalt.

The scatterplot which show the trade off between correctly identified landslides and non-landslides is shown in Figure 2. We chose an influence point of 67 for the landslides pixels, and 20,132 for non-landslide pixels. This point corresponded to a probability value of 0.005 from equation 1. Our selection of the influence point was determined by the desire to set the probability of making an error equal for both landslides and non-landslides.

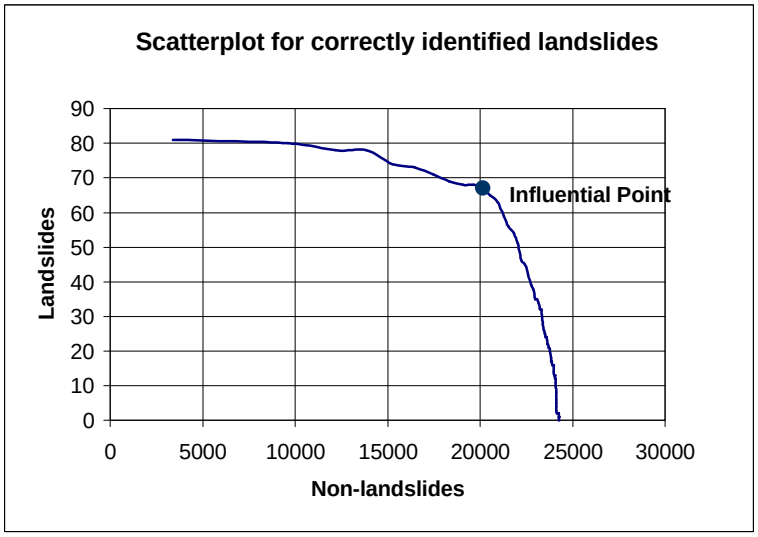

Figure 2. Scatterplot From the Correctly Identified Pixels From the Classification Table

Probability lower than the threshold (0.005) were mapped as Low Hazard, and probability higher than (0.005) were mapped as High Hazard. The resulting map is shown in Figure 3. It appears that 82.7% of the landslide pixels and 82.6% of the non-landslide pixels were correctly identified by the model.

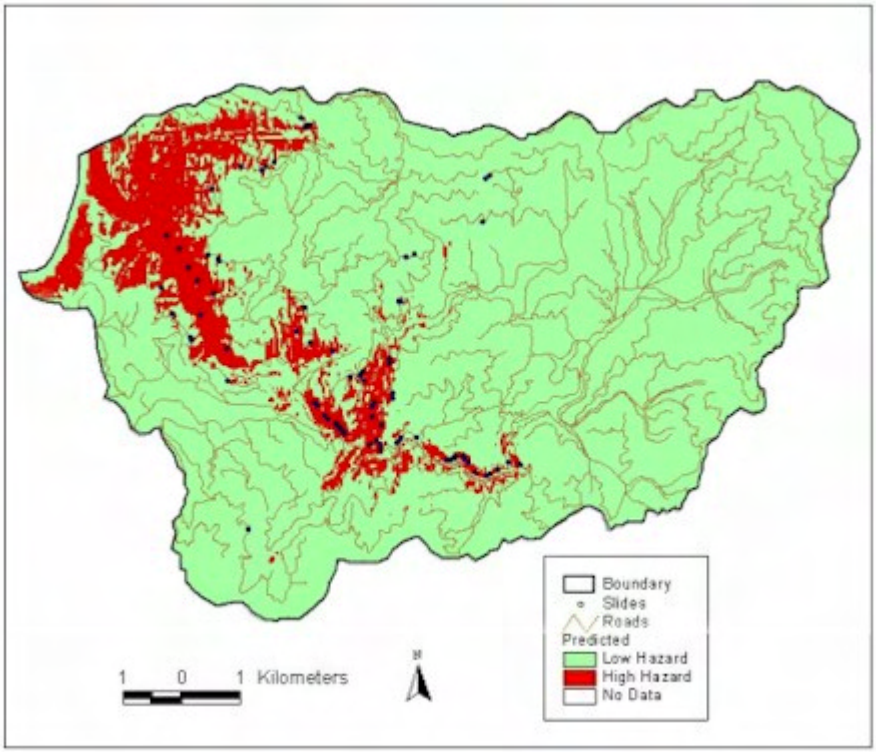

Figure 3. Predicted Landslide Hazard Assuming a Road in Each Pixel

DISCUSSION

The landslide hazard map presented in Figure 3 represents the road-related landslide hazard assuming that each pixel contained a road. While this is not the case, it presents, at a glance, the hazard associated with having a road in each pixel. The same analysis method presented in this paper, but using non-road containing pixels could be used to generate a similar map. That map would present the inherent hazard under the assumption of no roads. Comparison of the two maps would reveal risk reductions associated with road removal.

Our analysis did not include any attributes related to road construction technique which has been identified as important (Sessions et al., 1987). A further refinement of the proposed model would include this important attribute.

CONCLUSION

We developed a landslide hazard map of a 85.9 km^2 basin using a combination of logistic regression and principal component methods. Landscape characteristics were derived from a DEM. The map showed high and low risk areas for road placement. This tool can be used by land managers to focus limited resources toward the prevention of future landslides. The next step in our analysis is to include an attribute reflecting the road construction technique.

ACKNOWLEDGEMENTS

The research and work presented in this paper was supported through data provided by Potlatch Corporation and the Rocky Mountain Research Station in Moscow, Idaho.

REFERENCES

Allison P.D., 1999. Logistic Regression Using the SAS System: Theory and Application, Cary, NC: SAS Institute Inc., 1999. 304 pp.

Carrera A., 1983. Multivariate Models for Landslide Hazard Evaluation, Mathematical Geology, Vol. 15, No. 3, 1983

Carrera A, M. Cardinali, and F. Guzzetti 1992. Uncertainty in Assessing Landslide Hazard and Risk. ITC Journal, No. 2, pp. 172-183.

Carrera A., M. Cardinali, R. Detti, F. Guzzetti, V. Pasqui, and P. Reichenbach 1991. GIS Techniques and Statistical Models in Evaluating Landslide Hazard. Earth Surface Processes and Landforms, Vol. 16, 427-445 (1991)

Carrera A., M. Cardinali, F. Guzzetti, and P. Reichenbach, 1995. GIS Technology in Mapping Landslide Hazard, Geographical Information Systems in Assessing Natural Hazards (A. Carrera and F. Guzzetti, editors, Kluwer Academin Publishers, Dordrecht, The Netherlands, pp. 135-175.

Chung C.F., A.G. Fabbri and C.J. van Westen, 1995. Multivariate Regression Analysis for Landslide Hazard Zonation, Geographical Information Systems in Assessing Natural Hazards (A. Carrera and F. Guzzetti, editors, Kluwer Academin Publishers, Dordrecht, The Netherlands, pp. 107-133.

Chung C.F., and A.G. Fabbri, 1999. Probabilistic Prediction Model for Landslide Hazard Mapping. Photogrammetric Engineering and Remote Sensing. Vol. 65, No. 12 1999

ESRI Inc, 1998. Environmental Systems Research Institute, Inc. Computer Software Version 7.2.1, Redlands, CA: ESRI Inc.

Gallant J.C. and J.P. Wilson 1996. TAPES-G: A Grid-based Terrain Analysis Program for Environmental Sciences, Computers & Geosciences, Vol. 22, No. 7, pp. 713-722, 1996

Gorsevski P.V., P.E. Gessler, and R.B. Foltz 2000a. Spatial Prediction of Landslide Hazard Using Logistic Regression and GIS, 4th International Conference on Integrating GIS and Environmental Modeling (GIS/EM4):Problems, Prospects and Research Needs. Banff, Alberta, Canada, September 2 - 8, 2000.

Gorsevski P.V., P.E. Gessler, and R.B. Foltz 2000b. Spatial Prediction of Landslide Hazard Using Discriminant Analysis and GIS, GIS in the Rockies 2000 Conference and Workshop: Applications for 21st Century. Denver, Colorado. September 25 – 27, 2000.

Mark R.K., and S.D. Ellen 1995. Statistical and Simulation Models for Mapping Debris-Flow Hazard, Geographical Information Systems in Assessing Natural Hazards (A. Carrera and F. Guzzetti, editors, Kluwer Academin Publishers, Dordrecht, The Netherlands, pp. 93-106.

Montgomery D.R., and W.E. Dietrich 1994. A physically based model for the topographic control on shallow landsliding. Water Resources Research. Vol. 30. No. 4 Pages 1153-1171. April 1994.

Okimura T. and R. Ichikawa 1985. A prediction method for surface failures by movements of infiltrated water in a surface soil layer. Natural Disaster Science 7:41-51

SAS Institute Inc., 1996 SAS/STAT Software: Changes and Enhancements Through Release 6.12. Cary, NC: SAS Institute Inc.

Sessions J., J.C. Balcom, and K.Boston 1987. Road Location and construction practices: Frequency and size in the Oregon Coast Range. Western Journal of Applied Forestry, 2(4):119-124.

Williams C.J., S.S. Lee, R.A. Fisher, and L.H. Dickerman 1999. A Comparison of Statistical Methods for Prenatel Screening for Down Syndrome. Applied Stochastic Models and Data Analysis 15. 000-000 (1999)

Wu W., R.C. Sidle 1995. A distributed Slope Stability Model for Steep Forested Basins. Water Resources Research, 31 2097-2110.

ENTRAINMENT REVISITED: HIGH-FREQUENCY MEASUREMENTS OF FORCES ON SEDIMENT PARTICLES IN TURBULENT FLOW

Jonathan M. Nelson, U.S. Geological Survey, Lakewood, Colorado; Mark W. Schmeeckle, Geological Sciences, Florida State University, Tallahassee, Florida; Ronald L. Shreve, School of Oceanography, University of Washington, Seattle, Washington

Abstract: The entrainment of sediment particles from a bed underlying a turbulent flow is investigated using direct measurements of lift and drag forces on both spherical and naturally shaped sediment grains. In addition to quantifying the relations between mean near-bed flow and mean forces on sediment grains, the measurements show that flow variability is critically important for producing relatively high forces of lift and drag responsible for entrainment of sediment grains. Instantaneous values of drag from a time series measured using a grain resting on a gravel bed of the same nominal diameter are as much as four times the mean drag, and instantaneous lift values are as much as six times the mean lift. For the case of a 2cm particle on a bed of the same median particle size, time series of lift and drag were measured for conditions where some bed particles were in motion. The possibility of entrainment is evaluated from the force time series using a static force balance. This evaluation suggests that only rare flow events initiate sediment movement, even for very well exposed particles.

INTRODUCTION

Current methodologies for predicting sediment particle entrainment and transport rates for various flows are based on temporally and/or spatially averaged flow variables. However, observations show that some particles can move even when mean flow conditions suggest they should not. This is especially apparent in coarse-bedded channels. Typically, this apparent contradiction is handled by simply calibrating entrainment models with real data. For example, although Shield' s entrainment (critical shear stress) criteria suggests significant motion occurs only above a Shield' s stress of 0.06, applications in coarse channels often use values of 0.02 or even lower to match observations of motion. While some of the apparent disparity is related to the definition of "significant" motion, at least some of it is due to variations in particle placement on the bed and temporal and spatial variability in the flow field. Variability associated with the bed is usually parameterized in terms of the particle exposure to the flow, and to the pocket geometry (or friction angles) of the particles themselves, as explored by several researchers (e.g., Kirchner et al, 1990; Buffington et al, 1992; Johnston et al, 1998). There have been several studies of particle protrusion and pocket geometries over the past few decades to investigate the effects of bed particle variability, but few examinations of the effects of flow variability.

To develop a clearer understanding of the variability in the flow processes governing sediment entrainment and motion, and noting that the forces of lift and drag ultimately move sediment particles, we made direct measurements of horizontal and vertical force on a variety of stationary particles in several uniform and nonuniform flows. The measurements were made using a newly developed transducer, which measures forces on particles at turbulence-resolving frequencies (up to 200 Hz). The measurements show that rare lift and drag events occur that are much larger than the mean values of those quantities. Thus, mean flow conditions are unlikely to produce

significant entrainment relative to rarer high-amplitude events, which appear to dominate the initiation of particle motion (at least near the threshold of entrainment). The measurements also show that distributions of lift and drag on particles on a sediment bed are strongly dependent on both the magnitude and frequency content of the near-bed velocity distributions, which are in turn sensitive to rates of local acceleration. For example, flows with the same values of boundary shear stress but different turbulence structure (due to, for example, spatial acceleration) produce much different distributions of lift and drag on bed particles. The information from the force transducer allows construction of models which predict particle motion from a direct computation of forces using a predicted or measured velocity time series, i.e., without using some averaged surrogate for the flow information, such as bed stress.

In this paper, information from the force transducer is used along with a static force balance to examine when entrainment might occur for a single grain. For this computation, measurements of lift and drag were made for flow conditions that produced sediment motion on the bed, and the test particle was relatively well exposed. Thus, flow events with sufficient magnitude to produce entrainment of the particle were expected to occur.

EXPERIMENTAL PROCEDURE

The goal of the experiments discussed in this paper was to collect synchronous, high-frequency measurements of velocity and force on a particle in rough and smooth boundary layers. In the past, there have been several investigations describing the coupling between the mean flow characteristics and mean forces on grains, but there have been very few measurements of the temporal variability and frequency distributions of forces on grains in a turbulent flow. Apperley and Raudkivi (1989) measured time series of horizontal and vertical force, and were able to determine the frequency response of the grain and the variability in the measured forces. In the experiments described here, this idea is extended to include velocity measurements made with a laser-Doppler velocimeter (LDV), which allows examination of the relation between flow and forces on grains in a near instantaneous sense. In addition, particle image velocimetry (PIV) techniques are used to allow correlation of certain force events with the complete spatial structure of the local flow field. Data were collected in a variety of flow situations, including well-developed smooth and rough turbulent boundary layers, and interaction zones with both wake-like and boundary-layer characteristics. We used several test particles, including spheres, cubes, and several different natural grains. The experiments were carried out in a recirculating, racetrack, water flume, which has been extensively described by Nowell et al. (1989). This is the first set of data in which the instantaneous lift and drag on a particle near the bed can be directly correlated with the instantaneous velocity at various locations near the particle and with the entire flow structure around the particle. For a complete discussion of the various experimental measurements and results, the reader is referred to Schmeeckle (1998).

In order to make high-frequency measurements of force on a sediment grain, a new transducer was developed in cooperation with William Bruner of Hylozoic Products in Seattle, Washington (trade name is for identification only and does not constitute endorsement by the USGS). This transducer is capable of force measurements in two dimensions at frequencies approaching 200Hz. As one of the principal goals of the experiments was to examine the effects of turbulence, this frequency resolution was required. Further details on the force transducer can be found in Schmeeckle (1998) and in Nelson et al. (2000). The transducer was calibrated both

statically using weights and springs, and dynamically using a magnetic particle and a set of orthogonal coils driven by a frequency generator. The force transducer was mounted below a false bed in the flume as shown in Figure 1 with a slender, aerodynamic stalk protruding through an aperture in the flume floor to hold the test particle.

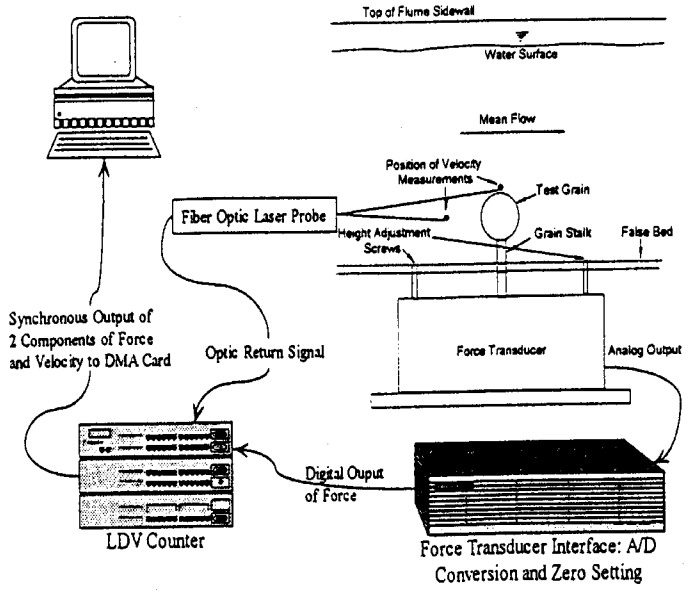

Figure 1. Schematic diagram of the force transducer and laser-Doppler velocimeter used to make synchronized measurements of force and velocity.

Data from the force transducer was collected directly in the data stream of the LDV system using a specially constructed interface, so that forces and velocities were saved in a single file. Details on the LDV system can be found in Nelson et al. (1995).

EXPERIMENTAL RESULTS

Over two hundred time series of velocity and force were collected using a variety of particle shapes and sizes in three different flow situations. These flows included both smooth and rough boundary layers and flow behind a backward step. The most common test particle was a 1.9cm sphere, although other simple shapes and a variety of natural grains also were employed. The sphere has the advantage that form lift effects are eliminated, and there is a great deal of existing information on drag and lift on spheres. A set of experimental time series is shown in figure 2.

Using the measured time series of forces and velocities, we computed drag and lift coefficients for both mean and fluctuating components of force and velocity, correlation coefficients, and other statistics for relating the flow structure to the forces on the test grain. Briefly, these measurements resulted in five major conclusions. (1) Drag coefficients for spheres in the near-bed region are higher (0.76) than the classical results found for settling spheres (0.4-0.5, e.g., Schlichting, 1979). This conclusion appears to be supported by the earlier work of Roberson and Chen (1970) and Apperly and Raudkivi (1989). (2) Drag coefficients for natural particles in the near-bed regions were even higher (about 0.9). (3) Both mean and fluctuating components of drag are fairly well correlated with streamwise velocity (with some caveats, see

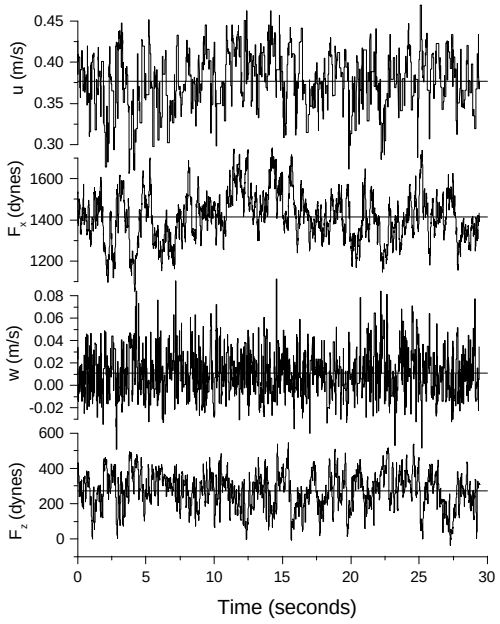

Figure 2. Typical times series of horizontal and vertical velocity and force. Velocities were measured one diameter upstream of the test particle. Horizontal lines represent mean values.

Schmeeckle, 1998). (4) Mean and fluctuating lift are not correlated with local velocity upstream or immediately above the test grain, suggesting that simple shear-lift formulations may be incomplete. (5) The maximum values of lift are often much larger than mean values (e.g., 4-6 times), suggesting that mean values may not be very important. (6) Rare high amplitude lift values appear to be associated with specific spatial structures in the flow field, and appear to depend critically on the pressure field under the grain. The reader is referred to Schmeeckle (1998) and Nelson et al. (2000) for more specific details on these conclusions.

In general, the most striking result from the experiments was the clear importance of flow variability for producing high drag and lift forces on particles. In figures 3 and 4, distributions of lift and drag on a spherical test particle from a 500Hz time series are shown for a simple, hydraulically smooth boundary layer, a developing boundary layer under a wake produced by a backward step 20 step heights upstream of the test particle, and for a gravel bed with the same median diameter as the test sphere. In the first two cases, the bed under the particle was smooth and the particle was 5mm from that bed; in the gravel bed case, the particle centerline was at the same level as the tops of the surrounding gravel. Maximum drag is about 25% greater than the mean drag in the simple boundary layer, over twice the mean in the developing boundary layer, and even higher for the gravel. Maximum lifts in the simple boundary layer are about twice the mean; they are about six times the mean in the other two cases. The results for the backward step case show that the effect of the overlying wake turbulence is dominant, not only near the reattachment point at 6-7 heights from the step, but even 20 step heights downstream. The effect of overlying wake turbulence has a profound effect on the boundary layer structure and on sediment transport (Nelson et al., 1995). Notably, measurements of forces on a grain in a gravel bed show even greater variability in lift and drag than those measured 20 step heights from a backward step.

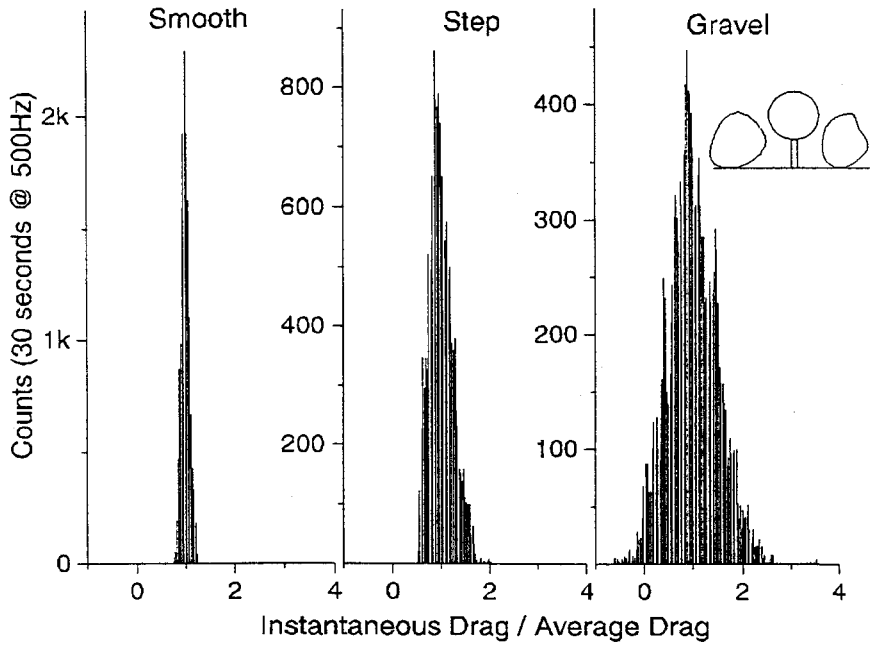

Figure 3. Distributions of drag for a 1.9cm particle 5mm above the bed in a smooth turbulent boundary layer, 5mm from the bed and 20 step heights from a backward step 2 grain diameters high, and positioned as shown in the inset for a gravel bed of approximately the same diameter.

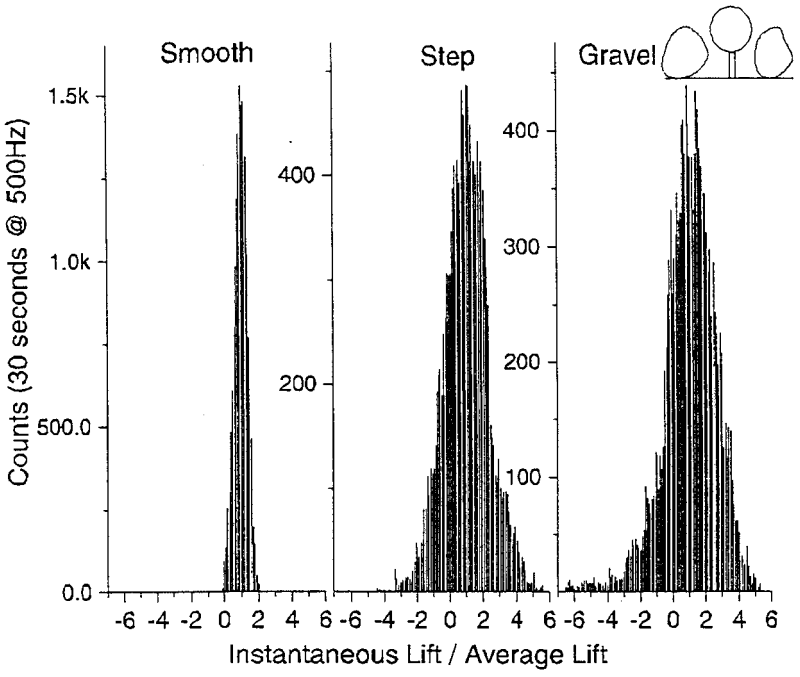

Figure 4. Distributions of lift for a 1.9cm particle 5mm from the bed in a smooth turbulent boundary layer, 5mm from the bed and 20 step heights from a backward step 2 grain diameters high, and positioned as shown in the inset for a gravel bed of approximately the same diameter.

Figures 3 and 4 indicate that variability is important for predicting if and when grains can be entrained from the bed, because they show that instantaneous forcing is often much larger than mean forcing. To investigate that aspect of this problem further, we carried out a set of experimental measurements of lift and drag for a well-exposed test particle located on a gravel bed. The flow conditions were adjusted to produce transport of the gravel making up the bed at a relatively low rate. Before the actual test measurements were made, the bed was allowed to move for a short length of time to ensure that the pocket geometries were representative of a natural sediment bed. The idea behind this set of measurements was to evaluate the time series of lift and drag in a simple force balance to see if the observed entrainment was consistent with the force measurements. In order to collect measurements of force for a case in which we might expect the particle to be entrained, the test particle was located with its centerline below the tops of the highest grains on the bed, but above most bed particles. This relatively well-exposed position was chosen so that the measurements were likely to show some particle-entraining events.

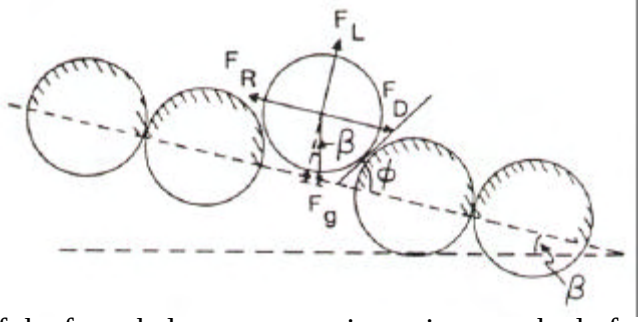

Figure 5. Schematic of the force balance on a grain resting on a bed of similarly sized particles.

To evaluate the possibility of entrainment, a simple force balance was used. Using the schematic diagram shown in figure 5, where F_D, F_L, F_R and F_g are the drag, lift, resisting and gravitational forces respectively, b is the bed slope and j is the friction angle (or particle angle of repose), The force balance when the particle is at the threshold of entrainment is given by the following expression:

$$\frac{F_D + F_G \sin b}{F_G \cos b - F_L} = \tan j \tag{1}$$

Equation 1 can be manipulated to define E, where E is one when the particle is at the threshold of motion, less than one if no motion occurs, and greater than one if the particle is accelerating out of its pocket. E is defined by the following:

$$E = \frac{F_D + F_L \tan j}{F_G(\tan j \ \cos b - \sin b)} \tag{2}$$

This expression allows evaluation of the entrainment of a particle using only the horizontal and vertical components of force, the slope of the bed, and the particle friction angle. In figure 6, the results from Equation 2 are shown using a measured time series of forces and assuming the bed slope equal to zero. Median friction angles for well-sorted beds are 50 to 60 degrees (e.g., Buffington et al. 1992), but for this value, E never exceeds one using the force time series

measured during grain motion. Typically, the lowest friction angles present in any significant proportion on sediment beds are 20 or 30 degrees (Buffington et al., 1992), so 30 degrees was used to compute E for figure 6. This value is consistent with the fact that the measured grain was well exposed (about half the grain was above the tops of the surrounding grains).

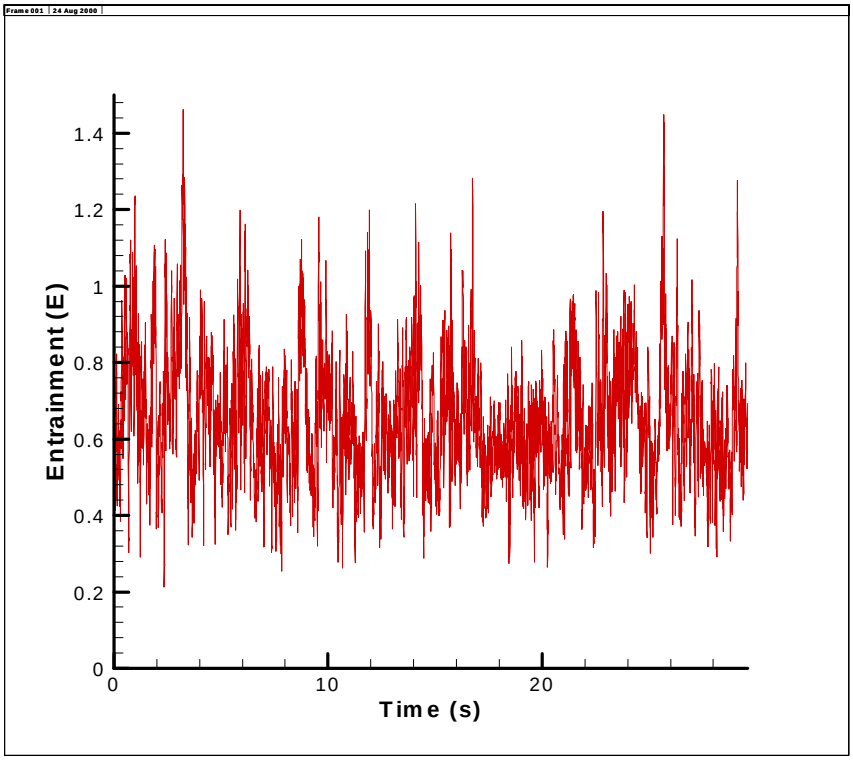

Figure 6. The entrainment E (see Equation 2) as a function of time for a 1.9 cm test particle on a gravel bed of the same approximate diameter.

Figure 6 shows that numerous events occur during the run that yield values of E greater than one, but that the mean value of E, even for this choice of friction angle, is well below one. Although the length of this paper prohibits an in-depth discussion, consideration of the time required to move a particle out of its pocket indicates that, although E is greater than one many times in the time series, most of these events last too short a time to move the grain any significant portion of its diameter. Only the event at about T=2.5s is large enough in magnitude and long enough in duration to move the particle more than half a grain diameter. Thus, many of the apparent events would probably only lead to the grain momentarily vibrating within its pocket. Thus, during this 30s time series, only a single rare flow event is of sufficient strength to move the test particle, and the mean conditions are inconsequential for entrainment.

CONCLUSIONS

Entrainment events that occur at very low values of the Shields stress are almost certainly related to situations where both the pocket geometry of the particle and its exposure to the flow are favorable, and when local flow structure produces a rare high lift and drag event. The immediate implication is that models that attempt to predict initiation of motion in low-Shields number

conditions, as are typically found in gravel-bed channels, must include parameterization of flow variability and its effect on forces on sediment grains. In a more general sense, our measurements suggest that mean flows are only capable of moving the average particle (i.e., with average protrusion and friction angle) when bottom stress is many times the critical value. Thus, in the majority of situations, mechanical models for entrainment based on mean flow and particle characteristics are not capturing the salient physics of the entrainment process. Accurate treatment requires the inclusion of flow variability, as in the model of Schmeeckle (1998).

REFERENCES

Apperley, L.W., and Raudkivi, A.J., 1989, The entrainment of sediments by the turbulent flow of water: *Hydrobiologia*, 176/177, p. 39-49.

Buffington, J.M., Dietrich, W.E., and Kirchner, J.W., 1992, Friction angle measurements on a naturally formed gravel streambed: Implications for critical boundary shear stress, *Water Resources Research*, 28(2), 411-425.

Kirchner, J.W., Dietrich, W.E., Iseya, F., and Ikeda, H., 1990, The variability of critical shear stress, friction angle, and grain protrusion in water-worked sediments, *Sedimentology*, 34, 647-672.

Johnston, C.E., Andrews, E.D., and Pitlick, J., 1998, In situ determination of particle friction angles of alluvial gravels, *Water Resources Research*, 34(8), 2017-2030.

Nelson, J.M., Schmeeckle, M.W., and Shreve, R.L., 2000, Turbulence and particle entrainment, in: Gravel-Bed Rivers V, NIWA, New Zealand, in press.

Nelson, J. M., Shreve, R. L., McLean, S. R., and Drake, T. G., 1995, Role of near-bed turbulence structure in bedload transport and bedform mechanics: *Water Resources Research*, v. 31, p. 2071-2086.

Nowell, A.R.M., Jumars, P.R., and Self, R.F.L., 1989, The effects of sediment transport and deposition in deposit feeders: results obtained in a specially designed flume. In: Lopez, G.R., and Taghon, G.L., eds., *Deposit Feeding*, Springer-Verlag, New York.

Roberson, J.A., and Chen, C.K., 1970, Flow in conduits with low roughness concentration: *Journal of the Hydraulics Division, ASCE*, 96, p. 941-957.

Schlichting, H., *Boundary Layer Theory*, 7th ed., McGraw-Hill, New York, 1979, 817 pp.

Schmeeckle, M.W., 1998, *The Mechanics of Bedload Sediment Transport*, Ph.D dissertation, Dep't of Geography, Univ. of Colorado, Boulder, 150 pp.

HYDRAULIC PERFORMANCE TESTING OF STIFF GRASS HEDGES

By Darrel Temple, Research Leader, USDA-ARS, PSWCRL, Stillwater, Oklahoma; Seth Dabney, Research Agronomist, USDA-ARS, NSL, Oxford, Mississippi

Abstract: Although stiff grass hedges are being used as vegetative barriers to concentrated flow for the purpose of decreasing erosion and encouraging sediment deposition, the data describing their hydraulic behavior have been limited. Sixteen hedges were tested with discharges being increased incrementally until the hedges failed through local overtopping. Following testing, half of the hedges were cut to remove the damaged stems, while the remainder were allowed to recover without disturbance. Preliminary data analyses and qualitative observation of the behavior of the tested hedges are reported. Test observations included: 1) the interior rows of the three and four-row hedges suffered from lack of light, making the additional rows less effective, 2) the amount of vegetal debris in the flow approaching the hedge had a significant impact on the head loss through the hedge at a given discharge, 3) the head loss through the hedge (depth of water ponded) was the dominant factor in determining the point of hydraulic failure (overtopping) of the hedge, 4) the switchgrass tended to perform better overall for the conditions tested and remained erect with water ponded to a depth of approximately 1.5 ft, and 5) removing the damaged stems by mowing following testing resulted in more rapid recovery of the hedge.

INTRODUCTION

Stiff grass hedges may be used in the management of upland erosion to assist in keeping the topsoil on the field and reducing sediment delivery to the stream and river system. These hedges normally consist of narrow, parallel strips of stiff-stemmed grass planted close to the contour. The strips may be continuous, or may be used locally to control ephemeral gullies or other areas of concentrated flow. Hedges may be used independently or in conjunction with other conservation measures (Dabney et al., 1993).

Stiff grass hedges reduce erosion and sediment delivery by forming a porous barrier to flow that ponds water upstream and spreads the flow over a large area as it leaves the hedge. This causes sediment to be deposited upstream of the hedge and reduces the erosion and sediment transport capacity of the flow downstream of the hedge (Dabney et al., 1995). Over time, contour hedges may form terraces due to the induced erosion/deposition pattern. Terraces thus formed will tend to be stable while the hedges remain in place.

Although stiff grass hedges have been shown to be a valuable conservation tool, the data related to their hydraulic behavior have been somewhat limited. Hedges are designed to function erect with flow through, rather than over, the vegetal elements, making much of the work on flow resistance of grasses inapplicable (Temple et al., 1987). Meyer et al. (1995) studied the hydraulic behavior of hedges brought into a laboratory flume and found them capable of ponding water to depths on the order of 1.5 ft (0.5 m). The effect of moving the hedges to the flume on their hydraulic behavior was unclear. Dalton et al. (1996) provided limited data on the hydraulic behavior of vetiver grass hedges, but the data were limited to a single hedge width and to vetiver grass as the plant material. Several other plant materials have been used for hedges, as discussed by Lane and Douglas (1996) and Dabney et al. (1999).

The present study was undertaken to provide additional information on the hydraulic characteristics of hedges with specific attention to alternate plant materials and hedge width. This report provides a description of the tests conducted and the behavior observed, along with preliminary data analyses. Focus is on a description of the observed behavior that may be of value to those utilizing hedges for erosion and sediment control. More detailed data analyses are planned and will be published at a later date.

DESCRIPTION OF TESTS

In preparation for testing, sixteen hedges were transplanted to test channels in the outdoor laboratory. The hedges were each 3 ft (0.9 m) in length, crossing the channels perpendicular to the direction of flow. Two repetitions of one-, two-, three-, and four-row hedges of switchgrass (*Panicum virgatum*) and eastern gamagrass (*Tripsacum dactyloides*) were established. For multiple row hedges, the rows were spaced 1 ft (0.3 m) apart. Sufficient plants were placed in each row to allow growth of a dense hedge. Initial transplanting density was approximately two plants per foot (7 plants/m). Transplanting for establishment of the hedges was done in April 1997.

The channels into which the hedges were placed were established 3-ft (0.9-m) wide channels, each 96 ft (29 m) long separated by 2-ft (0.6-m) concrete strips and isolated by a gravel bed 1.5 ft (0.46 m) below the surface. Two-ft (0.6-m) wooden sidewalls were mounted on the concrete dividers immediately prior to testing (Fig. 1). Instrumentation carriages for measuring devices were also mounted on the concrete. Between the hedges, the channels were covered with mixed grasses with bermudagrass dominating the cover. Except for the hedges, the cover was maintained in the mown condition. The grass between the hedges was mown and the loose material removed using a lawn rake immediately prior to testing.

Tests were conducted in July 1999, approximately two years after establishment. During the interim, the hedges had been maintained by irrigation and fertilization to maintain vigorous growth. The hedges were not mown or clipped at any time between establishment and testing.

Figure 1. Test channels with 2-ft sidewalls and instrument carriage mounted on the concrete dividers between channels.

In addition to mounting the channel sidewalls and instrument carriage, and mowing the grass other than the hedges, preparation for testing included documenting the condition of the hedges and establishing measurement stations immediately upstream and downstream of each hedge. The bed elevation at these measurement stations was determined before and after the tests,

and the stations were used to measure water surface elevations during the tests. Water was delivered to the channels using a 12-inch (0.3-m) pipe. Calibrated orifice plates placed in the pipe were used to measure the flow into the channel.

Tests were conducted with increasing discharge until the hedge was considered failed. The hedge was considered failed when bending and overtopping of a portion of the hedge was observed. Discharges in the 3-ft (0.9-m) wide channels were nominally set at 0.25, 0.5, 1, 2, 3, 4, and 6 cfs (0.007, 0.014, 0.028, 0.056, 0.084, 0.11, and 0.17 m^3/s). Additional intermediate flows were used in some channels when observation suggested the possibility of imminent change. Each flow was set at approximately the nominal discharge and conditions allowed to stabilize. After conditions appeared to have stabilized, water surface and discharge measurements were taken. Digital photography was used to visually document hedge performance.

Following the completion of all tests, one of each the hedge repetitions was hand clipped to a height of approximately 2 inches, and the cover removed. The other repetition of each hedge was left in the condition created by testing to failure. Recovery was monitored and documented photographically.

OBSERVATIONS AND TEST RESULTS

General Observations: During the period of establishment, the switchgrass hedges appeared well suited to the environment and management. The eastern gamagrass seemed less well adapted to the limited rooting depth and central Oklahoma climate. However, all hedges appeared dense and healthy at the time of testing.

The central rows of the multi-row hedges of both grasses tested showed evidence of poor health due to shading by the outer rows. Visually, this was more evident for the taller switchgrass than for the gamagrass, and was variable in all cases. Additional analysis is planned to identify a means of quantifying this effect.

Despite the attempt to develop consistent conditions between the hedges and the removal of vegetal debris prior to testing, the amount of debris in the flow varied significantly between tests. For reasons that are still unclear, portions of the mixed grass cover upstream of the hedges was detached by the flow in some areas, while remaining intact in others. Therefore, the amount of vegetal debris available to be trapped by the hedges varied from hedge to hedge. In some instances, this had a major effect on the depth of water ponded by a hedge for a given discharge. This effect is shown in figure 2a for the four-row switchgrass hedges. The hedge represented by the line showing the steepest initial slope experienced the greatest residue trapping and plugging of any hedge tested, while the hedge represented by the other line experienced only minimal plugging and allowed passage of substantially more flow for the same upstream depth. Figure 2b shows the same plot for the repetitions of the two-row switchgrass hedges where neither hedge experienced significant debris clogging. Figures 2a and 2b represent the worst and best consistency in test repetitions, respectively.

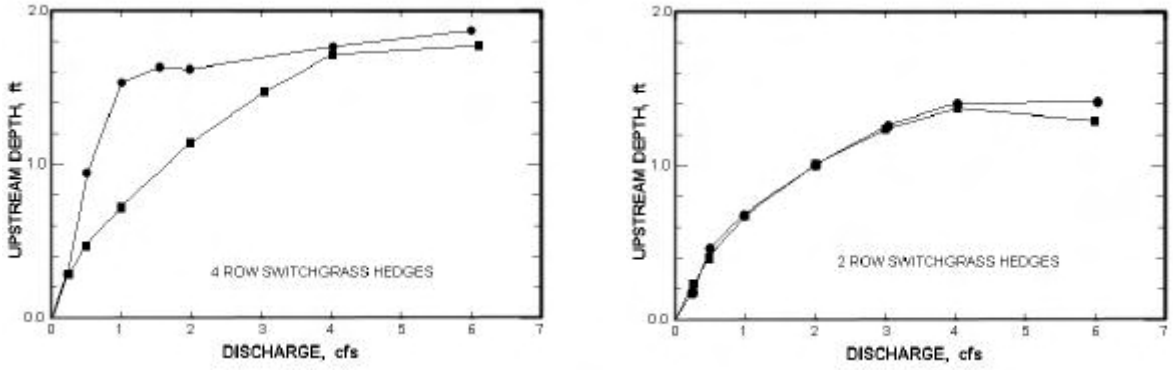

(a) *(b)*

Figure 2. Plots of upstream ponded depth vs. discharge for a) the four-row switchgrass hedges and b) the two-row switchgrass hedges.

Hydraulic Performance: Despite the problems associated with debris clogging, the general hydraulic behavior was the same for all tests as demonstrated by figures 2 and 3. For low discharges, the upstream depth increased rapidly with discharge. As the depth approached the maximum that the hedge was able to retain, upstream depth became relatively insensitive to discharge until the hedge failed locally due to bending and breaking of the stems.

When energy loss per unit of flow through the hedge (head loss) is plotted versus discharge, as is done in figure 3 for the same two- and four-row hedges represented in Fig. 2, the behavior near the point of failure becomes clearer. As additional energy is added to the system in the form of additional flow, the hedge dissipates this energy until a point is reached where flow begins to find a path over, rather than through, the hedge. The head loss then begins to decrease with increasing flow rate. This point of maximum head loss is used as the defining point of hedge failure for the remaining discussion.

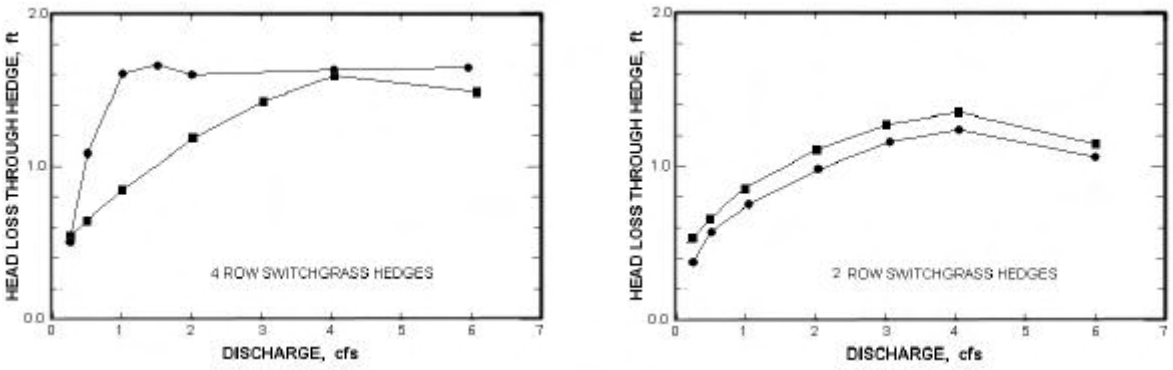

(a) *(b)*

Figure 3. Plots of energy head loss through a) the four-row switchgrass hedges, and b) the two-row switchgrass hedges.

By defining the point of hydraulic failure as the point of maximum energy head loss, we can observe trends for the hedges tested. Figure 4 shows the upstream depth at failure for each of the 16 hedges tested. The upstream depth at failure is observed to increase only slightly with the number of rows and to be on the order of 1.4 to 1.6 ft (0.4 to 0.5 m) for the switchgrass hedges and 0.9 to 1.1 ft (0.3 to 0.35 m) for the gamagrass hedges.

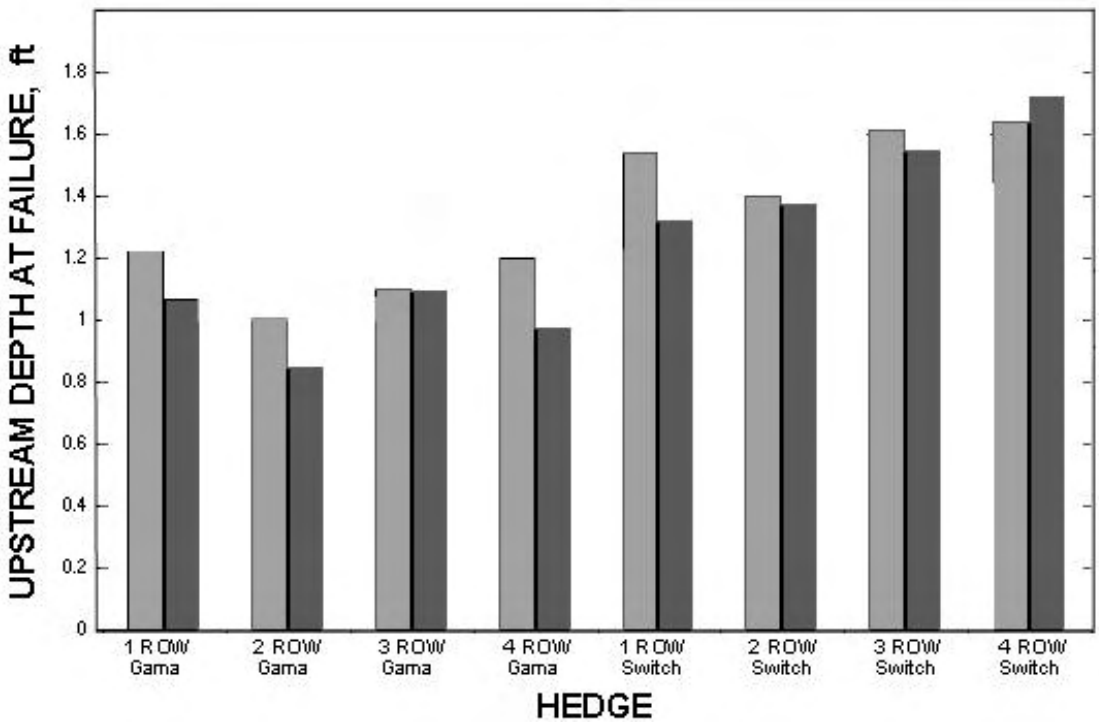

Figure 4. Upstream ponded depth at failure (maximum energy head loss) for all hedges tested.

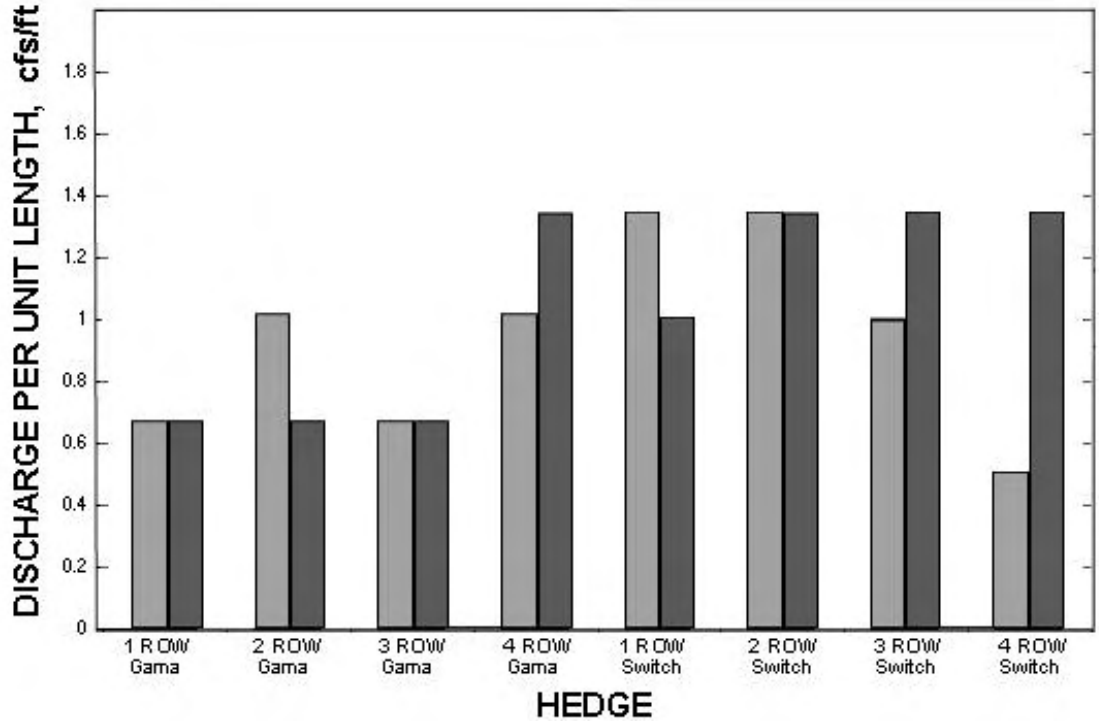

Figure 5. Discharge per foot of hedge at failure (maximum energy head loss) for all hedges tested.

Figure 5 plots the discharge per unit length of hedge (width of channel) at failure for each of the hedges tested. Discharge at failure shows significantly more scatter than upstream depth. This is due, in part, to the debris clogging problem previously discussed. Despite the scatter, an approximate specific discharge at failure may be extracted from the figure. For the tests where clogging was minimal, the discharge at failure was on the order of 1.0 to 1.3 cfs/ft (0.09 to 0.12 $m^3/s/m$) for the switchgrass hedges and approximately 0.7 cfs/ft (0.06 $m^3/s/m$) for the gamagrass. This finding is generally consistent with NRCS (1999), where, for a hedge designed to control concentrated runoff, it is recommended that a level length perpendicular to the flow direction, (measured in feet) be numerically greater than the contributing area (measured in acres). This recommendation implies a specific discharge of 1.0 cfs/ft with a runoff rate of 1in/h (2.5cm/h).

The fact that both the discharge and the upstream depth at failure tend to be relatively insensitive to the number of rows suggests that, even without significant debris clogging, the initial head loss on entry into the hedge is forming a hydraulic control. Weakening of the row interaction by shading internal rows would also contribute to this behavior. Additional data and analysis may clarify the physics of this behavior further.

Vegetal Recovery: The recovery of the hedges following testing offered few surprises. The hedges that were clipped recovered faster than did those that were left in the damaged state with a portion of the stems broken over. The difference was most notable at the end of the growing season following testing (approximately 2 months after the tests). All hedges recovered and appeared upright and healthy shortly after the beginning of the next growing season.

SUMMARY

Sixteen stiff grass hedges were established in the outdoor laboratory and tested to hydraulic failure. These hedges represented two repetitions each of one-, two-, three-, and four-row hedges of switchgrass (*Panicum virgatum*) and eastern gamagrass (*Tripsacum dactyloides*). The preliminary findings of these tests may be summarized as:

- Variation in plugging of the hedges by vegetal debris had a major impact on the depth of upstream ponding for a given discharge even though the conditions upstream appeared equivalent in all tests prior to introducing flow.
- Interior rows in multi-row hedges appeared weakened by shading from external rows, reducing the impact of using multiple rows.
- The switchgrass tended to be more adapted to the test environment and performed better hydraulically in that the discharge and ponding depth at failure tended to be greater.
- The switchgrass hedges ponded water to an upstream depth on the order of 1.4 to 1.6 ft (0.4 to 0.5 m), and the gamagrass ponded water to an upstream depth of 0.9 to 1.1 ft (0.3 to 0.35 m).
- Clipping or mowing the hedges following hydraulically damaging the stems tended to hasten recovery, but left a time period when no hedge was present.

Additional data analyses and testing may allow more detailed quantification of hedge performance. However, the difficulty in quantifying the quantity of debris available to the flow and the sensitivity of flow resistance through the hedge to this debris will make precise prediction of this resistance difficult.

REFERENCES

Dabney, S. M., McGregor, K. C., Meyer, L. D., Grissinger, E. H., Foster, G. R., 1993, Vegetative Barriers for Runoff and Sediment Control, pp. 60-70. In *Integrated Resources Management and Landscape Modification for Environmental Protection*, ed. J. K. Mitchell, ASAE, St. Joseph, MI.

Dabney, S. M., Meyer, L. D., Harmon, W. C., Alonso, C. V., Foster, G. R., 1995, Depositional Patterns of Sediment Trapped by Grass Hedges. Transactions of the ASAE, 38(6), 1719-1729.

Dabney, S. M., Liu, Z., Lane, M., Douglas, J., Zhu, J., Flanagan, D. C., 1999, Landscape Benching from Tillage Erosion Between Grass Hedges. Soil and Tillage Research 51, 219-231.

Dalton, P. A., Smith, R. J., Truong, P. N. V., 1996, Vetiver Grass Hedges for Erosion Control on a Cropped Flood Plain: Hedge Hydraulics. Agricultural Water Management 31, 91-104.

Lane, M., Douglas, J., 1996, Evaluation of Plant Species for Vegetative Hedges. Technical Note, Jamie L. Whitten Plant Materials Center, Coffeeville, MS.

Meyer, L. D., Dabney, S. M., Harmon, W. C., 1995, Sediment-Trapping Effectiveness of Stiff-Grass Hedges. Transactions of the ASAE. 38(3), 809-815.

NRCS, 1999, Vegetative Barriers. Chapter 3i in "Buffer Practices," CORE4 Key Conservation Practices, pp. 131-150. USDA-NRCS, Washington, D.C.

Temple, D. M., Robinson, K. M., Ahring, R. M., Davis, A. G., 1987, *Stability Design of Grass-Lined Open Channels*. U.S. Department of Agriculture, Agriculture Handbook 667, 175 p.